AUS DEM LEHRSTUHL
FÜR INNERE MEDIZIN I
PROF. DR. MARTINA MÜLLER-SCHILLING

FAKULTÄT FÜR MEDIZIN
UNIVERSITÄT REGENSBURG

FAT1 EXPRESSION AND FUNCTION IN CHRONIC LIVER DISEASE AND HEPATOCELLULAR CARCINOMA

Inaugural – Dissertation
zur Erlangung des Doktorgrades
der Biomedizinischen Wissenschaften

der
Fakultät für Medizin
der Universität Regensburg

vorgelegt von
Daniela Valletta

2012

AUS DEM LEHRSTUHL
FÜR INNERE MEDIZIN I
PROF. DR. MARTINA MÜLLER-SCHILLING

FAKULTÄT FÜR MEDIZIN
UNIVERSITÄT REGENSBURG

FAT1 EXPRESSION AND FUNCTION IN CHRONIC LIVER DISEASE AND HEPATOCELLULAR CARCINOMA

Inaugural – Dissertation
zur Erlangung des Doktorgrades
der Biomedizinischen Wissenschaften

der
Fakultät für Medizin
der Universität Regensburg

vorgelegt von
Daniela Valletta

2012

Dekan:	Prof. Dr. Dr. Torsten E. Reichert
Betreuer:	Prof. Dr. Claus Hellerbrand
Tag der mündlichen Prüfung:	30.04.2013

Das schönste Glück des denkenden Menschen ist, das Erforschliche erforscht zu haben und das Unerforschliche zu verehren.

Für meine Eltern

Table of Contents

1 Summary

FAT1 is a member of the atypical cadherin FAT subfamily. The first identified member of this family was *Drosophila* Fat which has been regarded as a tumor suppressor because of its implication in tissue growth. In vertebrates FAT subfamily consists of 4 members, FAT1, -2, -3 and FAT-J (or FAT4). Only FAT1 has so far been studied more intensively. FAT1 is expressed in a wide range of tissues and a homozygous knockout for FAT1 in mice was perinatal lethal. *In vitro* studies indicate that it is involved in cell polarity and migration. Cancer research revealed deregulated FAT1 expression. In some tumors as breast cancer FAT1 is over-expressed while FAT1 expression is reduced or deleted in others as astrocytic tumors or cholangiocarcinoma.

In the present work, we first analyzed the role of FAT1 in chronic liver disease. We found FAT1 upregulation in a murine model of non-alcoholic steatohepatitis (NASH) and could confirm this result in human tissue from NASH patients. Moreover, we detected induced FAT1 expression in further murine models of chronic liver injury. Thus, bile duct ligation (BDL) as well as hepatotoxic thioacetamide (TAA) administration induced hepatic upregulation of FAT1 expression. Furthermore, FAT1 expression was significantly heightened in cirrhotic human liver tissue. Activated hepatic stellate cells (HSC) were identified as the main cellular source of FAT1 in chronic liver disease. Suppression of FAT1 by siRNA inhibited NFκB activation and thereto proinflammatory gene expression, and reduced apoptosis resistance in activated HSC.

Next, we investigated FAT1 expression and function in hepatocellular carcinoma (HCC). FAT1 expression was significantly upregulated in HCC cell lines as well as in HCC tumor tissue compared to primary human hepatocytes (PHH) and non-tumorous liver tissue. In human HCC tissues strong FAT1 expression correlated with tumor stage and proliferation rate. Stable suppression of FAT1 by shRNA transfection reduced proliferation as well as migratory potential of HCC cells. Moreover, cells with suppressed FAT1 expression demonstrated higher susceptibility towards apoptosis, induced by serum starvation. To evaluate the role of FAT1 in HCC *in vivo* we injected stable FAT1 suppressed cells into nude mice. We observed delayed tumor onset and more apoptotic cells in tumors derived from FAT1 suppressed cell clones.

Finally, we searched for mechanisms responsible for FAT1 upregulation in HCC. We found that hepatocyte growth factor (HGF), a factor secreted by activated HSCs, induced FAT1 expression *in vitro*. FAT1 expression was further increased in HCC cells under hypoxia, and this induction was strongly repressed by inhibition of hypoxia inducible factor 1 alpha (HIF1α). Hypoxia caused significantly reduced levels of the methyl group donor S-adenosylmethionine (SAM), and SAM supplementation inhibited the hypoxia induced FAT1 expression in HCC cells. Conversely, demethylating agents induced FAT1 expression in HCC cells, and expression analysis in 24 human HCC tissues showed a significant correlation between FAT1 and MAT2A, which is known to critically affect SAM levels in HCC.

In conclusion, increased FAT1 expression in chronic liver disease and HCC functionally promotes the course of disease and thereto may be a new therapeutic target for the prevention and treatment of hepatic fibrosis in chronic liver disease and hepatocellular carcinoma.

1.1 Zusammenfassung

FAT1 ist ein Mitglied der atypischen Cadherin-Subfamilie FAT. Das erste identifizierte Mitglied dieser Familie war *Drosophila* Fat. Dieses wurde aufgrund seiner Funktion im Gewebewachstum als Tumorsuppressor angesehen. In Vertebraten besteht die FAT Subfamilie aus 4 Mitgliedern: FAT1, -2, -3 und FAT-J (FAT4), von denen nur FAT1 genauer erforscht wurde. FAT1 wird in vielen Geweben exprimiert. Ein homozygoter Knockout von FAT1 in Mäusen ist perinatal letal. *In vitro* Studien zeigten, dass FAT1 an der Zellpolarität und Migration beteiligt ist. In der Krebsforschung wurde eine deregulierte Expression von FAT1 gefunden. In einigen Tumoren, wie z.B. im Brustkrebs, ist FAT1 überexprimiert, wohingegen in anderen Tumoren, wie z.B. in astrozytären Tumoren oder im Cholangiokarzinom, eine verminderte FAT1 Expression vorliegt.

In dieser Arbeit analysierten wir zuerst die Rolle von FAT1 bei chronischen Lebererkrankungen. Eine Hochregulation von FAT1 konnte in einem murinen Modell der Nicht-Alkoholischen-Steatohepatitis (NASH) festgestellt werden. Diese Ergebnisse wurden in humanen Geweben von NASH Patienten bestätigt. Desweiteren fanden wir eine induzierte FAT1 Expression in murinen chronischen Leberschädigungsmodellen. Die Gallengangsligation (bile duct ligation, BDL) sowie die Gabe von hepatotoxischem Thioacetamid (TAA) führten zu einer erhöhten FAT1 Expression. Außerdem konnte eine signifikante Hochregulation der FAT1 Expression in humanen zirrhotischen Lebergeweben gefunden werden. Als Hauptquelle für FAT1 in chronischen Lebererkrankungen wurden aktivierte hepatische Sternzellen (HSC) identifiziert. Die Suppression von FAT1 in aktivierten HSC mittels siRNA inhibierte die NFκB Aktivierung und verminderte dadurch sowohl die Expression von proinflammatorischen Genen als auch die Apoptoseresistenz.

Weiterhin beschäftigt sich diese Arbeit mit der Expression und Funktion von FAT1 im hepatozellulären Karzinom (HCC). Die FAT1 Expression in HCC Zelllinien sowie in HCC Tumorgeweben war im Vergleich zu primären humanen Hepatozyten (PHH) und nicht-tumorigenen Lebergeweben signifikant hochreguliert. In humanen HCC Geweben korrelierte eine starke FAT1 Expression

mit dem Tumorstaging und der Proliferationsrate. Die stabile Suppression von FAT1 mittels shRNA Transfektion verminderte die Proliferation sowie die Migration von HCC Zellen. Außerdem zeigten HCC Zellen mit supprimierter FAT1 Expression eine erhöhte Suszeptibilität gegenüber der durch Serumentzug induzierten Apoptose. Um die Rolle von FAT1 im HCC *in vivo* zu untersuchen injizierten wir stabil FAT1-supprimierte HCC Zellen in Nacktmäuse. Wir konnten feststellen, dass Tumoren aus FAT1-supprimierten Zellklonen später auftreten und mehr apoptotische Zellen enthalten als Tumoren aus Kontrollzellen.

Schließlich sollten Mechanismen gefunden werden, die für die FAT1 Hochregulation im HCC verantwortlich sind. Es konnte gezeigt werden, dass der Hepatozyten Wachstumsfaktor (hepatocyte growth factor, HGF), der von aktivierten HSCs sekretiert wird, die FAT1 Expression *in vitro* induziert. Die FAT1 Expression in HCC Zellen konnte weiterhin durch Hypoxie verstärkt werden. Diese Induktion wurde durch Inhibition des Hypoxie induzierten Faktors 1 alpha (HIF1α) stark vermindert. Hypoxie führte zu signifikant verminderten Level des Methylgruppen-Donors S-Adenosylmethionin (SAM) und die Supplementation von SAM inhibierte die durch Hypoxie induzierte FAT1 Expression in HCC Zellen. Demethylierende Agenzien induzierten dagegen die FAT1 Expression in HCC Zellen. Durch Expressionsanalysen in 24 humanen HCC Geweben konnte eine signifikante Korrelation zwischen FAT1 und MAT2A gefunden werden. Von MAT2A ist bekannt, dass es die SAM Level entscheidend beeinflusst.

Zusammenfassend lässt sich feststellen, dass die erhöhte FAT1 Expression in chronischen Lebererkrankungen und im HCC das Fortschreiten der Erkrankung fördert. Daher könnte FAT1 ein neues therapeutisches Ziel für die Prävention und die Behandlung der hepatischen Fibrose sowie des HCC darstellen.

2 Introduction

2.1 Liver

2.1.1 Anatomy

The liver is the largest parenchymal organ and the largest gland in the human body and located in right upper quadrant in the abdominal cavity just below the diaphragm, shielded by the costal arch. Macroscopically, the liver can be subdivided into four different lobes (*Lobus hepatis dexter, Lobus hepatis sinister, Lobus quadratus, and Lobus caudatus*) and is surrounded by connective tissue, the so called Glisson's capsule, which is linked to the intrahepatic connective tissue.

The liver is supplied with two blood vessels: the *Arteria hepatica propria* brings arterial oxygenated blood, and the *Vena portae hepatis* transports venous, but nutrient-rich blood, drained from the gastrointestinal tract. Blood outflow is accomplished *via* the liver sinusoids by the *Vena hepatica* to the *Vena cava inferior*.

2.1.2 Histology and function

Microscopically, the liver can be further divided into hepatic lobules consisting mostly of hepatocytes and containing a vein in the center (*Vena centralis*). In the contact area of several lobules the periportal field includes *Arteria and Vena interlobularis*, as well as bile ducts (*Ductuli interlobulares*) also known as Glisson's triangle.

Hepatocytes represent the main cell type of the liver and are divided by liver sinusoids, built by fenestrated, discontinuous endothelium without basal membrane. Kupffer cells are specialized macrophages sitting in the walls of the sinusoids. A 10 to 15 µm wide perisinusoidal space, the space of Disse, is found between hepatocytes and sinusoids. It contains blood plasma and hepatic stellate cells (HSC, also called Ito cells). HSCs store lipids and vitamin A (Figure 2.1).

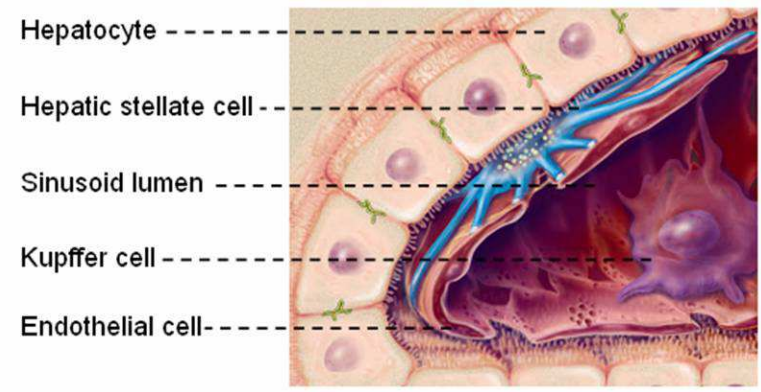

Figure 2.1 Graphical overview of the different liver cell types and their localization [modified from (Friedman and Arthur 2002)].

Being the central organ for metabolism and detoxification gives the liver specific tasks. It performs carbohydrate metabolism and thereby regulates blood glucose level in dependency on insulin and glucagon. Moreover, the liver takes part in lipid metabolism by the breakdown of lipids to free fatty acids and glycerol (lipolysis) and fatty acid as well as triglyceride synthesis (lipogenesis). Cholesterol is oxidized by the liver and can be discarded as bile acids. Further, the liver builds plasma proteins like albumin and coagulation factors and is involved in amino acid metabolism. During the degradation of amino acids ammonia is generated and will be used by the synthesis of urea. Additional functions of the liver are biotransformation of xenobiotica and for example heme and storage of iron.

2.2 Liver disease

Liver disease can be classified into acute and chronic liver disease. Acute liver injury can be induced by acute infections or intoxications. This rarely results in complete liver failure thanks to the regenerative response of the liver. Development of chronic liver disease upon ongoing hepatic injury is characterized by chronic hepatic inflammation which can contribute to liver fibrosis and ultimately cirrhosis.

2.2.1 Liver fibrosis

Liver fibrosis represents a wound healing process of the liver that leads to an excessive deposition of extracellular matrix (ECM) (Bataller and Brenner 2005; Friedman 2003). Major groups forming the properties of ECM are collagens, elastin, structural glycoproteins, and proteoglycans (Martinez-Hernandez and

Amenta 1995). Accumulation of ECM is either evolved from overproduction, deficient degradation or both. Current evidence indicates that HSC are central mediators of fibrogenesis (Friedman 2004; Friedman 2008).

Quiescent HSC are located in the space of Disse (see chapter 2.1) and constitute the main storage location for vitamin A. Upon hepatic injury, HSC transform to an activated myofibroblast-like phenotype (Pinzani 1995), which express α-smooth muscle actin (α-sma) and show enhanced proliferation, contractility, fibrogenesis, and proinflammatory signaling.

Fibrogenesis is characterized by deregulation of ECM remodeling with increased ECM deposition. Activated HSC secrete large amounts of collagen, predominantly the fibril-forming collagen I. Its expression is enhanced by activated gene transcription and on posttranscriptional level by increased mRNA stabilization (Stefanovic et al. 1997). Furthermore, the equilibrium between deposition and degradation of ECM is disordered. In healthy liver, matrix metalloproteinases (MMPs) are able to digest fibrotic scar tissue. MMPs are blocked by tissue inhibitors of matrix metalloproteinases (TIMPs), and upon activation HSCs show changes in the expression pattern of these enzymes. It has been shown that TIMP-1 expression is enhanced in response to liver injury, which prevents degradation of ECM (Benyon et al. 1996).

Moreover, activated HSCs are characterized by high resistance to apoptosis. They survive prolonged serum deprivation as well as established pro-apoptotic stimuli like e.g. Fas ligand (Novo et al. 2006).

One key transcription factor in the activation of hepatic stellate cells is NFκB. This signaling pathway is mediating apoptosis resistance (Oakley et al. 2005; Watson et al. 2008). But also, NFκB induces proinflammatory gene expression such as MCP1 and RANTES (Elsharkawy and Mann 2007; Hellerbrand et al. 1998; Schwabe et al. 2003).

2.2.2 Liver cirrhosis

The most advanced stage of fibrosis is cirrhosis. It is characterized by loss of liver function upon change of liver architecture. Nodules of regenerating hepatocytes and fibrotic septa are formed and replace normal parenchyma, which leads to hepatocellular dysfunction and obstruction of hepatic blood flow. The consequences are development of portal hypertension and hepatic insufficiency (Iredale 2003). Further complications are ascites, gastroesophageal varices,

bleeding resulting from decreased production of coagulation factors, hepatic encephalopathy and many more (Schuppan and Afdhal 2008). Moreover, presence of liver cirrhosis is the main risk factor for the development of HCC (Farazi and DePinho 2006).

2.3 Causes for chronic liver disease

2.3.1 Alcohol

Chronic alcohol abuse is a major cause of chronic liver disease in Western countries. Alcohol consumption of over 20 g/day for women and 40 g/day for men, respectively, can cause alcoholic liver disease (Gramenzi et al. 2006). Fatty liver develops in more than 90% heavy drinkers, about 30% develop more severe forms, such as fibrosis and cirrhosis, and approximately 1-2% of alcoholic cirrhotics develop HCC each year (Gao and Bataller 2011; Seitz and Stickel 2007). Important mechanisms contributing to the pathogenesis of alcoholic liver disease are alcohol induced hepatotoxicity due to formation of acetaldehyde/acetate and oxidative stress in consequence of formation of reactive oxygen species (ROS). Further, production of cytokines results in immune response and infiltration of immune cells. In this stage, disease has progressed to steatohepatitis. Upon both, ROS and cytokine release, HSCs become activated and development of fibrosis initiates (De Minicis and Brenner 2008).

2.3.2 Drug induced liver injury

Since one function of liver is metabolizing xenobiotics (see chapter 2.1.2), it is obvious that drug-induced liver disease is a frequent complication of pharmaceuticals. Acute liver failure (ALF) is the worst consequence leading to death or requiring liver transplantation. More than half of all cases of ALF in the U.S. are caused by drugs, and the majority (39%) is provoked by acetaminophen (paracetamol). However, more than 10% of ALF are called idiosyncratic, which means that hepatotoxicity occurs only infrequently in between 1 in every 1,000 patients to 1 in every 100,000 patients (Ostapowicz et al. 2002).

Pathology of drug-induced liver disease covers a broad spectrum, from acute hepatic necrosis, chronic hepatitis, cholestasis to neoplasms and depends on different mechanisms of hepatotoxicity, e.g. cell death resulting from direct binding

of the drug to cell proteins, disorganization of the cytoskeleton, and blockage of the mitochondrial function (Navarro and Senior 2006).

2.3.3 Autoimmune-related and genetic disorders

Liver disease can also be effected by autoimmune disorders. Autoimmune hepatitis (AIH) is a generally progressive, chronic hepatitis with fluctuating course (Krawitt 2006). Further, primary biliary cirrhosis (PBC) and primary sclerosing cholangitis (PSC) are cholestatic liver disease based on autoimmune related mechanisms (Boonstra et al. 2012). Moreover, genetic defects may affect liver. Patients with Gilbert's disease show reduced activity of UDP-glucuronosyltransferase (UGT1A), and therefore, they have increased bilirubin serum levels and jaundice. Accumulation of copper in liver and brain is characteristic for Wilson's disease, an autosomal recessive genetic disorder caused by mutations in the *ATP7B* gene (Ala et al. 2007). Similarly, in hemochromatosis the liver is harmed by iron overload. There are different forms of hereditary hemochromatosis with mutations in four diverse genes involved in iron metabolism (*HFE, HJV, HAMP, TfR2*) (Pietrangelo 2004). Further genetic disorders involving the liver are α1-antitrypsin deficiency, glycogen storage disease, and cystic fibrosis.

2.3.4 Viral hepatitis

Viral hepatitis is the consequence of infection with hepatitis virus A-E. Most relevant forms are presented below.

2.3.4.1 Hepatitis A

Hepatitis A is caused by the hepatitis A virus (HAV), a non-enveloped RNA virus and member of the *Picornaviridae* family. The predominant way of spreading is enteric transmission (faecal-oral) *via* person-to-person, or by consumption of contaminated water or food (e.g. bivalve molluscs). Areas of high endemicity are Asia, Africa, and Central and South America (Koff 1998).

Incubation period is 15-50 days and symptoms of acute infection may be fatigue, nausea, vomiting, and fever. Later on, there may be patients with cholestatic symptoms like jaundice and dark colored urine. Symptoms usually last less than two months and infection never takes chronic course. However, less than 1% of all

hepatitis A patients show a severe course of the disease with acute liver failure. Prevention of HAV infection is possible because HAV vaccines are available.

2.3.4.2 Hepatitis B

Hepatitis B virus (HBV) is an enveloped DNA virus and belongs to the *Hepadnaviridae* virus family. The genome is replicated by utilization of a reverse transcriptase. Hepatitis B infection is one of the most common infectious diseases in the world, and virus transmissions occur percutaneously, sexually, and perinatally. High endemic regions are China, South East Asia, and sub-Saharan Africa. Because of its envelope HBV is quite stable and it shows high resistance to disinfectants, but a safe vaccination with active immunization exists (Lavanchy 2004).

Around one-third of infections proceed asymptomatically, the other patients have symptoms after an incubation time of 45 to 120 days. Symptoms are similar to HAV infection and typical for acute virus hepatitis. 0.5-1% of all HBV infections take severe course with fulminant hepatic failure. More than 90% of infections are self-limiting and patients have acquired lifelong immunity against HBV. In up to 10% of patients virus infection persists and they suffer a chronic infection, which is a risk factor for developing cirrhosis and HCC (Dandri and Locarnini 2012).

2.3.4.3 Hepatitis C

The hepatitis C virus (HCV) is a member of the *Flaviviridae* family, comprising enveloped RNA virus. Transmission is possible by direct blood contact and perinatal from mother to child, in fewer cases also by sexual contact. High rates of chronic infection are found in Egypt, Pakistan and China. No protecting vaccine exists to date. Therefore, prevention of exposition is critical.

75% of all infected persons have no or no specific symptoms, and thereto virus infection is often not diagnosed. Only 25% of HCV infections cause mild hepatitis symptoms. Persistence of HCV infections occurs in the majority of HCV-infected individuals, leads to chronic liver damage and may cause fibrosis, cirrhosis and HCC (Bartosch et al. 2009).

2.3.4.4 Hepatitis D

Hepatitis D occurs only in individuals positive for the HBV surface antigen, seen as hepatitis delta virus (HDV) is a satellite virus, which is defective and requires a

coinfection with HBV for its replication. Hence, immunization against HBV also protects from a HDV infection. Acute HBV and HDV coinfection is more severe than HBV infection alone, and chronic HDV infection takes a more progressive course than HBV monoinfection (Wedemeyer and Manns 2010)

2.3.4.5 Hepatitis E

Hepatitis E is provoked by infection with hepatitis E virus (HEV), which forms the *Hepeviridae* family. HEV is a non-enveloped RNA virus and is shown to be transmitted *via* the oral-faecal route or by contaminated water. Clinically, HEV infection is comparable to hepatitis A, but develops to acute, severe liver disease in some cases, especially in pregnant women. Chronic HEV infection is described in organ transplanted patients (Wedemeyer et al. 2012).

2.3.5 Non-alcoholic fatty liver disease (NAFLD)

2.3.5.1 Definition and prevalence of NAFLD

It has been known for a long time that fatty livers of obese people can develop inflammation and fibrosis, but the term “non-alcoholic steatohepatitis (NASH)” has been introduced by Ludwig et al. (Ludwig et al. 1980). It describes hepatic steatosis and liver inflammation in patients without (significant) alcohol consumption. Meanwhile, the term “non-alcoholic fatty liver disease (NAFLD)” also includes fatty liver without hepatitis.

NAFLD can take a progressive course starting from hepatic steatosis, which is characterized by deposition of triglycerides as lipid droplets in hepatocytes, following the development of NASH with ballooning of hepatocytes and cell death.

Prevalence of NAFLD is estimated to be 20-30% in Western countries (Bedogni et al. 2005; Browning et al. 2004). The percentage of NAFLD patients is higher in obese people (57.5-74%) (Angulo 2002). In children prevalence of NAFLD is also increased in presence of obesity (Schwimmer et al. 2006). Moreover, advancing age is a risk factor for developing NAFLD (Frith et al. 2009).

Strong associations between NAFLD and obesity, insulin resistance, hypertension, as well as dyslipidaemia have been found and are the origin for considering NAFLD as the liver manifestation of the metabolic syndrome (de Alwis and Day 2008).

2.3.5.2 Etiology and pathogenesis

Day and James described a two-hit-model for the pathogenesis of NAFLD (Day and James 1998). The ‘first hit’ arises from an imbalance between lipid acquisition and removal and leads to hepatic fibrosis. Subsequently, a ‘second hit’ induces inflammation. This includes oxidative stress due to increased lipid oxidation and deregulated cytokine production and results in steatohepatitis. But since NASH doesn’t show progression to fibrosis and cirrhosis in every patient, a ‘third hit’ appear to be necessary.

2.3.5.3 Prognosis and therapy

Prognosis of simple steatosis is good, but 20-30% of patients with NASH develop hepatic fibrosis and 10-30% evolve cirrhosis within 10 years (Argo et al. 2009; Argo and Caldwell 2009). This NASH induced cirrhosis is further a risk factor for HCC.

Exercise, weight loss (diet-induced or by bariatric surgery) and treatment of the metabolic syndrome are recommended therapies since no established pharmacological treatment of NAFLD exists.

2.4 Liver cancer

The liver can be affected by metastatic cancer especially by spreading tumors of the gastrointestinal tract, breast, lung, pancreas and by malignant melanoma. Primary liver cancer is arising from liver cells and can be classified into different groups. Hepatocellular carcinoma (see chapter 2.4.1) and cholangiocarcinoma, a malignant tumor developing from the biliary tract represent 10%-25% of primary hepatic malignancies (Tyson and El-Serag 2011). Quite rare is the embryonal hepatoblastoma. Besides, there exist the mesenchymal angiosarcoma of the liver, a neoplasm of endothelial blood vessel cells forming 2 % of all primary liver tumors (Maluf et al. 2005).

2.4.1 Hepatocellular carcinoma

2.4.1.1 Prevalence and incidence

Hepatocellular carcinoma (HCC) is the sixth most common cancer worldwide with around 700,000 newly diagnosed cases per year and the most frequent form of primary liver cancer with about 85%-90% (El-Serag and Rudolph 2007; Forner et

al. 2012). Because of its high lethality it is the third most common cause of death from cancer worldwide. The disease is more frequent in men than in women, and highest occurrence rates are reported for Eastern and Southeastern Asia (Ferlay et al. 2010). But the incidence of HCC is increasing in developed countries. Reasons may be rising rates of HCV infections (see chapter 2.3.4) and non-alcoholic steatohepatitis (NASH, see chapter 2.3.5) as a consequence of diabetes and obesity (Venook et al. 2010).

2.4.1.2 Etiology

Hepatocarcinogenesis is a multi-step process based on cycles of inflammation, necrosis, oxidative stress and regeneration leading to genomic instability and epigenetic changes (Farazi and DePinho 2006). HCC mostly arises from an established background of chronic liver disease and cirrhosis (80%-90%), and the 5-year cumulative risk for developing HCC in patients with cirrhosis ranges from between 5% and 30% (El-Serag 2011). Cirrhosis is mostly caused by chronic HBV or HCV infection, chronic alcohol abuse or NASH. Less common causes include hereditary hemochromatosis, Wilson's disease, and α-1 antitrypsin deficiency (see chapter 2.3).

Another risk factor for HCC in tropical regions is intoxication with aflatoxin produced by the fungus *Aspergillus fumigatus via* contamination of food grains (El-Serag and Rudolph 2007).

2.4.1.3 Therapy and prognosis

Despite new strategies for the therapy, HCC remains a disease with poor prognosis attributed to frequently late diagnosis and aggressive tumor growth. A meta-analysis revealed a one year survival rate of 17.5% for untreated HCC patients (Cabibbo et al. 2010).

Resection of the tumor is the first choice of treatment for patients without cirrhosis because of their limited liver function. However, risk for recurrence of HCC is quite high with about 70% of the patients with tumor remission within 5 years (Forner et al. 2012). Another surgical option is liver transplantation, which seems to be optimal curing tumor and cirrhosis simultaneously. However, drawbacks are organ shortage and lifelong immunosuppression. And also in this case the risk of tumor recurrence is approximately 20%. (Zimmerman et al. 2008).

Different forms of ablation are possibilities to treat HCC, even while awaiting transplantation or to make the tumor resectable. Ablation destroys tumor tissue by modifying the temperature of neoplastic cells (e.g. radiofrequency ablation, RFA) or by using chemical substances (e.g. percutaneous ethanol injection, PEI) (Gervais and Arellano 2011).

Transarterial chemoembolization (TACE) is another therapy for unresectable HCC. Ischemic tumor necrosis is induced by occlusion of hepatic arteries with embolizing agents (gelantine, microspheres) together with chemotherapeutic drugs (Llovet and Bruix 2008). Another form of this principle is radioembolization (also called selective internal radiation therapy, SIRT). Here, microspheres coated with yttrium 90 (^{90}Y), a β-emitting isotope, are injected intraarterially. Thereby, embolization as well as radiation of malignant tissue can be achieved (Sangro et al. 2012).

Knowledge of molecular events taking place during tumor progression made it possible to develop therapies against new targets. For patients with advanced stage HCC systemic therapy with the multikinase inhibitor sorafenib is considered. It blocks Raf signalling and receptors for VEGF, PDGF, as well as c-Kit and thereby shows antiangiogenic and antiproliferative effects. It has been shown to prolong median overall survival and median time to radiologic progression, as compared with placebo (Llovet et al. 2008).

2.4.1.4 Tumor microenvironment

The tumor surrounding microenvironment largely consists of hepatic stellate cells, fibroblasts, immune cells, and endothelial cells. Cells within the tumor microenvironment influence tumor growth by multiple mechanisms. HCC is a highly vascularized tumor, and endothelial cells are essential for blood vessel formation. Activation, proliferation and migration of endothelial cells promote angiogenesis (Semela and Dufour 2004). Tumor infiltrating immune cells like lymphocytes and Kupffer cells secrete cytokines, growth factors and chemokines which increase cancer cell motility. Hepatic stellate cells can be detected around tumor sinusoids, fibrous septa and the capsule (Dubuisson et al. 2001; Faouzi et al. 1999; Le Bail B. et al. 1999). Activation of HSCs is not only the key event of hepatic fibrosis and progression to cirrhosis as a high risk factor for developing HCC (see chapter 2.2). Beyond that HSCs promote tumorigenesis by their ability to remodel the extracellular matrix. Moreover, they release different factors by

which HCC cells become directly affected and through the activation of signalling pathways triggered by HSCs migratory and proliferative capability of HCC cells are enhanced (Amann et al. 2009a).

2.5 Cadherins

Cell adhesion molecules (CAM) are required to direct cells to stay at one specific site, to form cell-cell and cell-matrix junctions, or to disrupt these associations and promote directional migration. CAM can be classified into four major protein families: the integrin family, the selectin family, the immunoglobulin superfamily, and the cadherin family.

Cadherins are characterized by conserved repeating motifs in their extracellular domains. The quantity of these cadherin repeats is variable. Moreover, the motif, which is structurally related to immunoglobulin (Ig) domains, mediates the calcium dependence by Ca^{2+} binding domains. Most cadherins are single-pass transmembrane glycoproteins (Angst et al. 2001).

The cadherin superfamily can be divided into two groups, classical and nonclassical cadherins. Classical cadherin family was identified first and is important for the formation of adherens junctions between cells. Cadherins usually link cells by homophilic mechanism. Here, the extracellular tails of molecules of the same kind bind to each other. The cytoplasmic tail of classical cadherins mainly interacts with the actin cytoskeleton *via* β-catenin. Best studied protein members of the classical cadherin family are E-cadherin and N-cadherin. They play a role in mesenchymal-epithelial-transition (MET) during development and also in epithelial-mesenchymal-transition (EMT) during cancer metastasis (Peinado et al. 2004).

A subfamily of the nonclassical cadherins is called desmosomal cadherin family, because of its role in the arrangement of desmosomes, like desmocollin or desmoglein. These cadherins interact with intermediate filaments *via* plakoglobin (Gumbiner 2005).

Furthermore, the nonclassical cadherin group contains some cadherins which cannot be assigned to a specific family, called atypical cadherins, like Fat, Dachsous, and Flamingo.

2.6 FAT family

The cadherin subfamily FAT is characterized by large extracellular domains containing 34 cadherin motifs, a variable number of epidermal growth factor (EGF)-like repeats, one or two laminin A/G domains, and a single transmembrane domain (Tanoue and Takeichi 2005).

Drosophila fat was the first identified gene of this protein family (Mahoney et al. 1991). Mutations at this gene locus caused hyperplastic overgrowth of all larval imaginal discs, which led to the suggestion that Fat regulates tissue growth and operates as a tumor suppressor protein (Bryant et al. 1988). Several studies revealed Fat as a member of the Hippo signaling pathway controlling cell proliferation and survival (Bennett and Harvey 2006). Recent studies discovered a role of Fat in the regulation of planar cell polarity (PCP). PCP signaling regulates the establishment of polarity within the plane of an epithelium and involves Fat and Dachsous (Sopko and McNeill 2009).

Another Fat subfamily cadherin, Fat-like, was identified in *Drosophila*. It is involved in morphogenesis and maintenance of tubular structures of ectodermal origin and has no influence on growth or PCP (Castillejo-Lopez et al. 2004).

In vertebrates Fat subfamily consists of 4 members, FAT1, -2, -3 and FAT-J (or FAT-4). Analysis for similarities has shown that FAT-J could be the ortholog of *Drosophila* Fat. FAT1 and FAT3 revealed highest resemblance and can form a subgroup together with FAT2 and *Drosophila* Fat-like (Tanoue and Takeichi 2005). Information about function of vertebrate FAT proteins is limited, only FAT1 has so far been studied more intensively.

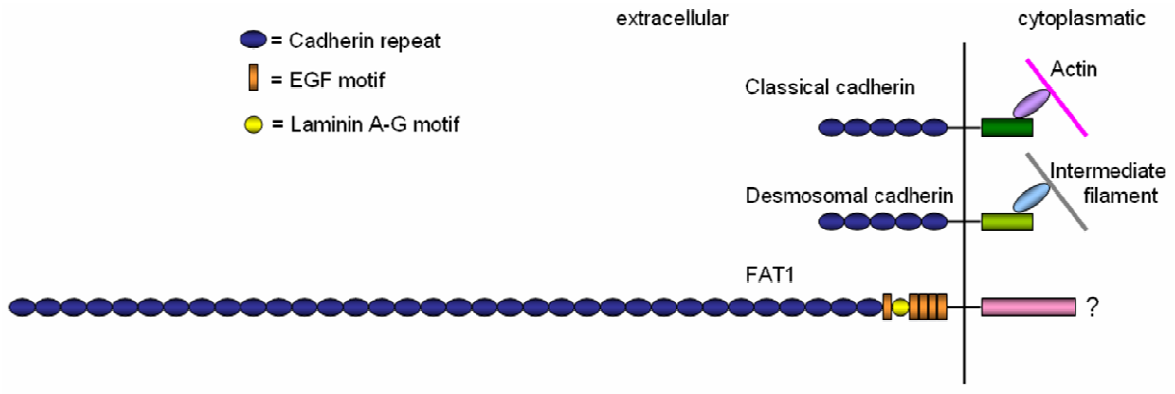

Figure 2.2 Schematic representation of the cadherin superfamily [modified from (Tanoue and Takeichi 2005)].

2.6.1 FAT1

Dunne et al. identified human FAT1 as the first Fat-like protein in vertebrates. FAT1 was shown to be expressed in a wide range of tissues (e.g. kidney, lung, eye, and pancreas) with higher expression in fetal opposed to adult tissue. *In situ* hybridization revealed localization of the gene encoding *FAT1* on chromosome 4q34-q35 (Dunne et al. 1995). Thereafter, FAT1 has been described in rat, mouse, and zebrafish (Cox et al. 2000; Down et al. 2005; Ponassi et al. 1999). Further studies investigated FAT1 expression in the kidney, where it is located at cell-cell contacts and where it forms an element of glomerular slit diaphragms (Inoue et al. 2001). Moreover, FAT1 is found to be expressed in the Langerhans islets of the pancreas (Rinta-Valkama et al. 2007).

2.6.1.1 Function, interaction and modification

As a first step to get an insight in the function of FAT1 its gene expression has been silenced, but the homozygous knockout of *FAT1* locus in mice was perinatal lethal with defects in kidney and brain (Ciani et al. 2003). Further findings concerned cellbiological function of FAT1. FAT1 is localized to cell-cell contacts as well as lamellipodia and filopodial tips, where it organizes actin filaments and promotes migration. Interaction of FAT1 with Enabled/vasodilator-stimulated phosphoproteins (Ena/VASP) is shown to be essential for regulation of actin dynamics and cell polarization (Moeller et al. 2004; Tanoue and Takeichi 2004). Ena/VASP proteins are actin-binding proteins involved in promotion and inhibition of actin-dependent processes and are thereby implicated in polarization and migration, too (Krause et al. 2003). The interaction of FAT1 with Ena/VASP proteins is mediated by Ena/VASP homology I (EVHI) domains, for which functional binding sites have been found in FAT1 (Tanoue and Takeichi 2004).

These binding sites have also been described to bind Homer proteins (Schreiner et al. 2006). Homer proteins are scaffolding proteins found in many tissues, but are best characterized in neurons. They are implicated in many signalling pathways by binding different key proteins like metabotropic glutamate receptors, inositol trisphosphate dependent Ca^{2+} channels, small GTPases and others (Shiraishi-Yamaguchi and Furuichi 2007).

In vascular smooth muscle cells (VSMC) FAT1 expression is upregulated in response to arterial injury, and knockdown of FAT1 limited migration but improved

proliferation (Hou et al. 2006). Further, FAT1 has been shown to interact with Atrophins. Atrophin proteins are conserved transcriptional repressors and their family includes two different members in vertebrates: Atrophin 1 (synonym DRPLA) and Atrophin2 (synonym RERE) (Wang and Tsai 2008). Like FAT1, Atrophin1 and 2 are upregulated upon injury in VSMC, but their downregulation has no effect on proliferation. In contrast, suppression of Atrophin 2 led to enhanced VSMC migration, for which FAT1 expression was essential (Hou and Sibinga 2009).

Another interaction partner of FAT1 is β-catenin. Binding is accomplished by the acidic and prolin-rich FC domains in the FAT1 intracellular part ($FAT1_{IC}$). Besides, expression of FAT1 affects cellular distribution and transcriptional activity of β-catenin. Moreover, FAT1 can be spliced and the cytoplasmic domain is able to translocate into the nucleus due to a putative nuclear localization sequence (NLS) (Hou et al. 2006; Magg et al. 2005; Nishikawa et al. 2011).

FAT1 can be modified posttranscriptionally by alternative splicing in the cytoplasmic domain. Thereby, two additional variants can be generated: FAT1(+12) (additional 12 aa in frame), FAT1(+32) (additional 32 aa in frame), and FAT1 (+8TR) (termination after 8aa). FAT1(+32) and FAT1 (+8TR) are specifically expressed within the central nervous system (CNS). In the rat kidney epithelial cell line NRK-52E, splicing is regulated upon cell density. Quiescent cells express predominantly the FAT1(+12) isoform, whereas in proliferating or migrating cells, respectively, a preponderance of wildtype FAT1 can be determinated, and this isoform is even sufficient for migration (Braun et al. 2007).

Proteolytical cleavage is another mechanism of FAT1 modification. In HaCaT cells, an immortalized human keratinocyte cell line, FAT1 is processed into two products (p430 and p85), before achieving cell surface expression as a heterodimer. The cleavage is dependent on the proprotein convertase furin, and leads to almost complete loss of the full length p500. In melanoma cells an additional product, p65, has been identified, which has lost the ability to associate with the extracellular domain and can be found in the cytoplasm (Sadeqzadeh et al. 2011).

2.6.1.2 FAT1 in cancer

In cancer research contradictory results have been found regarding FAT1 expression. Frequent loss of heterozygosity (LOH) of FAT1 has been described in

oral squamous cell carcinomas (OSCC) and astrocytic tumors (Chosdol et al. 2009; Nakaya et al. 2007). LOH describes the deficiency of one allel of a gene in which the other allel was already inactivated and is mostly concerning tumorsuppressors. In cholangiocarcinoma immunohistochemical staining of FAT1 demonstrated reduced expression at the normal membranous location (Settakorn et al. 2005). However, a study about breast cancer revealed FAT1 overexpression and its diffuse expression in both, *carcinoma in situ* and invasive carcinoma (Kwaepila et al. 2006). Further, FAT1 is expressed in leukemia cell lines, whereas in normal peripheral blood cells and in the bone marrow no expression of FAT1 was detectible. High FAT1 expression in precursor B-cell (preB) acute lymphoblastic leukemia (ALL) was prognostic for shorter relapse-free and overall survival (de Bock et al. 2012).

2.7 Hypoxia and hypoxia inducible factor (HIF)-1

Oxygen is essential for most aerobic organisms. In vertebrates, O_2 is necessary as final electron acceptor during cellular respiration. In the process of oxidative phosphorylation ATP is generated and O_2 is reduced to water. Oxygen deficiency is called hypoxia and plays an important role in many pathological conditions. Hypoxia leads to activation of different adaption processes in the cell.

2.7.1 The transcription factor HIF-1

HIF-1 has been discovered as a main mediator of hypoxic adaption. Under hypoxic conditions, HIF-1 transcriptionally regulates expression of many target genes, and thereby promotes activation of required mechanisms on cellular, local, and systemic level (Wenger 2002). Identification of HIF-1 has been made together with a specific regulatory element (enhancer) of the human *erythropoieti*n gene (*epo*) (Semenza and Wang 1992). EPO mediates production of erythrocytes and herewith, improves oxygen supply. Later on, it has been clarified that HIF-1 is a heterodimer composed of a 120 kDa HIF-1α and a 91 kDa HIF-1β subunit (Wang and Semenza 1995). HIF-1β, also known as aryl hydrocarbon receptor nuclear translocator (ARNT), is constitutively expressed and located in the nucleus, whereas HIF-1α is immediately degraded under normoxia. Upon hypoxic conditions HIF-1α is stabilized. Thus it accumulates and translocates to the nucleus, where it forms the dimer with HIF-1β.

Meanwhile, two HIF-1α homologes have been identified: HIF2α and HIF3α.

HIF2α (EPAS) shows high sequence similarity with HIF1α, but its expression is more constricted. Since HIF1α is quite ubiquitinously expressed, HIF2α can only be found in certain tissues (Park et al. 2003). This aspect and the fact that HIF1α knockout embryos are non-viable (Iyer et al. 1998; Kotch et al. 1999; Ryan et al. 1998) let infer that HIF1α is essential and cannot be replaced by its homologue.
HIF3α (IPAS) lacks a transactivation domain, binds to HIFα subunits and has an antagonistic effect, which may represent a feedback regulation because HIF3α expression is upregulated by HIF1α in hypoxic conditions (Gu et al. 1998; Makino et al. 2001; Makino et al. 2007).

HIF1α and HIF1β are members of the bHLH (basic helix-loop-helix)/PAS protein family. The bHLH domain mediates dimerization of both subunits, whereas the PAS domain, named after the first three proteins (PER, ARNT, SIM) in which this structure has been found, is important for binding to a consensus HIF DNA binding site (HBS) (5'-ACGTG-3') in the so called hypoxia responsive element (HRE) (Jiang et al. 1996; Wang et al. 1995). Furthermore, transactivation domains (TAD) exist in both subunits to facilitate interaction with cofactors (CBP, p300) (Jiang et al. 1997). The oxygen dependency is established by two ODD (oxygen dependent degradation domain) in HIF1α protein (Ivan et al. 2001; Jaakkola et al. 2001).

2.7.2 Regulation of HIF1α

Degradation of HIF1α under normoxic conditions starts with hydroxylation of two proline residues in the ODD. This reaction is mediated by prolyl hydroxylases (PHD) and is oxygen-, iron-, 2-oxoglutarate-, and ascorbate-dependent (Kivirikko and Myllyharju 1998).
Thereafter, pVHL (von Hippel-Lindau tumor suppressor) recognizes hydroxyproline, and hence, binds to HIF1α. pVHL is a component of the E3 ubiquitin ligase complex. It ubiquitylates and thereby designates the protein for proteasomal degradation (Tanimoto et al. 2000). Furthermore, the factor inhibiting HIF-1 (FIH-1) hydroxylates asparagyl residues in the TAA domain of HIF1α. Thus, cofactors like CBP or p300 are no longer capable to bind to HIF1α (Schofield and Ratcliffe 2005).
Hypoxic conditions prevent both hydroxylations, mediated by PHD as well as by FIH-1. Therefore, no degradation of HIF-1α takes place; it can translocate into the nucleus and in form of the dimer with HIF-1β promotes gene expression.

2.8 Aim of the thesis

Based on the fact that to date no data regarding FAT1 in the liver exists, neither healthy nor pathologically changed, the aim of this thesis was to analyze expression and function in chronic liver disease and in hepatocellular carcinoma. Another focus of the analysis was regulation of FAT1 expression in HCC and the influence of hypoxia which was shown to be important in HCC.

3 Materials and Methods

3.1 Chemicals and Reagents

Agarose SeaKem ® LE	Biozym, Hess/Oldendorf, Germany
Agar	Difco Laboratories, Augsburg
Ampicillin	Sigma-Aldrich, Deisenhofen, Germany
β-Mercaptoethanol	Sigma-Aldrich, Deisenhofen, Germany
Ciprofloxacin	Fresenius Kabi, Bad Homburg, Germany
Collagenase type IV	Sigma-Aldrich, Hamburg, Germany
Fluconazol	B. Braun, Melsungen, Germany
DMEM medium	PAA Laboratories, Cölbe, Germany
DMSO	Sigma-Aldrich, Deisenhofen, Germany
FCS (fetal calf serum)	PAN-Biotech, Aidenbach, Germany
Milk powder	Carl Roth, Karlsruhe, Germany
Geneticin	Invitrogen, Karlsruhe, Germany
Penicillin	Invitrogen, Karlsruhe, Germany
Streptomycin	Invitrogen, Karlsruhe, Germany
Trypsin/EDTA	PAA Laboratories, Cölbe, Germany
Cycloheximid	Sigma-Aldrich, Deisenhofen, Germany
5-Azacytidine (Aza)	Sigma-Aldrich, Deisenhofen, Germany
Adenosine periodate oxidized (Adox)	Sigma-Aldrich, Deisenhofen, Germany
2,2-dipyridyl (DP)	Sigma-Aldrich, Deisenhofen, Germany
Thioacetamide (TAA)	Sigma-Aldrich, Deisenhofen, Germany
Staurosporine (STS)	Alexis Biochemicals, Lausen, Switzerland

3.2 Laboratory expendables

CryoTube vials	Nunc, Roskilde, Denmark
Pipet tips (10, 20, 100 und 1000 µl)	Eppendorf, Hamburg, Germany
Falcon tubes (50 ml)	Corning, New York, USA
Glassware (various)	Schott, Mainz, Germany
Multiwell plates	Corning, New York, USA

Pipettes (stripettes ®) (5, 10, 25, 50 ml)	Corning, New York, USA
Reaction vessels (1.5 and 2 ml)	Eppendorf, Hamburg, Germany
Strip tubes (0.2 ml)	Peqlab, Erlangen , Germany
Cell culture flasks T25, T75, T175	Corning, New York, USA

3.3 Laboratory instruments

Heating block:	
Thermomixer comfort	Eppendorf, Hamburg, Germany
PCR-cycler:	
GeneAmp® PCR System 9700	Applied Biosystems, Foster City, USA
LightCycler® Real-Time PCR System	Roche Diagnostics, Mannheim, Germany
Pipettes:	
Eppendorf Research (1000 µl, 200 µl, 100 µl, 20 µl, 10 µl, 2 µl)	Eppendorf, Hamburg, Germany
Pipette controllers:	
Accu-jet®	Brand, Wertheim, Germany
Shaking devices:	
KS 260 Basic Orbital Shaker	IKA® Werke, Staufen, Germany
Power Supplies:	
Consort E145	Peqlab, Erlangen, Germany
Power Supply-EPS 301	Amersham Biosciences, Munich, Germany
Spectrophotometer:	
EMax® Microplate Reader	MWG Biotech, Ebersberg, Germany
SPECTRAFluor Plus	Tecan, Männedorf, Switzerland
Scale:	
MC1 Laboratory LC 620 D	Sartorius, Göttingen, Germany

Water bath:	
Haake W13/C10	Thermo Fisher Scientific, Karlsruhe, Germany
XCELLigence system:	
Real-Time Cell Analyser (RTCA)	Roche Diagnostics, Mannheim, Germany
Centrifuges:	
Biofuge fresco	Heraeus, Hanau, Germany
Megafuge 1.0 R	Heraeus, Hanau, Germany
Microscope:	
Olympus CKX41 with ALTRA20 soft imaging system	Olympus Hamburg, Germany

3.4 Buffers

PBS buffer	140 mM	NaCl	
	10 mM	KCl	
	6.4 mM	Na_2HPO_4	
	2 mM	KH_2PO_4	pH 7.4
TE buffer	10 mM	Tris/HCl	
	1 mM	EDTA	pH 8.0

3.5 Plasmids

pBS/U6 ploxPneo	by courtesy of Prof Dr. C. Deng, NIH, Bethesda, USA
pcDNA3.1	Invitrogen, Karlsruhe, Germany
pCMX	Addgene, Cambridge, USA
pIC-Cre	by courtesy of Prof Dr. T. Hehlgans, University Regensburg, Germany
pRL-TK	Promega, Mannheim, Germany
NFκB luc	Promega, Mannheim, Germany

dnHIF1α	by courtesy of Dr. C. Warnecke, Erlangen, Germany

3.6 Working with bacteria

3.6.1 Bacterial strains

Top10	Invitrogen, Karlsruhe, Germany
294-Cre: Cre-recombinase expressing Escherichia coli	Gene Bridges, Heidelberg, Germany

3.6.2 Liquid media and agar plates

LB medium	10 g/l	peptone
	5 g/l	yeast extract
	10 g/l	NaCl
	Suspended in H_2O and autoclaved	
For plates	+ 15 g/L	Agar
For selection	+ 100 µg/ml	Ampicillin

3.6.3 Bacterial culture

E. coli strains were cultivated on solid LB-agar as well as in liquid medium. Ampicillin was added to LB medium for selection of insert-containing clones after transformation. Bacteria were spread out on agar plates using a Drigalski spatula and incubated overnight at 37°C. Liquid cultures were inoculated by a single bacterial colony with a sterile pipette tip and grown overnight at 37°C on a shaking device (250 rpm).

3.6.4 Preparation of competent cells

Calcium chloride treatment of E.coli facilitates uptake of free plasmid DNA. Bacterial culture was incubated in LB medium at 37°C to an optical density (OD_{650}) of 0.2-0.5.

After incubation for 5 min on ice cells were centrifuged (1500 g, 10 min, 4°C), resuspended in chilled calcium chloride solution (50 mM), centrifuged and

resuspended again in chilled calcium chloride (50 mM). The suspension containing 15% glycerol was aliquoted and shock frozen in liquid nitrogen for long-term storage.

3.6.5 Transformation

Chemically competent E.coli (50 µl) were thawed on ice and 100 ng plasmid DNA were added. After 30 min incubation on ice cells were heat shocked at 42°C for 45 s and immediately cooled on ice. Thereafter, 250 µl pre-warmed SOC medium was added and the cell suspension was incubated for 1 h at 37°C with shaking. Then 50-150 µl of the transformation mix were plated and incubated over night at 37°C on LB-agar containing the antibiotic necessary for selection of transformed cells.

3.6.6 Isolation of plasmid DNA (mini and midi preparation)

For mini preparation of plasmid DNA a single E.coli colony was picked and cultured with 3 ml LB-selection medium at 37°C over night (250 rpm).
To obtain greater amounts of plasmid DNA 50 µl of this preculture was added to 50 ml LB-selection medium and incubated again at 37°C over night (250 rpm). Then plasmids were isolated using HiSpeed^{TM} Plasmid Midi Kit (Qiagen, Hilden, Germany) following the supplier's instruction. Plasmid DNA was eluated with 500 µl sterile $H_2O_{dest.}$ and stored at -20°C.

3.7 Molecular cloning

3.7.1 Restriction digestion

The cleavage of DNA by restriction enzymes (Roche, Mannheim, Germany) was performed in a volume of 20 µl with about 0.5 µg plasmid DNA, 5-10 units of corresponding enzyme and 2 µl of the manufacturer's recommended reaction buffer. After incubation for 1 to 2 hours at the optimal reaction temperature, reaction was stopped by incubating for 15 min at 65°C and products are separated by agarose gel electrophoresis.

3.7.2 Dephosphorylation of plasmid DNA with alkaline phosphatase

To prevent re-ligation of cohesive ends digested vectors were treated with shrimp alkaline phosphatase (SAP) to remove 5'-phosphate at 37°C for 10 min followed by heat-inactivation of the SAP for 15 min at 65°C.

3.7.3 Purification of plasmid DNA by gel extraction

The DNA vector was purified by running on an ethidium bromide containing agarose gel, excising the band containing the fragment under UV illumination and subsequent gel extraction using QIAquick Gel extraction Kit (Qiagen, Hilden, Germany) following the manufacturer's instructions.

3.7.4 Ligation

In the presence of ATP and Mg^{2+} ions T4 DNA ligase is able to covalently join blunt or cohesive ends between a 5'-phosphate and a 3'-OH group.
Following reaction mix was incubated for 16 h at 16°C:

2 µl	reaction buffer
0.1-0.3 µg	target vector
0.3-1.5 µg	insert DNA
400 units	T4 DNA ligase
ad 20 µl	$H_2O_{dest.}$

3.7.5 FAT1 shRNA plasmid

Preparation of the plasmid containing FAT1 shRNA was performed according to the protocol "RNAi-based conditional gene knockdown in mice using a U6 promoter driven vector" (Shukla et al. 2007). The selected siRNA sequences (Table 3.1) were inserted twice as a palindrome. The U6 promoter is inactivated by insertion of a loxP flanked Neomycin cassette which can be deleted by Cre recombinase.

Table 3.1 Oligonucleotides for cloning of the FAT1 shRNA plasmid

oligonucleotide	sequence
FAT1_2 sense	5'-GGCAGGACGTGTATGATACTCTAAAGCTTTAGAGTATCATACACGTCC TGCCCTTTTTG-3'
FAT1_2 antisense	5'-TTAAGTTTTTCCCGTCCTGCACATACTATGAGATTTCGAAATCTCATAG TATGTGCAGGAC-3'
FAT1_3 sense	5'-GGCACGTTACTTACCATATTGTAAAGCTTTACAATATGGTAAGTAACGT GCCCTTTTTG-3'
FAT1_3 antisense	5'-TAAGTTTTTCCCGTGCAATGAATGGTATAACATTTCGAAATGTTATACC ATTCATTGCACGG-3'

First, the vector was digested with ApaI restriction enzyme and overhanging ends were filled with Klenow enzyme. Subsequently, linearized vector was additionally digested with EcoRI. The insert containing siRNA sequences was prepared by annealing of both oligonucleotides. Thereby an overhang in form of an EcoRI recognition site was formed and the insert could have been ligated with the digested vector. After transformation and mini preparation of plasmid DNA restriction digestion was performed to verify integration of annealed oligonucleotides.

Vectors containing the shRNA construct were then transformed into Cre-recombinase expressing Escherichia coli (294-Cre) to delete the Neomycin cassette and thereby activate the promoter.

3.8 Human tissues and tissue microarray

Paired HCC and non-neoplastic liver tissues were obtained from HCC patients undergoing surgical resection. Tissue samples were immediately snap-frozen and stored at -80°C until subsequent analysis. A tissue microarray (TMA) of paraffin-embedded HCC samples was constructed as described (Amann et al. 2009b). Clinicopathological patient characteristics are summarized in Table 4.1.

Experimental procedures were performed according to guidelines of the charitable state controlled foundation HTCR (Human Tissue and Cell Research) with the informed patient's consent.

3.9 Cell culture

3.9.1 Cell culture medium

DMEM (high glucose/10% FCS)	4.5 g/l	Glucose
	300 µg/ml	L-Glutamine
	supplemented with:	
	10% (v/v)	FCS
	400 U/ml	Penicillin
	50 µg/ml	Streptomycin
HSC medium	DMEM (high glucose/10% FCS)	
	supplemented with:	
	10 µg/ml	Fluconazol
	4 µg/ml	Ciprofloxacin
Freezing medium	5 Vol	DMEM (high glucose/10% FCS)
	3 Vol	FCS
	2 Vol	DMSO

3.9.2 Cultivation of cell lines

Cell culture work was always performed within a laminar flow biosafety cabinet (Hera Safe, Heraeus, Osterode, Germany). Cells were cultivated in a Binder series CB incubator (Binder, Tuttlingen, Germany) in 10% CO_2 atmosphere at 37°C. For passaging adherent cells were washed with PBS and detached with trypsin (0.05%)/EDTA (0.02%) (PAA Laboratories, Cölbe, Germany) at 37°C. Trypsination was stopped adding DMEM containing 10% FCS. Subsequently, cells were centrifuged at 500 g for 5 min and the obtained cell pellet was resuspended in fresh culture medium and distributed to new cell culture flasks achieving a cell density thinning factor of 5 to 10. Medium was changed every second day. Cell growth and morphology were controlled and documented with a microscope (Olympus CKX41 with ALTRA20 Soft Imaging System, Olympus, Hamburg, Germany). Cell culture waste was autoclaved before disposal with a Sanoclav autoclave (Wolf, Geislingen, Germany).

3.9.3 Human hepatocellular carcinoma cell lines

HepG2	ATCC HB-8065
PLC	ATCC CRL-8024
Hep3B	ATCC HB-8064

Cell lines were obtained from the American Type Culture Collection (ATCC).

3.9.4 Cell line of activated human hepatic stellate cells

Activated human hepatic stellate cells have been immortalized by infection with a retrovirus expressing hTERT (human telomerase reverse transcriptase) (Schnabl et al. 2002).

3.9.5 Isolation of primary human hepatocytes

Primary human hepatocytes (PHH) were isolated in cooperation with the Center of Liver Cell Research (Department of Paediatrics and Juvenile Medicine, University of Regensburg, Germany) from human liver resections using a modified two-step EGTA/collagenase perfusion procedure (Hellerbrand et al. 2007; Hellerbrand et al. 2008; Pahernik et al. 1996; Ryan et al. 1993; Weiss et al. 2002). Experimental procedures were performed according to guidelines of the charitable state controlled foundation HTCR (Human Tissue and Cell Research) with the informed patient's consent.

3.9.6 Isolation of human hepatic stellate cells

Human hepatic stellate cells (HSC) were isolated in cooperation with the Center of Liver Cell Research (Department of Paediatrics and Juvenile Medicine, University of Regensburg, Germany). After perfusion and separation of hepatocytes by an initial centrifugation step at 50 g (5 min, 4°C) the supernatant containing the non-parenchymal cells were centrifuged at 700 g for 7 min (4°C). The obtained cell pellet was resuspended in HSC medium and cells were seeded into T75 flasks. Within the first week, the medium was replaced daily, from the second week on medium change took place every 2-3 days. Under these conditions only HSC proliferate. Liver sinusoidal endothelial cells (LSEC) die within the first 24h. By cultivation on uncoated plastic HSC activate within the first 2 weeks and transdifferentiate to myofibroblast-like cells. Liver disease mediated HSC activation can be simulated *in vitro* that way. After 2 weeks the cell culture was

split 1:3 by incubating the cells with Trypsin (0.05%)/EDTA (0.02%) solution. Thereby, only HSC detach whereas Kupffer cells remain adherent to the plastic surface. Therefore, after the first passage only activated HSC remain in the cell culture which was confirmed by previously done analysis (Muhlbauer et al. 2006).

3.9.7 Determination of cell number and viability

Cell number and viability was determined by trypan blue exclusion test. The cell suspension was diluted 1:2 with trypan blue solution (Sigma, Deisenhofen, Germany) and applied on a Neubauer hemocytometer (Marienfeld GmbH, Lauda-Königshofen, Germany). Cell with impaired cell membrane integrity are stained blue, and therefore, can be clearly distinguished from intact cells which appear white under microscopic inspection. The cell number could be calculated after counting cells in all four quadrants of the hemocytometer, each containing sixteen smaller squares, with the following equation:

Cell number/ml = Z x DF x 10^4 ÷ 4

Z: counted cell number

DF: dilution factor (in the described procedure the factor is 2)

The ratio of viable cells could be determined by setting the number of unstained cells in relation to the total cell number (blue and unstained cells).

3.9.8 Collection of conditioned medium

For the purpose of studying potential effects of factors secreted from activated HSC on HCC cells *in vitro*, conditioned medium (CM) from activated HSC was collected. 2 x 10^6 cells were seeded into T75 flasks, washed twice with serum-free DMEM, and then incubated for 24 h with serum-free DMEM (15 ml/T75). Serum-free DMEM incubated for 24 h in cell culture flasks without cells served as control. Medium was then collected, centrifuged at 500 g for 10 min and the supernatant was stored at -80°C until use.

3.9.9 Transient siRNA transfection

siRNA (Table 3.2) and HiPerFect Transfection Reagent® were purchased from Qiagen (Hilden, Germany).

Table 3.2: Used siRNA and their target sequences

name	target sequence
FAT1 siRNA1: Hs_FAT_2	CAGGACGTGTATGATACTCTA
FAT1 siRNA2: Hs_FAT_3	CACGTTACTTACCATATTGTA
All stars negative control siRNA	not disclosed

Transfection of cells was performed according to the manufacturer's fast-forward siRNA transfection protocol.

Shortly before transfection, 2 x 10^5 cells per well were seeded on a 6 well plate in 2,300 µl DMEM culture medium containing 10% FCS. 150 ng siRNA per well was diluted in 100 µl DMEM without FCS and 12 µl of HiPerFect Transfection Reagent was added to the diluted siRNA and mixed. The samples were incubated for 10 min at room temperature to allow the formation of transfection complexes which were then added drop-wise onto the cells. After 24 h cell medium was changed. Successful gene silencing was documented on the mRNA and protein levels by quantitative RT-PCR and Western blotting.

3.9.10 Transient and stable plasmid transfection

Lipofectamine method with Lipofectamine™ and PLUS™ reagent (Invitrogen, Karlsruhe, Germany) was used to transfect cells with plasmid DNA (see 3.5).

For transfection 2x10^5 cells per well were seeded on a 6 well plate. After 3 hours medium was changed and cells are cultivated in DMEM without FCS over night. On the next day medium was again changed to DMEM containing 10% FCS (1 ml per well) and after 3 hours cells transfection mix was added to the cells. Transfection mix was prepared according the manufacturer's instructions containing 0.5 µg plasmid DNA per well. Cell medium was changed after incubation over night.

For generation of stable transfected cell lines an expression vector containing a resistance gene was transfected into the cells. By addition of the antibiotic Geneticin® (Invitrogen, Karlsruhe, Germany) selection took place and only cells containing the vector with the resistance gene could survive.

3.9.11 NFκB reporter gene assay

Regulatory DNA sequences can be examined by using reporter gene analysis. To determine the activity of a promoter, the corresponding DNA fragment containing the promoter region, is cloned into the reporter plasmid pGL3 basic prior to the firefly luciferase gene. Expression of the reporter gene is then proportional to the activation potential of the cloned DNA fragment. By addition of a substrate (luciferin) for the luciferase enzyme chemiluminescence is achieved which can be measured in a luminometer.

Considering different transfection efficiencies in individual experimental assays, cells were cotransfected with an additional vector containing the luciferase gene from Renilla reniformis (pRL-TK). Chemiluminescence of Renilla luciferase was also measured in the luminometer and used for the normalization of the values depending on the transfection efficiency. Dual-Luciferase® Reporter Assay System (Promega, Mannheim, Germany) was used to perform luciferase assays.

2×10^5 cells per well were seeded on a 6-well plate and transfected with 0.5 µg NFκB reporter construct (Promega, Mannheim, Germany) or empty control plasmid and pRL-TK using lipofectamin (see 3.9.10). After 24 h medium is removed and cells are rinsed twice with water. Subsequently, 300 µl lysis buffer are added per well and cells were gently shaked for 20 min at room temperature. Then, 50 µl of each approach were measured in the luminometer using the provided chemicals in the kit.

3.10 Isolation and analysis of RNA

3.10.1 RNA isolation and determination of RNA concentration

RNA isolation was performed with the RNeasy® mini kit (Qiagen, Hilden, Germany) according to the manufacturer's instructions. The principle of RNA isolation is based on the absorption of RNA to hydrophilic silicon-gel membranes in presence of suitable buffer systems. Biological samples were first lysed and homogenized in the presence of a highly denaturing guanidine isothiocyanate containing buffer, which immediately inactivates RNases to ensure isolation of intact RNA. To homogenize tissue samples a MICCRA D1 homogenizer (ART Prozess- & Labortechnik, Müllheim, Germany) was used.

After lysis, ethanol has been added to provide ideal conditions for the binding of RNA to the silica-gel membranes. Contaminants have been washed away with

suitable buffers before RNA was eluted in water and stored at -80°C. The concentration of RNA was measured with the NanoDrop® ND-1000 UV/VIS spectrophotometer (Peqlab, Erlangen, Germany).

3.10.2 Reverse transcription of RNA to cDNA

Transcription of RNA to complementary DNA (cDNA) was conducted with the Reverse Transcription System Kit (Promega, Mannheim, Germany) which uses avian myeloblastosis virus reverse transcriptase (AMV-RT). The working solution was pipetted with contamination-free aerosol filter pipet tips after the following pipetting scheme:

0.5 µg	RNA
4 µl	$MgCl_2$ (25 mM)
2 µl	10x reverse transcription buffer
2 µl	dNTP mix (10 mM)
1 µl	random primer
0.5 µl	RNasin ribonuclease inhibitor
0.6 µl	AMV RT
ad 25 µl	$H_2O_{dest.}$

For reverse transcription samples have been incubated in a GeneAmp® PCR cycler (Applied Biosystems, Foster City, USA) for 30 min at 42°C. For denaturation of the AMV RT the temperature has been raised to 99°C for 5 min. After cooling down to 4°C the obtained cDNA was diluted with 75µl $H_2O_{dest.}$ and used immediately or stored at -20°C.

3.10.3 Quantitative real time polymerase chain reaction

To quantify the expression of specific mRNA, quantitative real time polymerase chain reaction (qRT-PCR) has been performed with the LightCycler® 480 System (Roche Diagnostics, Mannheim, Germany). The qRT-PCR is principally based on a conventional polymerase chain reaction (PCR), but offers the additional possibility of quantification, which is accomplished by fluorescence measurements at the end and/or during a PCR cycle. As fluorescent reagent SYBR® Green (SensiFAST™ SYBR No-ROX Kit, Bioline, Luckenwalde, Germany) has been used. SYBR® Green intercalates with double-stranded DNA whereby the fluorescence emission rises significantly. Therefore, the fluorescence signal increases proportionally with the amount of PCR products. To quantify the

expression of a specific gene of interest, the results have been normalized to the housekeeper 18s rRNA. The results were evaluated with the LightCycler® 480 software release 1.5.0 SP4 following the manufacturer's instructions. qRT-PCR was performed according following protocol:

2.5 µl	$H_2O_{dest.}$
0.25 µl	forward primer (20 µM)
0.25 µl	reverse primer (20 µM)
5 µl	SYBR® Green

Following standard scheme has been used and adapted to particular primer melting point temperature:

Initial denaturation:	95°C	2 min
Two step PCR (45 cycles):	95°C	5 s
	60°C	18 s
Analysis of melting curve:	95°C	5 s
	65°C	1 min
	97°C	0 s

For validation, after qRT-PCR PCR product has been mixed with loading buffer (Peqlab, Erlangen, Germany) and loaded on a agarose gel with ethidium bromide (50 µg/100 ml gel) to determine the PCR product length. Each experimental condition was performed in triplicates and experiments were repeated at least three times.

Table 3.3 Used primers for qRT-PCR, species: mouse or human

name	forward primer	reverse primer
18s	5' AAA CGG CTA CCA CAT CCA AG	5' CCT CCA ATG GAT CCT CGT TA
Coll I, human	5' CGG CTC CTG CTC CTC TT	5' GGG GCA GTT CTT GGT CTC
E-Cad, human	5'-ATC CTC CGA TCT TCA ATC CCA CCA C	5'-GTA CCA CAT TCG TCA CTG CTA CGT G
FAT1, human	5' GTG TTT GTT CTC TGC CGT AAG	5' TAG GCT TCT GGA TGG AGT CG
FAT1, murine	QIAGEN QuantiTect Primer Assay	
MAT2A, human	5'-CCA CGA GGC GTT CAT CGA GG	5'-AAG TCT TGT AGT CAA AAC CT
MCP1, human	5'-CGC GAG CTA TAG AAG AAT CAC	5'-TTG GGT TGT GGA GTG AGT GT
RANTES, human	QIAGEN QuantiTect Primer Assay	
SNAIL, human	QIAGEN QuantiTect Primer Assay	
TNF, human	QIAGEN QuantiTect Primer Assay	
VEGF, human	QIAGEN QuantiTect Primer Assay	

Primers were synthesized by SIGMA Genosys (Hamburg, Germany) or purchased as QuantiTect Primer Assays from Qiagen (Hilden, Germany). The lyophilized

primers (SIGMA Genosys primers) were solved in $H_2O_{dest.}$ or TE buffer (QuantiTect Primer Assays), respectively, and stored at -20°C.

3.11 Protein analysis

3.11.1 Preparation of protein extracts

To extract whole cell protein from cell lines cultivated in 6-well plates the cell culture medium was discarded and cells were washed once with PBS, then scraped off with a cell scraper (Corning, New York, USA) and taken up into 350 µl cell lysis buffer (Cell Signaling Technology, Boston, USA) supplemented with 1 mM PMSF and a protease inhibitor cocktail (cOmplete Mini Protease Inhibitor Cocktail Tablets from Roche Diagnostics, Mannheim, Germany). Liver tissue extracts were obtained by homogenization of snap-frozen liver tissue in cell lysis buffer containing 1 mM PMSF and protease inhibitors using a MICCRA D1 homogenizer (ART Prozess- & Labortechnik, Müllheim, Germany). Subsequently, probes were treated with an ultrasonoscope (Sonoplus hp 70, Bandelin electronics, Berlin, Germany) 5 x 3 s at an intensity of 70% for cell lysis. Subsequently, the solved proteins were separated from the non-soluble cell components by centrifugation at 20,000 g (15 min, 4°C). The protein solution was transferred into new reaction tubes and stored at -20°C.

3.11.2 Determination of protein concentration

To determine the protein concentrations of protein solutions the BCA™ Protein Assay Kit (Pierce, Rockford, USA) was used. The assay combines the reduction of Cu^{2+} to Cu^{1+} by protein in an alkaline medium with the highly sensitive and selective colorimetric detection of the cuprous cation Cu^{1+} by bicinchoninic acid (BCA). The first step is the chelation of copper with protein in an alkaline environment to form a blue-colored complex. In this reaction, known as biuret reaction, peptides containing three or more amino acid residues form a colored chelate complex with cupric ions in an alkaline environment. One cupric ion forms a colored coordination complex with four to six nearby peptides bound. In the second step of the color development reaction, BCA, a highly sensitive and selective colorimetric detection reagent reacts with the cuprous cation Cu1+ that was formed in step 1. The purple-colored reaction product is formed by the chelation of two molecules of BCA with one cuprous ion. The BCA/copper complex

is water-soluble and exhibits a strong linear absorbance at 562 nm with increasing protein concentrations. 200 µl of alkaline BCA/copper(II) solution (50 parts of solution A mixed with 1 part of solution B) was added to 2 µl of protein solution using a 96-well plate and were incubated for 15 min at 37°C. Thereafter the purple color was measured at 562 nm with a spectrophotometer (EMax® Microplate Reader, MWG Biotech, Ebersberg, Germany). The optical absorbance values could be translated into specific protein concentrations by parallel quantification of a BSA standard.

3.11.3 SDS polyacrylamid gel electrophoresis (SDS-PAGE)

Used buffers:

Laemmli buffer	62.5 mM	Tris/HCl; pH 6.8
	2% (w/v)	SDS
	10% (v/v)	Glycerine
	5% (v/v)	β-Mercaptoethanol
Running buffer	25 mM	Tris/HCl; pH 8.5
	200 mM	Glycine
	0.1% (w/v)	SDS
10% Resolving gel	7.9 ml	$H_2O_{dest.}$
	5.0 ml	1.5 M Tris/HCl; pH 8.8
	0.2 ml	10% (w/v) SDS
	6.7 ml	Acrylamide/Bisacrylamid 30%/0.8% (w/v)
	0.2 ml	Ammonium persulfate 10% (w/v)
	0.008 ml	TEMED
5% Stacking gel	2.7 ml	$H_2O_{dest.}$
	0.5 ml	1.0 M Tris/HCl; pH 6.8
	0.04 ml	10% (w/v) SDS
	0.67 ml	Acrylamide/Bisacrylamid 30%/0.8% (w/v)
	0.04 ml	Ammonium persulfate 10% (w/v)
	0.004 ml	TEMED

For SDS-PAGE of larger proteins like FAT1 the NuPAGE® -System (Invitrogen, Karlsruhe, Germany) was used.

Gel:	NuPAGE® 3-8% Tris-Acetate Gel 1.0 mm10 well
Buffer:	25 ml NuPAGE® Tris-Acetate SDS Running Buffer
	475 ml $H_2O_{dest.}$
	500 µl NuPAGE® Antioxidant

The protein solutions were heated at 95°C for 5 min in Laemmli buffer and applied on a SDS polyacrylamid gel for protein fractionation by size at 35 mA/150 V (XCell SureLock™ Mini-Cell, Invitrogen, Karlsruhe, Germany). As size marker HiMark™ Pre-Stained High Molecular Weight Protein Standard (Invitrogen, Karlsruhe Germany) and peqGOLD Protein-Marker V (Peqlab, Erlangen, Germany) were used.

3.11.4 Western Blotting

Used buffers:

Standard transfer buffer	10% (v/v)	Methanol
	25 mM	Tris
	190 mM	Glycine

NuPAGE® transfer buffer	25 ml NuPAGE® Transfer Buffer (20x)
	50 ml Methanol
	425 ml $H_2O_{dest.}$
	500 µl NuPAGE® Antioxidant

To detect the proteins after SDS-PAGE by use of specific antibodies proteins were transferred electrophoretically to a nitrocellulose membrane (Invitrogen, Karlsruhe, Germany) at 220 mA/300 V for 1.5 h (XCell II Blot Module, Invitrogen, Karlsruhe, Germany). To block unspecific binding sites, the membrane was bathed in PBS containing 3% BSA or 5% milk powder for 1 h at RT. Then, the membrane was incubated with a specific primary antibody (Table 3.4) over night at 4°C. After washing, the membrane was incubated with a secondary horseradish peroxidase (HRP) conjugated antibody (Table 3.4) for 1 h at RT. Thereafter, the membrane was washed and incubated with ImmunStar™ WesternC™ Kit (BioRad, München, Germany) for 3 min. This system utilizes chemiluminescence technology which was detected by the ChemiDoc XRS (BioRad, München, Germany) imaging system.

Table 3.4 Used primary and secondary antibodies for Western Blot analysis

Primary antibody	**Dilution**
rabbit anti-FAT1 (Atlas Antibodies AB, Stockholm, Sweden)	1:1000
rabbit anti-collagen I (Rockland, Gilbertsville, PA, USA)	1:5000
mouse anti-α-sma (Abcam, Cambridge, UK)	1:500
rabbit anti-IκBα (Cell Signaling, Beverly, MA, USA)	1:1000
mouse anti-β-actin (Sigma-Aldrich, Deisenhofen, Germany)	1:20,000
mouse anti-α-Tubulin (Santa Cruz Biotechnology, Santa Cruz, CA, USA)	1:200
mouse anti-HIF1α (Santa Cruz Biotechnology, Santa Cruz, CA, USA)	1:200
Secondary antibody	
anti-mouse HRP (Santa Cruz Biotechnology, Santa Cruz, CA, USA)	1:3000
anti-rabbit HRP (Santa Cruz Biotechnology, Santa Cruz, CA, USA)	1:3000

3.11.5 Quantification of caspase-3/7 activity

Caspases, or cysteine-aspartic acid proteases, are a family of cysteine proteases, which play essential roles in apoptosis. There are two types of apoptotic caspases: initiator (apical) caspases and effector (executioner) caspases. Initiator caspases (*e.g.* caspase-2, -8, -9, -10) cleave inactive pro-forms of effector caspases, thereby activating them. Effector caspases (*e.g.* caspase-3, -6, -7) in turn cleave other protein substrates within the cell, to trigger the apoptotic process. To analyze caspase-3/7 activity we used the Apo-One Homogeneous Caspase-3/7 Assay Kit (Promega, Mannheim, Germany) according to the manufacturer's instructions. We used 6000 cells/well (96-well plate) and incubated cells with the provided caspase substrate Z-DEVD-R110 for 1h. Cleavage of the non-fluorescent caspase substrate Z-DEVD-R110 by caspase-3/7 liberates the fluorescent rhodamine 110, which was detected fluoro-spectrometrically with a SPECTRAFluor Plus microplate reader (Tecan, Männedorf, Switzerland) at wavelengths of 485 nm (excitation) and 520 nm (emission). Each experimental condition was performed in triplicates and experiments were repeated at least twice.

3.11.6 S-Adenosylmethionine (SAM) extraction and analysis

For analysis of S-Adenosylmethionine (SAM) in cell culture medium, cells were cultured in serum free medium for 24 h. Subsequently, medium was collected, centrifuged, and the supernatant was snap-frozen and stored at -80°C. Further,

cell number in corresponding cell culture plates was determined by counting the trypsinized cells.

Samples were further processed by the Institute of Functional Genomics, University of Regensburg. Briefly, cell culture medium was spiked with stable isotope-labeled standards, dried by means of an infrared evaporator, and the residues were reconstituted in 0.1 mol/L acetic acid.

Liquid chromatography-electrospray ionization-tandem mass spectrometry (LC-ESI-MS/MS) was performed as described (Stevens et al. 2010).

3.12 Flow cytometry

3.12.1 Annexin V / Propidium iodide double staining

At early stages of apoptosis cells change the structure of their membrane, which leads to the exposure of phosphatidylserine on the membrane surface. In living cells, phosphatidylserine is transported to the inside of the lipid bilayer by the aminophospholipid translocase, a Mg^{2+} ATP dependent enzyme. At the onset of apoptosis, phosphatidylserine is translocated to the external membrane and serves as a recognition signal for phagocytes.

Annexins are ubiquitous homologous proteins that bind phospholipids in the presence of calcium. Since the redistribution of phosphatidylserine from the internal to the external membrane surface represents an early indicator of apoptosis, Annexin V and its conjugates can be used for the detection of apoptosis because they interact strongly and specifically with exposed phosphatidylserine.

The differentiation between apoptotic and necrotic cells can be performed by simultaneous staining with propidium iodide (PI), a dye that stains by intercalating into nucleic acid molecules. The cell membrane integrity excludes PI in viable cells, whereas necrotic cells are permeable to PI. Thus, dual parameter flow cytometric analysis allows for the discrimination between viable, early apoptotic and late apoptotic/necrotic cells.

To quantify apoptotic cells we used the Annexin V-FITC Detection Kit (PromoKine, Heidelberg, Germany). Therefore, we resuspended 2 x 10^5 cells in 500 µl of the provided binding buffer and added 5 µl of the FITC-labeled Annexin V reagent and 5 µl of PI solution. After incubation for 5 min at room temperature in the dark flow cytometric analysis was performed. The FITC-Annexin V signal was detected at a wavelength of 525 ± 12.5 nm, the PI signal at a wavelength of 620 ± 12.5 nm. The

result of the dual parameter flow cytometric analysis were depicted as dotplot and evaluated by quadrant analysis. The y-axis of the dotplot shows PI fluorescent signal intensity, the x-axis FITC-Annexin V fluorescent signal intensity. Discrimination of viable, early apoptotic and late apoptotic/necrotic cells were done by means of different intensities of FITC-Annexin V of PI fluorescent signals. Viable cells show low FITC-Annexin V and PI fluorescence (lower left quadrant), early apoptotic cells show high FITC-Annexin V but low PI fluorescence (lower right quadrant) and late apoptotic/necrotic cells show both high FITC-Annexin V and PI fluorescence (upper right quadrant).

To asses the effects of a specific apoptosis or necrosis inducing reagent the percental distribution of viable, early apoptotic and late apoptotic/necrotic cells related to the total of counted cell (10^4 cells) were calculated.

3.13 Functional assays

3.13.1 XTT

Cell proliferation was quantified with the XTT kit (Roche Diagnostics, Mannheim, Germany). The assay is based on the ability of metabolic active cells to reduce the tetrazolium salt XTT (2,3-bis(2-methoxy-4-nitro-5-sulfophenyl)-5-[phenylamino)carbonyl]-2H-tetrazolium hydroxide) to orange colored compounds of formazan. The dye formed is water soluble and dye intensity can be read with a spectrophotometer at a wavelength of 450 nm and a reference absorbance wavelength of 650 nm. The intensity of the dye is proportional to the number of metabolic active cells.

To quantify the effects of siRNA treatment on cell proliferation, cells were seeded in 96-well tissue culture plates (4000 cells per well) and incubated for different time intervals. At the chosen time points XTT reagent was added and the intensity of the forming dye was measured two hours later with an EMax Microplate Reader (MWG Biotech, Ebersberg, Germany). Values of optical density (OD) at individual time points were corrected for background by subtracting the OD value of blank wells without cells. Each experimental condition was performed in triplicate and experiments were repeated three times.

3.13.2 Attachment and proliferation assay (xCELLigence System, Roche)

By the use of so-called E-plates it is possible to examine attachment and proliferation of cells in the xCELLigence System from Roche (Penzberg, Germany). Each well on ePlates contains a sensor with two microelectrodes which measures the resistance between two electrodes on the bottom of the well. This value correlates with the number of cells and is transmitted in real time as a change in cell index on the connected laptop. The more cells settle to the well bottom, the higher the resistance, and thus the cell index. ePlates were coated at the beginning of the experiment with 100 µl DMEM with FCS and equilibrated for 30 minutes at room temperature. 2000 cells/100 µl DMEM with FCS were added after the measurement of background resistance. Following incubation for 10 minutes at room temperature ePlate was inserted into the analyzer. Data was evaluated with the appropriate software.

3.13.3 Migration (96-well)

The migratory potential of cells was quantified using the Cultrex 96 Well Cell Migration Assay (Trevigen, Gaithersburg, USA) according to the manufacturer's instructions. This assay is based on two medium-filled compartments separated by a microporous membrane. In general, cells are placed in the upper compartment and are allowed to migrate through the pores of the membrane to the lower compartment, in which chemotactic agents are present. After an appropriate incubation time, migrated cells are detached from the lower side of the membrane by a detachment buffer and quantified using calcein acetoxymethylester (calcein AM). Calcein AM is internalized by the cells, and intracellular esterases cleave the acetomethylester moiety to generate free calcein, which can be detected fluorometrically.

Cells were seeded into the upper compartment of the provided 96-well plate ($4x10^4$ cells/well) in DMEM. The lower compartment was filled with DMEM supplemented with conditioned medium from fibroblasts and 10% FCS as chemoattractants. After incubation at 37°C for 5 h cell migration was quantified by fluorimetry using a SPECTRAFluor Plus microplate reader (Tecan, Männedorf, Switzerland). Each experimental condition was performed in triplicates and experiments were repeated twice.

3.13.4 Migration (xCELLigence System, Roche)

In contrast to the above-mentioned migration assay which only allows endpoint analysis, the xCELLigence System allows to observe behavior of the cells in real time.

The lower compartment of so called CIM plates was filled with 160 µl conditioned medium from fibroblasts. After assembly with the upper part 27 µl DMEM without FCS was given on the membrane and CIM plate was equilibrated for 1 hour at 37°C. $4x10^4$ cells /100 µl DMEM without FCS were added following the measurement of background resistance. After incubation for 30 minutes at room temperature ePlate was inserted into the analyzer. Data was evaluated with the appropriate software.

3.14 Animal experiments

Animals were purchased at Charles River Laboratories (Sulzfeld, Germany) and housed in a 22°C controlled room under a 12 h light-dark cycle with free access to food and water. After one week of acclimatization mice were used for different experimental settings.

3.14.1 Bile duct ligation

Experimental cholestasis induced by bile duct ligation (BDL) is a commonly used model of liver injury. BDL or sham surgeries were performed in 4 female C57Bl/6 mice each as described (Gabele et al. 2009). After midline laparotomy the common bile duct was exposed and ligated. Then, the abdomen was closed again in layers. After 3 weeks, blood and livers were collected for further analysis.

3.14.2 Thioacetamid induced liver fibrosis

Thioacetamide (TAA) is a hepatotoxin, which induces liver fibrosis by injury. It is a commonly used chemically induced model of fibrosis (Brodehl 1961).

TAA induced liver fibrosis was caused in female C57Bl/6 by administering TAA at a dose of 300 mg/L in drinking water for 14 weeks.

3.14.3 Experimental NASH model

Male BALB/c mice were purchased at 6 weeks of age, divided into two groups (n=5 each) and fed either with control diet or a non-alcoholic steatohepatitis (NASH) inducing high fat diet containing 30% lard, 1.25% cholesterol and 0.5%

sodium cholate (Matsuzawa et al. 2007). After 30 weeks feeding animals were sacrificed and liver tissue was immediately frozen.

3.14.4 Tumor cell inoculation and measurement of tumor growth in NMRI (nu/nu) mice

To analyze tumor growth *in vivo* tumor cells were injected subcutaneously into immunodeficient NMRI (nu/nu) mice. This experiment was performed in cooperation with Dr. Thilo Spruss (animal care facility, University of Regensburg). Mice were housed in a 22°C controlled room under a 12 h light-dark cycle with free access to food and water in the central animal laboratories.

Cells were harvested after incubation with PBS containing 0.05% trypsin and 0.04% ethylenediaminetetraacetic acid (Sigma-Aldrich, Steinheim, Germany). Tumor cells were washed twice with serum-free Dulbecco's modified Eagle's medium at room temperature and were resuspended in Dulbecco's modified Eagle's medium at a concentration of 5 x 10^6 cells/ml. For each of the cell lines, a group of 10 NMRI (nu/nu) mice with a mean body weight of 32 g was formed. All mice were injected subcutaneously with a cell suspension of 0.1 ml containing 5 x 10^5 cells of a single line. Tumor growth kinetics were recorded by weekly measurement of tumor diameters at the inoculation site (region of the thoracic mammary fat pad) with an electronic caliper. Tumor areas were calculated as the product of two perpendicular diameters, one measured across the greatest width of the tumor. For ethical reasons, mice were sacrificed at day 21 after the first tumors underwent ulceration, and the tumors were taken out and stored for subsequent analysis.

3.15 Histology and Immunohistochemistry

For histological and immunohistochemical analysis tissue was fixed for 24 hours in buffered formaldehyde solution (3.7% in PBS) at room temperature, dehydrated by graded ethanol and embedded in paraffin. Sections were cut at 5 µm and stuck on glass slides.

3.15.1 Hematoxylin/Eosin staining

Paraffin embedded tissue sections stuck on a glass slide were deparaffinized with xylene. Then, the tissue was rehydrated and dipped into an aequeous solution of hematoxylin. Hematoxylin binds to basophilic structures such as the anionic

phosphate groups of nucleic acids. Following dehydration in alcohol, the tissue was dipped into an alcoholic solution of eosin. Eosin carries a negative charge and reacts with cationic groups common to amino acids (eosinophilic structures). Once stained, the tissue was covered with a thin glass cover slip (Carl Roth, Karlsruhe, Germany) attached by mounting medium (Vector Laboratories, Burlingame, USA). In general, the eosin imparts a pink to red color to proteins, and hematoxylin stains the basophilic structures, usually containing nucleic acids, such as ribosomes and the chromatin-rich cell nucleus, from blue to purple. Digital images were captured with an Olympus CKX41 microscope equipped with the ALTRA20 Soft Imaging System (Olympus, Hamburg, Germany).

3.15.2 Immunohistochemical analysis of FAT1 and Ki67

For visualization of FAT1 and Ki67 positive cells the LSAB+ System HRP-Kit (Dako, Hamburg, Germany) was used according to the manufacturer's instructions. The technique used in this kit is based on the LSAB (labelled streptavidin biotin) method.

Used buffer:

TBS-T buffer	6.1 g/L	Tris	
	8.8 g/L	NaCl	
	37 ml	1 N HCl	
	ad 1L	$H_2O_{dest.}$	pH 7.6
	0.05%	TWEEN 20	

Table 3.5 Used antibodies for immunohistochemical staining

Antibody	Dilution (in TBS + 1%BSA)
rabbit anti-FAT1 (Atlas Antibodies AB, Stockholm, Sweden)	1:50
rabbit anti-Ki67 (Abcam, Cambridge, UK)	1:50

Deparaffinated and rehydrated tissue sections on glass slides were incubated for 5 min in 3% H_2O_2 to quench endogenous peroxidase activity. Subsequently, tissue was incubated for 30 minutes with a primary antibody (Table 3.5) at RT in a humid chamber. After washing in TBS-T buffer, sequential incubations with the biotinylated link antibody (15 min) and peroxidase-labeled streptavidin (15 min) were performed. Staining is completed after incubation with the provided

substrate-chromogen (3,3'-diaminobenzidine) solution (5 min). Tissue was then counterstained in an aqueous solution of hematoxylin for 1 min, rinsed with $H_2O_{dest.}$ and covered with a thin glass cover slip (Carl Roth, Karlsruhe, Germany) attached by mounting medium (Vector Laboratories, Burlingame, USA). Digital images were captured with an Olympus CKX41 microscope equipped with the ALTRA20 Soft Imaging System (Olympus, Hamburg, Germany).

3.15.3 TUNEL staining (TdT-mediated dUTP-biotin nick end labeling)

Tissue sections of nude mice tumors were stained for apoptotic cells with the DeadEnd Fluorometric TUNEL System (Promega, Mannheim, Germany) according to the manufacturer's instructions. Thereby, free DNA ends, which are characteristic for apoptotic cells, are marked with Fluorescein-12-UTP by terminal desoxynucleotidyl transferase (TdT) and can be made visible, in this way. Nuclear staining was performed with DAPI (Hard Set Mounting Medium with DAPI, H-1500, Vectashield, Vector Laboratories, Burlingame, USA) and fluorescence was analyzed with a fluorescence microscope.

3.16 Statistical analysis

Values are presented as mean ± SEM or mean ± SD as indicated. All experiments were repeated at least three times. Comparison between groups was made using the Student's unpaired t-test. A p-value < 0.05 was considered statistically significant. Contingency table analysis and the two-sided Fisher's exact test were used to study the statistical association between clinicopathological and immunohistochemical variables. Calculations were performed using the statistical computer package GraphPad Prism (GraphPad Software, San Diego, CA, USA) or SPSS (SPSS, Chicago, IL, USA).

4 Results

As described in the introduction FAT1 is involved in different pathological circumstances, however, with regards to the role of FAT1 in liver cells or liver disease respectively, no data are available at present. The aim of this thesis was to address this issue.

In particular, the focus was placed on two aspects:

4.1 Expression and function of FAT1 in liver fibrosis

4.2 Expression and function of FAT1 in hepatocellular carcinoma

4.1 Expression and function of FAT1 in chronic liver disease

4.1.1 FAT1 expression in non-alcoholic fatty liver disease (NAFLD)

To investigate the role of FAT1 in chronic liver disease, we first analyzed FAT1 expression in a murine dietary NASH model. Thereto, mice received a non-alcoholic steatohepatitis (NASH) inducing high fat diet or were fed with standard chow for 30 weeks.

Hepatic FAT1 expression was significantly higher after feeding a NASH inducing diet compared to mice fed with standard chow (Figure 4.1).

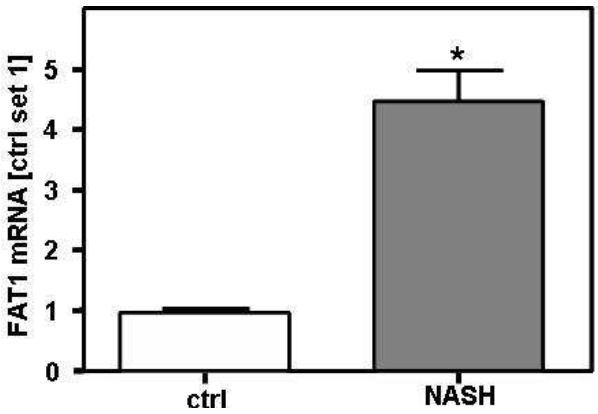

Figure 4.1 Analysis of FAT1 mRNA expression in the dietary murine NASH model (NASH, n=5) and control mice (ctrl, n=5). *p<0.05 compared to control.

In human NASH FAT1 expression revealed a high variation but significantly correlated (r=0.64, *p*=0.002) with the expression of collagen alpha I(1), the most abundant extracellular matrix protein of fibrotic liver tissue. In contrast, no significant correlation was found between the expression of FAT1 and tumor necrosis factor (TNF), a proinflammatory cytokine which is significantly elevated during liver inflammation (Figure 4.2).

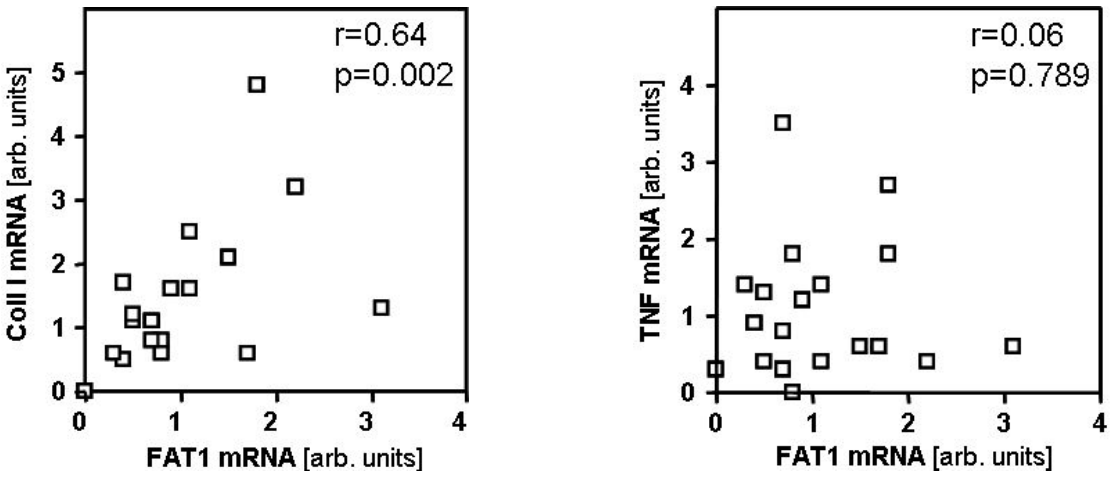

Figure 4.2 Correlation of FAT1 with collagen alpha I(1) (Coll I) (left panel) and tumor necrosis factor (TNF) mRNA expression (right panel) in hepatic tissues of patients with non-alcoholic fatty liver disease (n=20).

4.1.2 FAT1 expression in chronic liver disease

We further analyzed FAT1 expression in murine models of hepatic fibrosis. Experimental cholestasis induced by bile duct ligation (BDL) is a commonly used model to induce liver fibrosis (Iredale 2007). Three weeks after BDL, we analyzed FAT1 expression by qRT-PCR and found significant upregulation of FAT1 in response to BDL compared to sham treated mice (Figure 4.3).

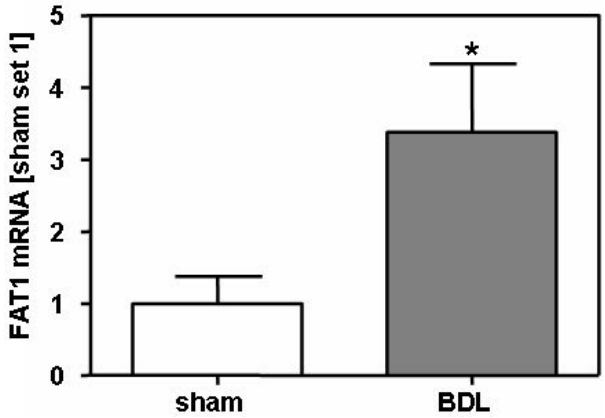

Figure 4.3 Analysis of FAT1 mRNA expression in bile-duct ligated (BDL, n=4) and sham-treated (sham, n=4) mice. *p<0.05 compared to sham.

Another model to induce liver fibrosis is iterative treatment with hepatotoxic agents. One of these is thioacetamide (TAA). FAT1 expression was enhanced in mice treated with TAA for 14 weeks compared to control mice (Figure 4.4).

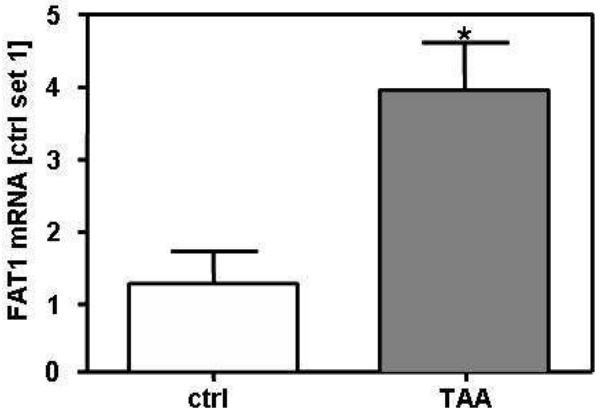

Figure 4.4 Analysis of FAT1 mRNA expression in TAA treated (TAA, n=3) and control (ctrl, n=3) mice. *p<0.05 compared to control.

Also in cirrhotic human liver tissue of patients with alcoholic liver disease and chronic viral hepatitis B or C infection FAT1 expression was significantly higher compared to normal human liver tissue (Figure 4.5).

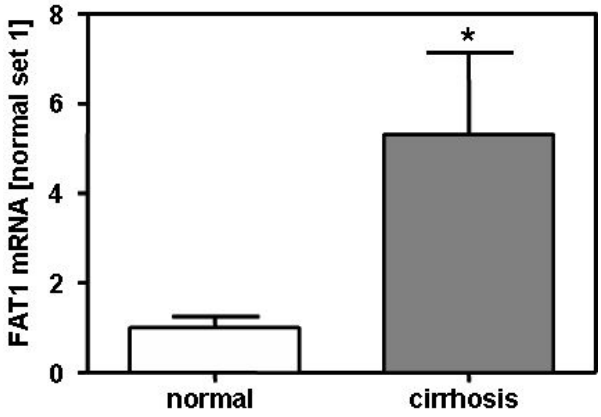

Figure 4.5 FAT1 mRNA expression in cirrhotic human liver tissue (n=6) compared to normal liver tissue (n=7). *p<0.05 compared to normal.

Immunohistochemistry revealed no significant differences in the staining intensity between normal and cirrhotic liver tissue. However, myofibroblast like cells in the fibrotic septa revealed a significant immunosignal (Figure 4.6).

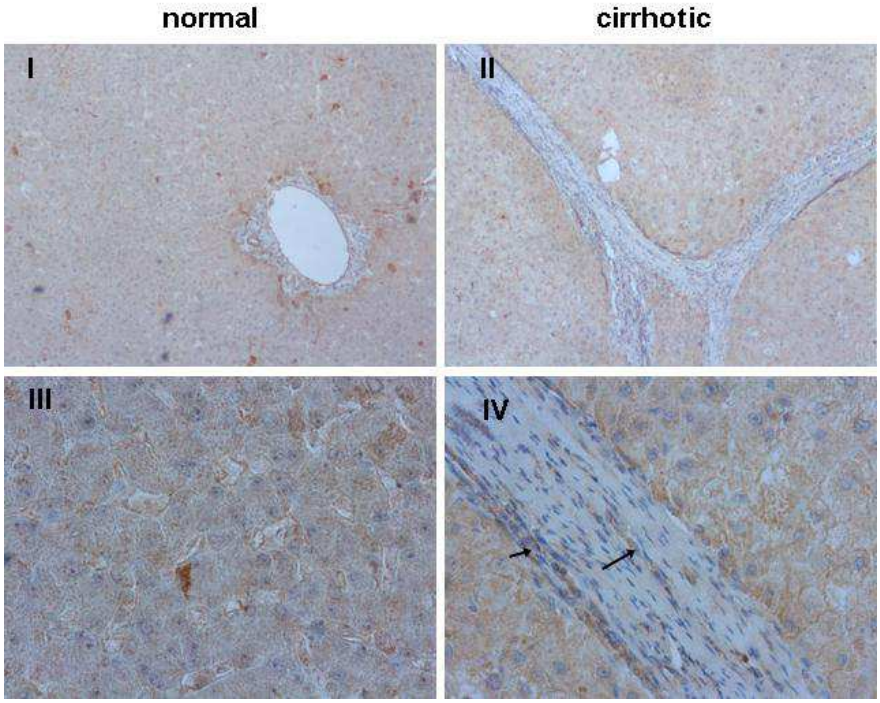

Figure 4.6 Immunohistochemical analysis of FAT1 in normal (panel I, III) and cirrhotic liver tissue (panel II and IV). Myofibroblast like cells in fibrotic septa revealed a strong FAT1 immunosignal (IV, black arrows).

4.1.3 Expression of FAT1 in hepatic stellate cells (HSCs)

These data indicated activated HSCs as cellular source of enhanced FAT1 expression. Therefore, we determined the expression of FAT1 during the course of *in vitro* activation of human HSCs by quantitative RT-PCR (Figure 4.7). There is a significant increase of FAT1 mRNA expression during activation of HSCs.

We confirmed FAT1 upregulation during activation of HSCs on protein level (Figure 4.8). In parallel to FAT1, we determined Coll I and α-sma to document the activation of HSCs during *in vitro* culture.

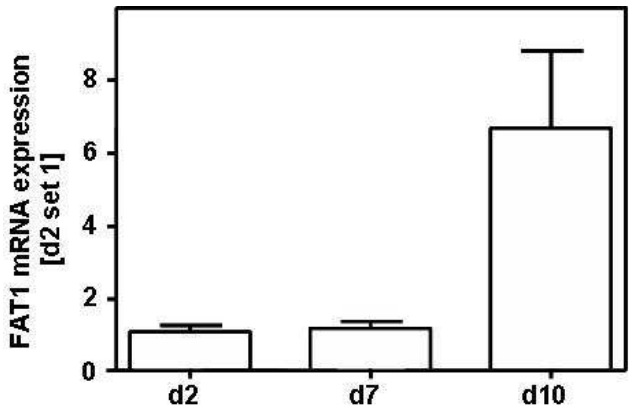

Figure 4.7 Analysis of FAT1 mRNA during *in vitro* activation of human HSCs. Freshly isolated HSCs were cultured on plastic and RNA was isolated after different times of culture (day 2, 7 and 10).

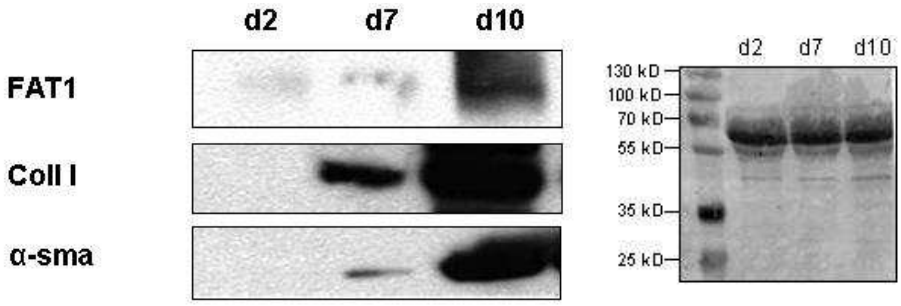

Figure 4.8 FAT1 protein expression during *in vitro* activation of human HSCs. Collagen alpha I(1) (Coll I) and alpha-smooth muscle actin (α-sma) were used as activation markers. Ponceau S staining of the same membrane was used to demonstrate equal protein loading.

4.1.4 Functional role of FAT1 in activated HSCs

To gain insight into the functional role of increased FAT1 in activated HSCs, FAT1 was suppressed by transfection with specific siRNA. Quantitative RT-PCR

analysis revealed a strong suppression of FAT1 mRNA expression in transfected primary HSCs in contrast to control transfected cells. Downregulation of FAT1 expression was confirmed on protein level by Western blot analysis (Figure 4.9).

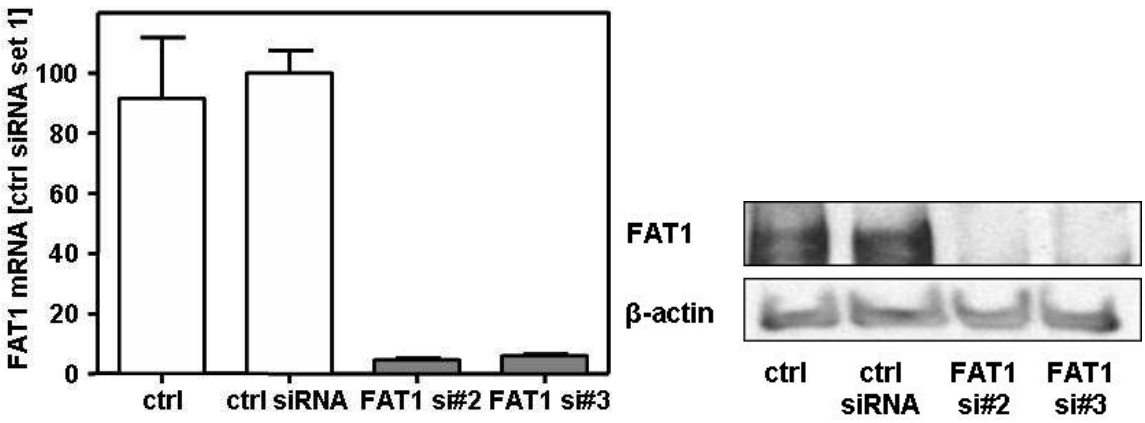

Figure 4.9 Analysis of FAT1 mRNA and protein in untransfected cells (ctrl), in control siRNA (ctrl siRNA), and FAT1 siRNA (FAT1 si#2, FAT1 si#3) transfected cells. β-actin served as housekeeper for Western Blot analysis.

Morphology did not differ between cells (Figure 4.10), but expression analysis revealed lower levels of the proinflammatory genes MCP1 and RANTES in FAT1 suppressed HSCs (Figure 4.11).

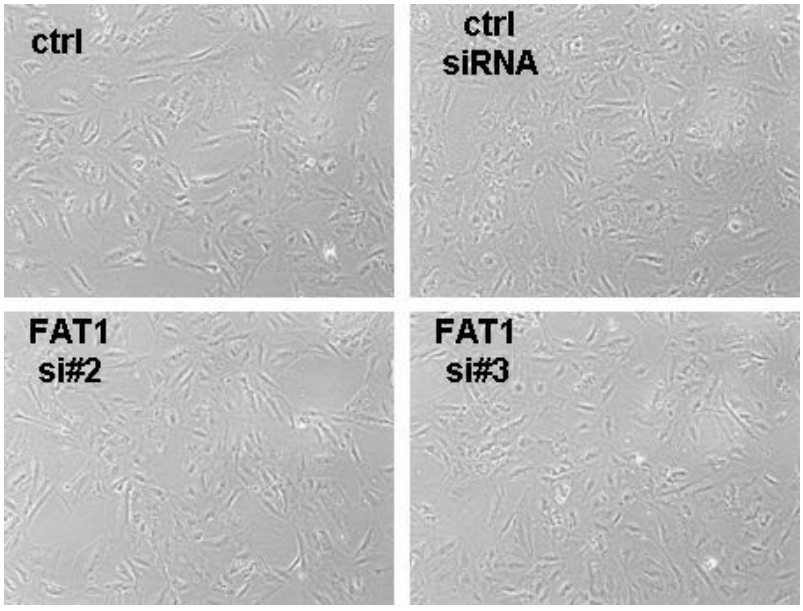

Figure 4.10 Morphology of untransfected cells (ctrl), control siRNA (ctrl siRNA), and FAT1 siRNA (FAT1 si#2, FAT1 si#3) transfected cells (magnification 40x).

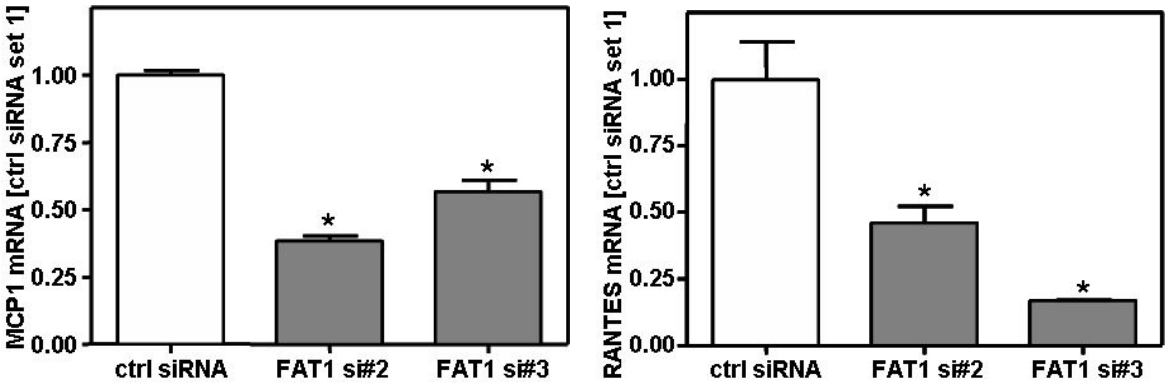

Figure 4.11 Effect of FAT1 suppression on expression of the inflammatory genes MCP1 and RANTES. *p<0.05 compared to control siRNA.

Both cytokines are regulated by NFκB, which plays a key role in regulating immune responses and cell survival. A decrease of NFκB activity is mainly considered as having anti-inflammatory and pro-apoptotic effects. The inactive form of NFκB is bound in the cytoplasm to IκBα and regulation of NFκB activity is mediated by phosphorylation, ubiquitinylation and subsequent degradation of IκBα. Consequently, NFκB is free and can translocate to the nucleus, where it binds to and activates the promoter of NFκB-dependent genes.

To analyze the activity of the NFκB pathway we performed Western blotting for IκBα. We could detect more IκBα in HSCs transfected with siRNA against FAT1. This indicates a reduced NFκB activity in FAT1 suppressed HSCs (Figure 4.12).

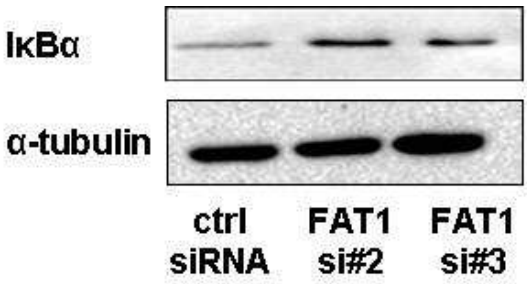

Figure 4.12 Western Blot analysis for IκBα and α-tubulin (housekeeper) in FAT1 suppressed cells and control cells.

Accordingly, an NFκB reporter gene assay confirmed reduced NFκB activity in FAT1 suppressed HSCs (Figure 4.13).

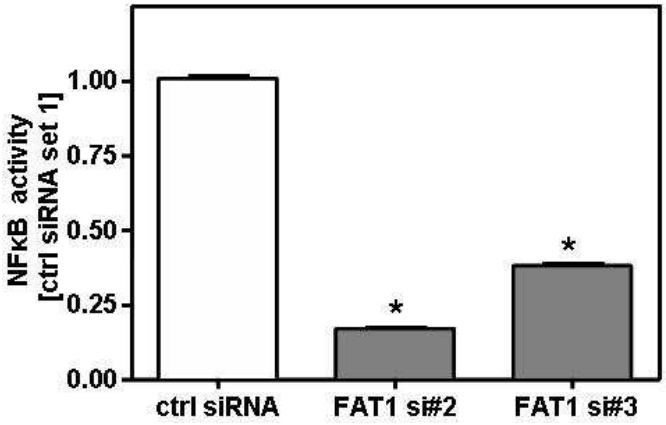

Figure 4.13 Reporter gene assay for NFκB activity in FAT1 suppressed (FAT1 si#2, FAT1 si#3) and control cells (ctrl siRNA). *p<0.05 compared to control siRNA..

In addition to its effect on proinflammatory gene expression NFκB has been shown to be critical for apoptosis resistance of activated HSCs (Hellerbrand et al. 1998; Oakley et al. 2005).

To investigate a functional role of FAT1 in apoptosis of HSCs we analyzed caspase-3/7 activity, which plays a key role in the cell death program. Caspase-3/7 activity was higher in staurosporine (STS) induced apoptotic cells after suppression of FAT1 compared to control cells (Figure 4.14).

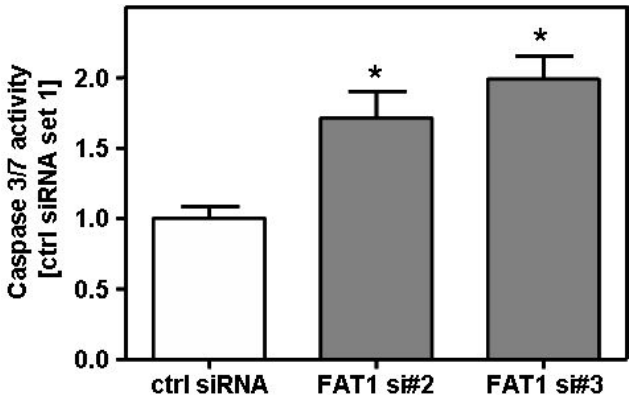

Figure 4.14 Analysis of caspase-3/7 activity in FAT1 suppressed and control HSCs after STS (500 nM; 4h) induced apoptosis. *p<0.05 compared to control siRNA.

In line with this, Annexin V and propidium iodide (PI) double staining and following FACS analysis of HSCs revealed higher STS-induced apoptosis rate of FAT1 suppressed cells compared to control cells (Figure 4.15).

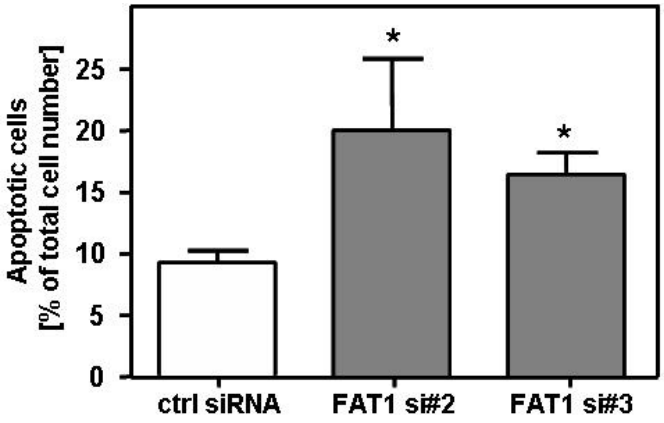

Figure 4.15 Assessment of STS-induced (500 nM, 4h) apoptosis by flow cytometry applying annexin V and propidium iodide (PI) staining. Depicted is the mean-percentage of total apoptotic cells from 3 independent experiments. *p<0.05 compared to control siRNA.

4.2 Expression and function of FAT1 in HCC

4.2.1 Expression of FAT1 in HCC cell lines and primary hepatocytes

First, the expression of FAT1 was analyzed in three different HCC cell lines (Hep3B, HepG2, and PLC) compared to primary human hepatocytes (PHH). Quantitative RT-PCR analysis showed an upregulation of FAT1 expression in HCC cells compared to PHH. HepG2 cells demonstrate highest FAT1 mRNA levels within the HCC cell lines, Hep3B and PLC display similar FAT1 expression (Figure 4.16).

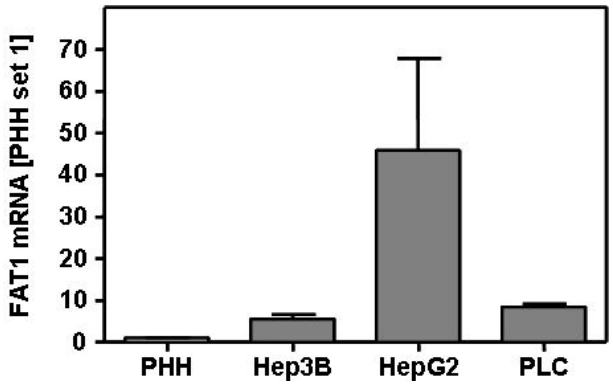

Figure 4.16 qPCR analysis of FAT1 mRNA in HCC cell lines (Hep3B, HepG2, PLC) and primary human hepatocytes (PHH).

To verify these results, we analyzed FAT1 protein expression in these cells by Western blotting. Thereby, overexpression of FAT1 in HCC cell lines compared to primary hepatocytes was shown (Figure 4.17).

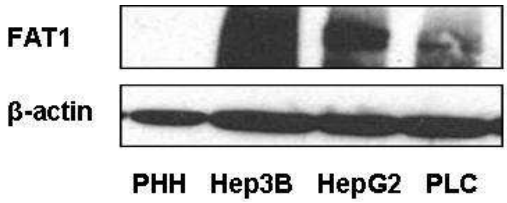

Figure 4.17 Western Blot analysis for FAT1 protein and β-actin in HCC cell lines (Hep3B, HepG2, PLC) and PHH.

To evaluate whether this result can be confirmed *in vivo* we next examined FAT1 expression in tumor tissues of 14 HCC patients compared to corresponding non-

neoplastic liver tissues. Similarly, quantitative RT-PCR revealed a significant upregulation of FAT1 expression in cancerous tissue (Figure 4.18).

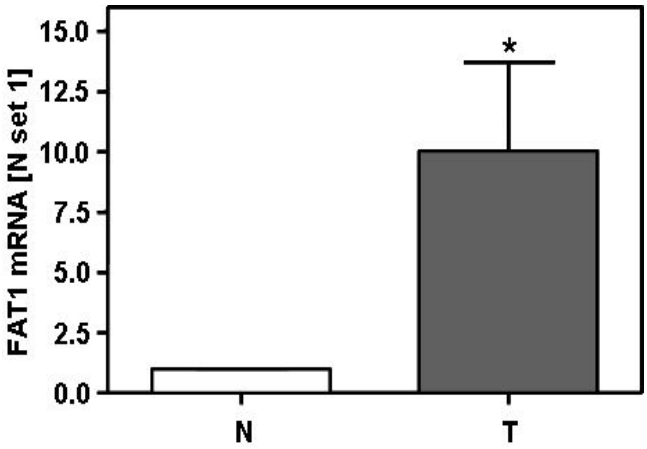

Figure 4.18 FAT1 mRNA expression in tumor tissue (T) and corresponding non-tumorous tissue (N). *p<0.05 compared to N.

To further evaluate the functional effects of FAT1 upregulation in HCC *in vivo*, we analyzed FAT1 protein expression in a series of 112 human HCC tissues, applying TMA technology. Membranous FAT1 staining intensity varied significantly in individual patients. For descriptive data analysis, HCC were separated into tissues with strong and weak immunosignal (representative examples are depicted in Figure 4.19), and immunohistochemical results were correlated with clinicopathological tumor characteristics (Table 3.1).

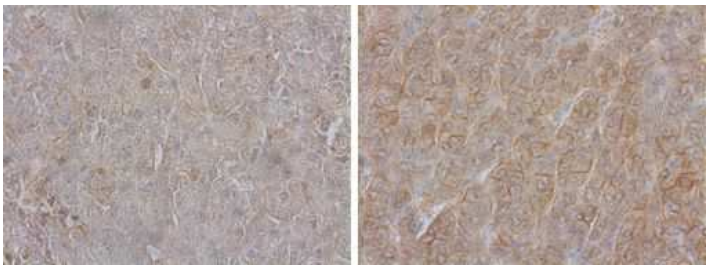

Figure 4.19 Immunohistochemical staining of FAT1 in HCC tissues with strong (right panel) and weak (left panel) membranous staining (magnification 100x).

A strong membranous FAT1 staining was significantly associated with higher tumor stage (p=0.042) and a higher proliferation index (Ki67 staining; p=0.040). No correlation was found between FAT1 expression and tumor staging, age, sex, or tumor size.

Table 4.1 FAT1 immunoreactivity (IR) in HCC-tissues of 112 patients in relation to clinicopathological characteristics and proliferation rate.

Variable	Categorization	n	%	**FAT1 IR negative**	**FAT1 IR positive**	***p****
Clinico-pathological characteristics						
Age at diagnosis						
	<60 years	40	*35,7*	13	27	1.000
	≥60 years	72	*64,3*	23	49	
Gender						
	female	17	*15,2*	3	14	0.259
	male	95	*84,8*	33	62	
Tumor stage						
	pT1	42	*37,5*	17	25	**0.042**
	pT2	27	*24,1*	12	15	
	pT3	38	*33,9*	6	32	
	pT4	3	*2,7*	1	2	
	nd	2	*1,8*	0	2	
Histological grade						
	G1	42	*37,5*	14	28	1.000
	G2	59	*52,7*	19	40	
	G3	11	*9,8*	3	8	
Tumor size						
	≤ 5 cm	60	*53,6*	19	41	0.921
	> 5 cm	36	*32,1*	11	25	
	nd	16	*14,3*	6	10	
Cirrhosis						
	no	31	*27,7*	13	18	0.246
	yes	77	*68,7*	23	54	
	nd	4	*3,6*	0	4	
Proliferation rate (MIB1-Index)						
	≤ 5%	46	*41,1*	20	26	**0.040**
	> 5%	66	*58,9*	16	50	

* Fisher's exact test (2-sided); bold face representing *p*-values <0.05.
(nd: no data available; IR: immunoreactivity)

4.2.2 Functional role of FAT1 in HCC cells

4.2.2.1 Suppression of FAT1 by siRNA transfection

To gain insight into the functional role of increased FAT1 in HCC cell lines, FAT1 was suppressed by transient transfection with specific siRNA. Quantitative RT-PCR analysis revealed a strong suppression of FAT1 mRNA expression in transfected cell lines after 3d, whereas no change of FAT1 expression was seen on protein level. It lasted as far as day 8 until a downregulation of FAT1 expression on protein level was achieved (Figure 4.20).

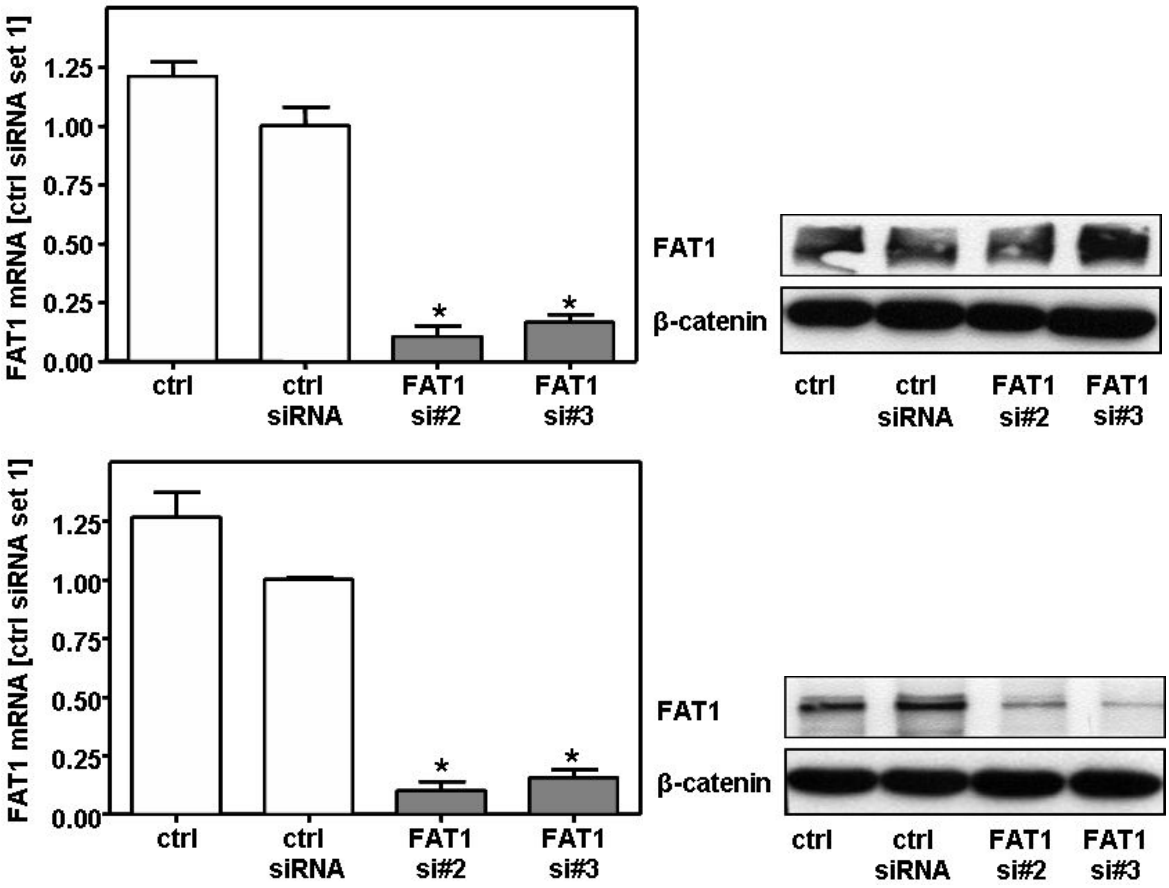

Figure 4.20 Analysis of FAT1 in control cells (ctrl), control siRNA (ctrl siRNA) and FAT1 siRNA (FAT1 si#2, FAT1 si#3) transfected HCC cells by qRT-PCR and Western Blot 3d (upper panel) and 8d (lower panel) after transfection. *p<0.05 compared to control siRNA.

These data indicated a high protein stability of FAT1. To further clarify this result protein synthesis was inhibited by cycloheximide (Cyclo). Subsequent Western Blot analysis showed that FAT1 protein expression can be detected until 48 h after blocking protein synthesis in HCC cells, and that confirmed a long half life of FAT1 protein (Figure 4.21).

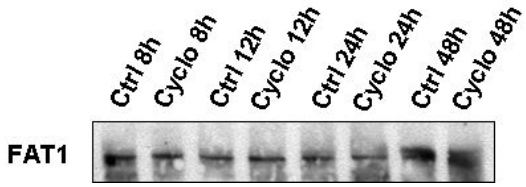

Figure 4.21 FAT1 protein analysis in HCC cell lines at different time points after stimulation with cycloheximide (Cyclo; 50 µg/ml).

4.2.2.2 Stable transfected cell clones

Since it required repeated and longtime (transient) transfection with siRNA to reach sufficient suppression of FAT1 (see 4.2.2.1) we prepared stable suppressed HCC cell clones. As a further advantage stably transfected cells allow the use for *in vivo* studies (see 4.2.3).

FAT1 was suppressed by stable transfection with a shRNA expressing vector containing the sequence of FAT1 siRNA (clone 1 and 2). The vector without an insert was used as a control (mock). Quantitative RT-PCR analysis revealed a suppression of FAT1 mRNA expression in the cell clones (FAT1 shRNA#1, FAT1 shRNA#2). Downregulation of FAT1 expression in the cell clones was confirmed on protein level by western blot (Figure 4.22).

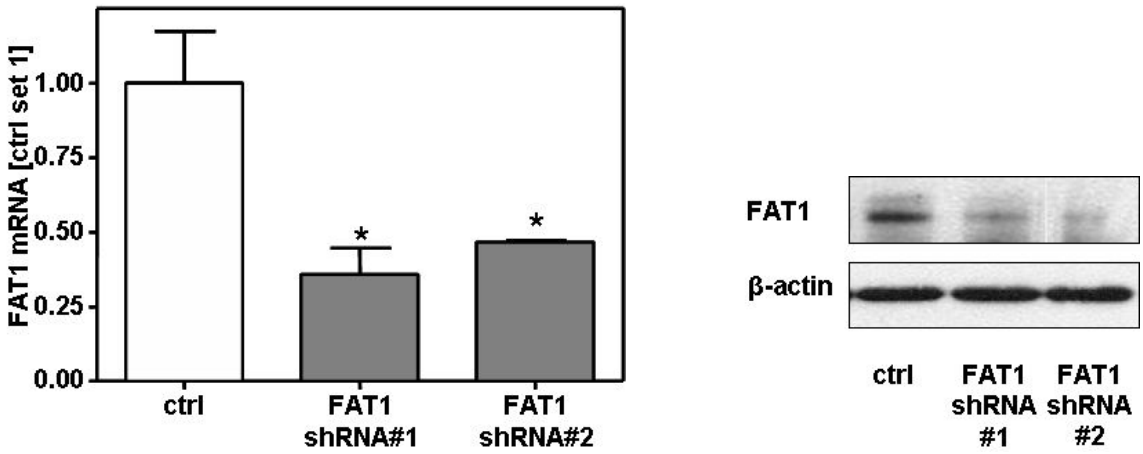

Figure 4.22 FAT1 mRNA (left panel) and protein (right panel) expression in stable transfected cell clones (FAT1 shRNA#1, FAT1 shRNA#2) and mock transfected controls (ctrl). **p*<0.05 compared to control.

Cell morphology did not differ between mock transfected controls and stable FAT1 suppressed HCC cells (Figure 4.23).

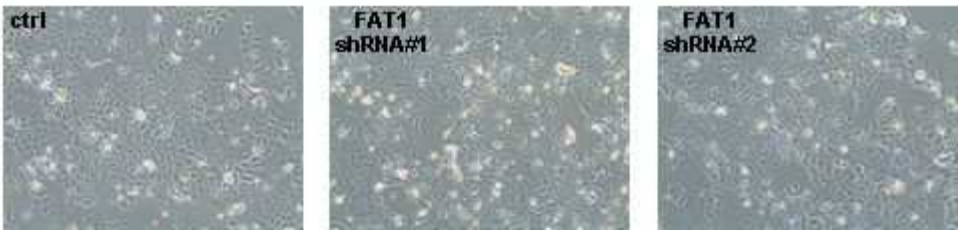

Figure 4.23 Morphology of mock-transfected cells (ctrl) and FAT1 shRNA (FAT1 sh#1, FAT1 sh#2) transfected cells (magnification 40x).

Further, expression of markers for cell differentiation E-Cadherin and Snail were not influenced by FAT1 suppression (Figure 4.24).

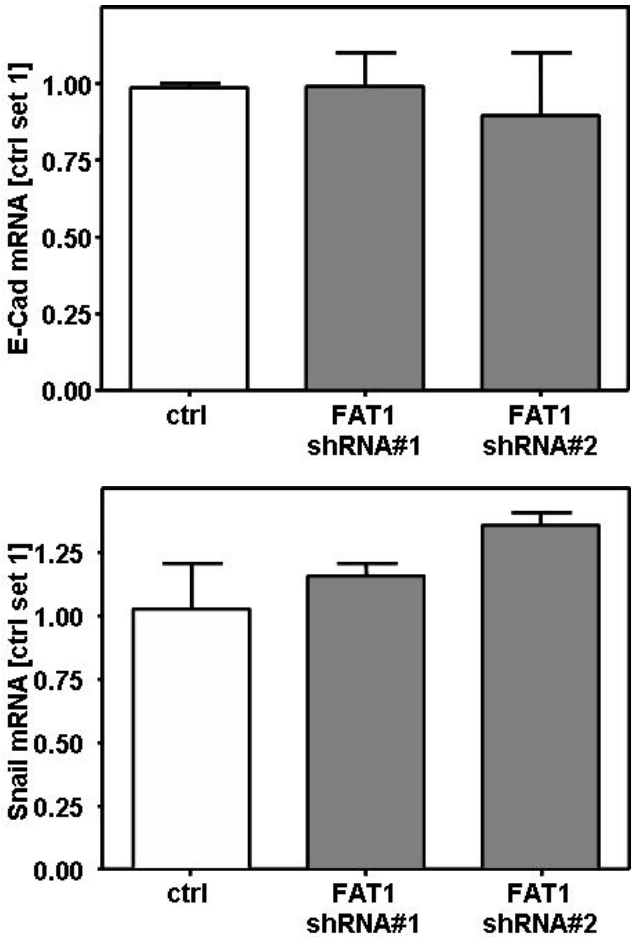

Figure 4.24 E-Cadherin (E-Cad) and Snail mRNA expression in FAT1 suppressed cells (FAT1 shRNA#1, FAT1 shRNA#2) and control cells.

4.2.2.3 Functional changes upon stable transfection

To ascertain the functional role of FAT1 in HCC, we performed functional *in vitro* assays with stable FAT1 suppressed cells.

HCC cells with stable suppressed FAT1 expression showed a prolonged doubling time (Figure 4.25).

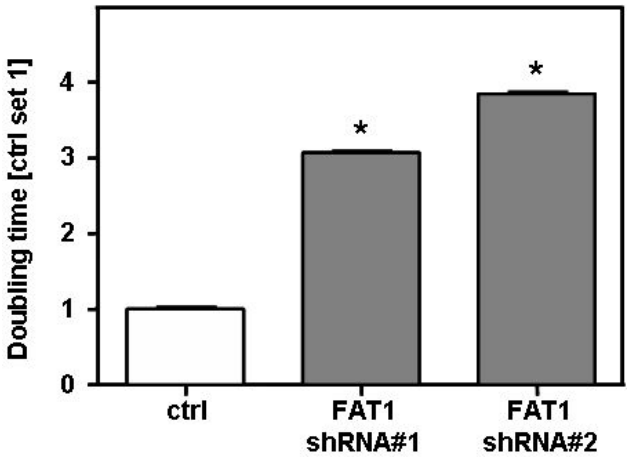

Figure 4.25 Doubling time of stable transfected cell clones (FAT1 shRNA#1, FAT1 shRNA#2) and control cells. **p*<0.05 compared to control.

Next, we analyzed whether FAT1 suppression affects the migratory potential of HCC cells. Therefore, the Cultrex cell migration assay and the ROCHE RTCA XCELLigence system were used (see also chapters 3.13.3 and 3.13.4) and a short time span of 5 h was chosen to exclude anti-proliferative effects of FAT1 suppression. Noteworthy, we observed a significant inhibition of cell migration after suppression of FAT1 (Figure 4.26).

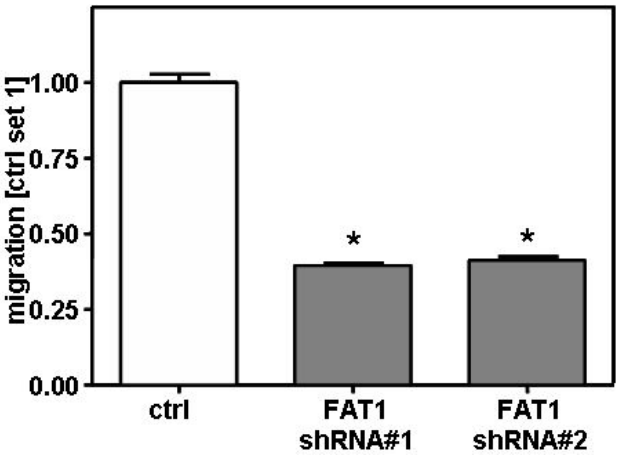

Figure 4.26 Migration analysis of stable FAT1 suppressed HCC cells (FAT1 shRNA#1, FAT1 shRNA#2) and mock transfected control cells. **p*<0.05 compared to control.

We further investigated the effect of stable FAT1 suppression on apoptosis in HCC cells after serum starvation for 48 h. Notably, Annexin V and propidium iodide (PI) double staining and following FACS analysis revealed a higher apoptosis rate in cells with suppressed FAT1 expression compared to control cells (Figure 4.27).

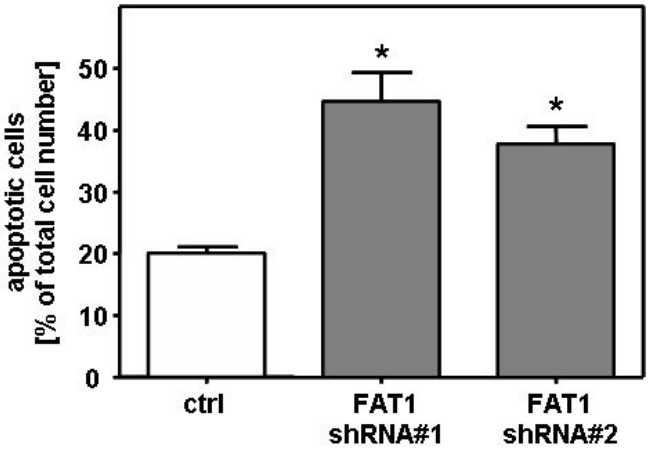

Figure 4.27 Assessment of apoptosis by flow cytometry applying annexin V and propidium iodide (PI) staining. Depicted is the mean-percentage of total apoptotic cells from 3 independent experiments. *p<0.05 compared to control.

In accordance with this, caspase-3 activity was significantly higher in FAT1 suppressed cells compared to control cells with serum starvation (Figure 4.28).

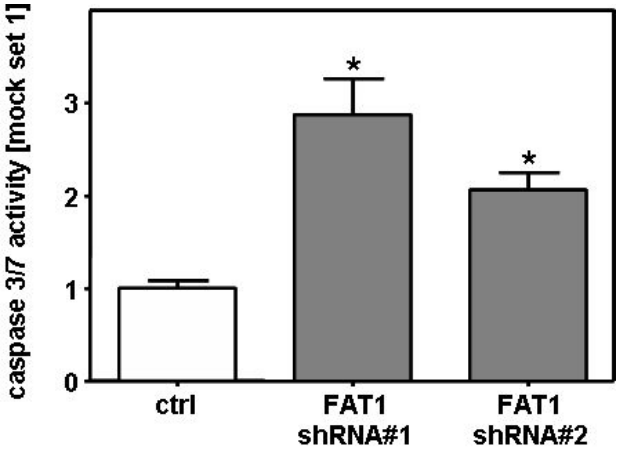

Figure 4.28 Analysis of caspase-3/7 activity in FAT1 suppressed (FAT1 shRNA#1, FAT1 shRNA#2) and mock transfected (ctrl) HCC cells after serum starvation. *p<0.05 compared to control.

4.2.3 Function of FAT1 in HCC cells *in vivo* in the nude mouse model

To test the effect of FAT1 on tumor growth *in vivo*, HCC cells stably suppressing FAT1 were injected subcutaneously into nude mice. Tumors derived from FAT1 suppressing HCC cell clones showed delayed tumor onset compared to tumors derived from mock transfected control cells (Figure 4.29).

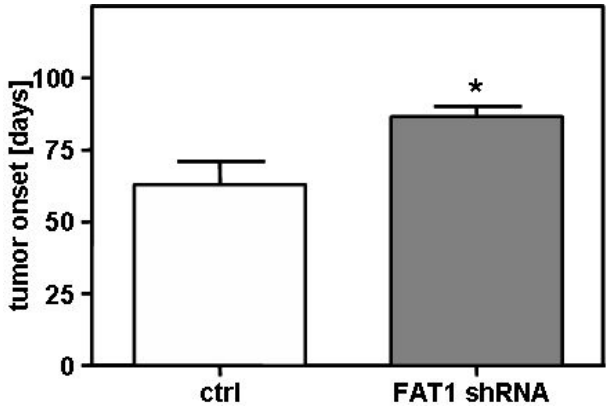

Figure 4.29 Onset of tumors derived from FAT1 suppressed (FAT1 shRNA, n=9) or control cells (ctrl, n=8) implanted in nude mice. *p<0.05 compared to control.

Expression analysis revealed preservation of FAT1 mRNA suppression in tumors derived from FAT1 suppressed cell clones compared to controls (Figure 4.30).

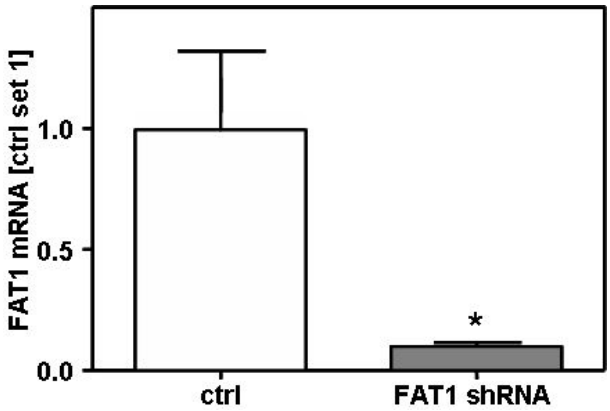

Figure 4.30 FAT1 mRNA expression in tumors derived from FAT1 suppressed HCC cells (FAT1 shRNA) and control cells (ctrl). *p<0.05 compared to control.

Further, we analyzed the proliferation rate by immunohistochemical staining for Ki67 in the tumor tissue. Ki67 labeling revealed very high mitogenic activity in both tumors derived from FAT1 suppressed and control cells. Therefore no significant difference in the proliferation rate could be observed (Figure 4.31).

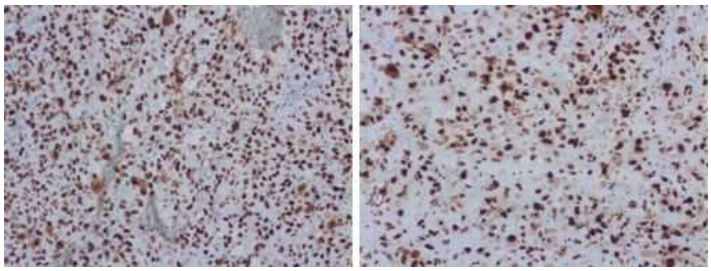

Figure 4.31 Immunohistochemical staining of Ki67 in tumors derived from control-transfected cells (left panel) or from FAT1 suppressed cell clones (right panel) (magnification 100x).

Analysis of apoptotic cells by using the terminal deoxynucleotidyl transferase dUTP nick-end labeling system (TUNEL staining) showed only few apoptotic cells in control-transfected HCC derived tumors, whereas the FAT1 suppressing tumors displayed large apoptotic areas (Figure 4.32).

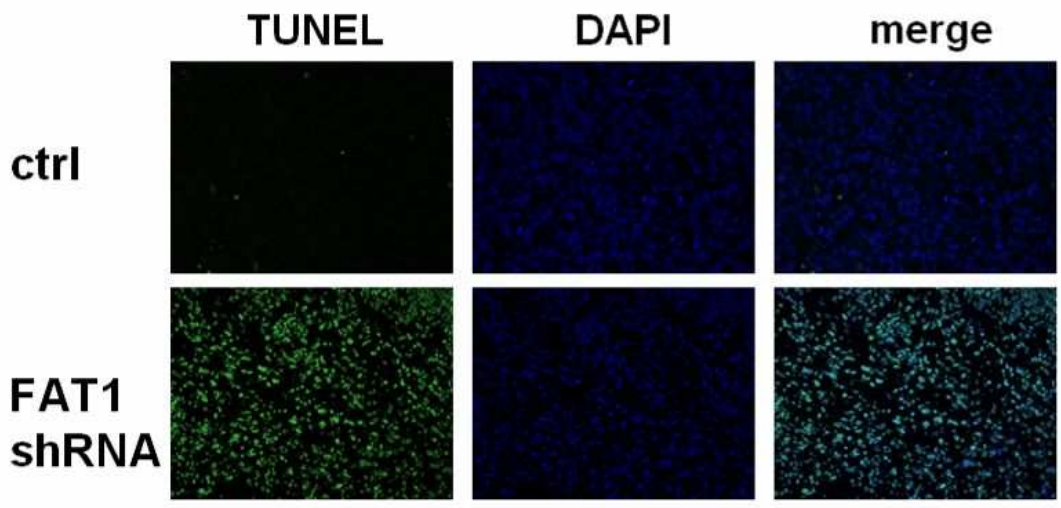

Figure 4.32 Analysis of apoptotic cells in tumor tissue derived from control transfected cells (ctrl) and FAT1 suppressed cell clones (FAT1 shRNA) using TUNEL staining (green) and DAPI staining for nuclei (blue) (magnification 40x).

In summary, data obtained in nude mice indicate that enhanced FAT1 expression induces tumorigenicity of HCC cells.

4.2.4 Regulation of FAT1 expression

4.2.4.1 Effect of activated HSCs on FAT1 expression in HCC cells

Our group has shown that hepatic stellate cells (HSCs) secrete factors by which they promote HCC progression *via* different signal cascades (Amann et al. 2009a). This prompted us to examine the effect of conditioned media (CM) from activated HSCs on FAT1 mRNA expression in HCC cells. Quantitative RT-PCR showed an increase of FAT1 mRNA after incubating HepG2 cells with CM (Figure 4.33).

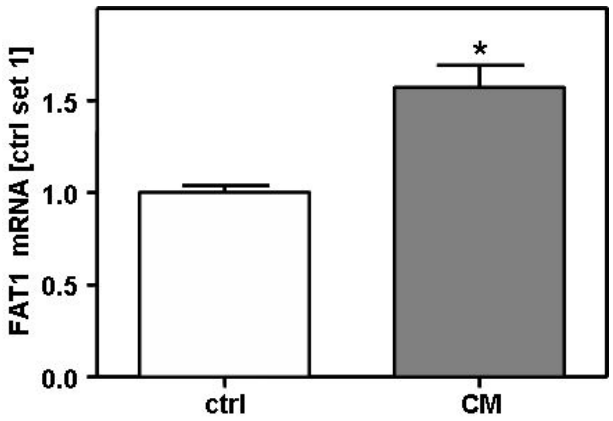

Figure 4.33 FAT1 mRNA expression in HepG2 cells stimulated with conditioned media from activated HSCs (CM) and control media (ctrl). *p<0.05 compared to control.

In search for the factors in CM of activated HSCs responsible for FAT1 upregulation we focused on hepatic growth factor (HGF), a factor known to act protumorigenic during hepatocancerogenesis. Stimulation of HCC cells with HGF induced a dose-dependent upregulation of FAT1 mRNA expression (Figure 4.34).

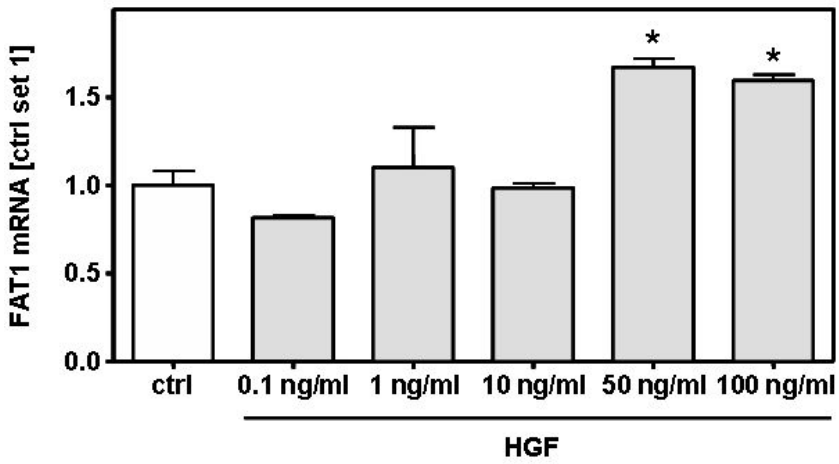

Figure 4.34 Analysis of FAT1 mRNA expression in HCC cells stimulated with different concentrations of HGF. *p<0.05 compared to control.

Western Blot analysis confirmed induction of FAT1 expression in HCC cells by HGF on protein level (Figure 4.35).

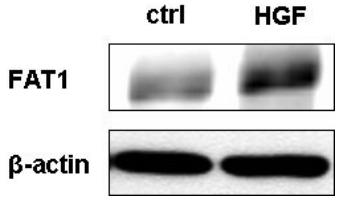

Figure 4.35 Analysis of FAT1 protein expression incubated with HGF [50 ng/ml].

Preincubation of CM of activated HSCs with anti-HGF antibodies completely abrogated the stimulating effect on FAT1 (Figure 4.36).

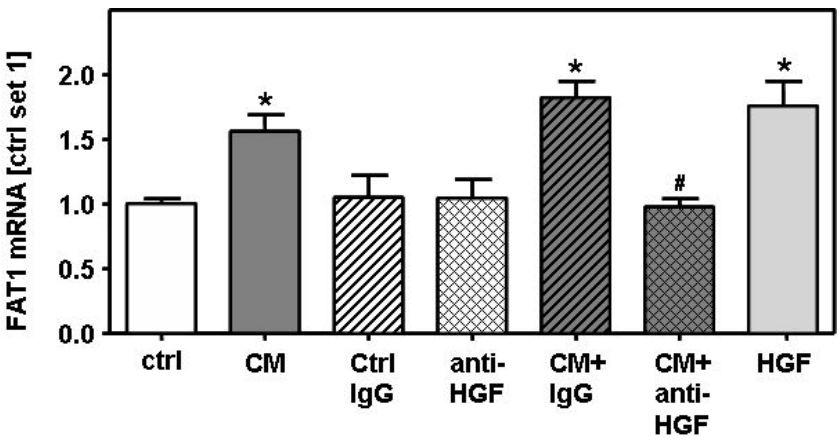

Figure 4.36 Effect of anti-HGF antibodies on FAT1 mRNA expression in the presence of CM. CM was preincubated with anti-HGF antibodies or isotype marched control antibodies (ctrl IgG). Stimulation with HGF (50 ng/ml) revealed a similar effect as CM. *p<0.05 compared to control; # p<0.05 compared to CM.

Together, these data indicate that activated HSCs induce FAT1 expression in HCC cells *via* HGF.

4.2.4.2 Regulation of FAT1 expression in HCC cells under anaerobic conditions

HGF has been shown to enhance hypoxia inducible factor 1 alpha (HIF1α) activity in HCC cells (Tacchini et al. 2001). This transcription factor is an important mediator of hypoxic adaption of tumor cells and promotes tumorigenicity (Kim et al. 2002). Induction of hypoxia by incubating the cells with reduced oxygen concentration (1%) or by incubation with the chemical inducer Dipyridyl (DP) caused a significant upregulation of FAT1 mRNA expression in HCC cells (Figure 4.37). Interestingly, Western Blot analysis demonstrated stabilization of HIF1α in DP treated cells (Figure 4.38).

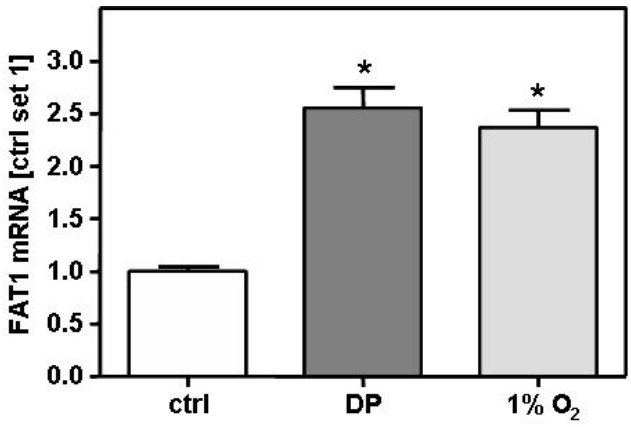

Figure 4.37 Analysis of FAT1 mRNA expression in HCC cells cultured under normoxic conditions, with pharmaceutical induction of hypoxia (DP, 100 µmol/L) or 1% oxygen (1% O_2). *p<0.05 compared to control.

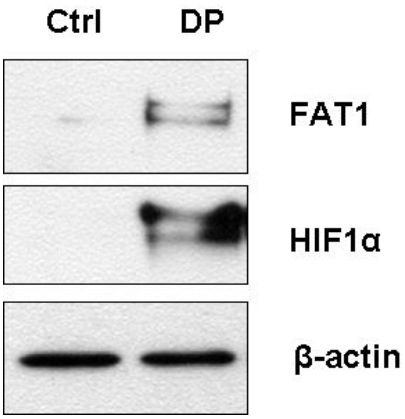

Figure 4.38 FAT1 and HIF1α protein expression after chemical induction of hypoxia by DP (100 µmol/L).

Further, FAT1 upregulation under DP-induced hypoxia was strongly repressed by echinomycin (Ech), a pharmaceutical inhibitor of HIF1α activity (Kong et al. 2005) (Figure 4.39).

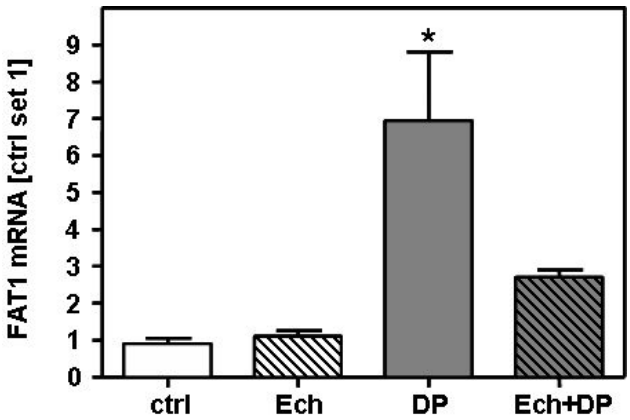

Figure 4.39 FAT1 mRNA expression with or without pharmaceutical induction of hypoxia (DP, 100 µmol/L) and HIF1α inhibition with echinomycin (Ech, 10 nmol/L).*p<0.05 compared to control.

In line with this finding, transient transfection with a dominant-negative variant of HIF1α (dnHIF1α) (Warnecke et al. 2004) led to diminished hypoxia induced FAT1 expression (Figure 4.40).

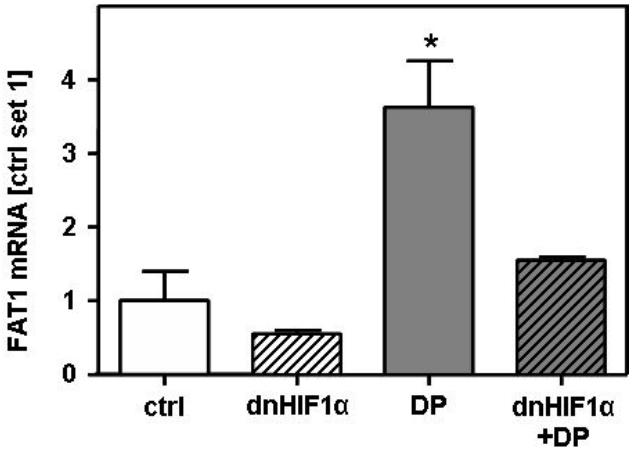

Figure 4.40 Analysis of FAT1 mRNA after transfection of HCC cells with a dominant-negative variant of HIF1α (dnHIF1α) or a control plasmid (ctrl) with or without stimulation with DP (100 µmol/L). **p*<0.05 compared to control.

In silico analysis of the FAT1 promoter did not shown an HIF1 binding site (Tess, http://www.cbil.upenn.edu/cgi-bin/tess/tess?RQ=WELCOME;Genomatix software). Furthermore, costimulation with cycloheximide, an inhibitor of protein synthesis, abolished hypoxia-induced upregulation of FAT1 mRNA expression in HCC cells (Figure 4.41).

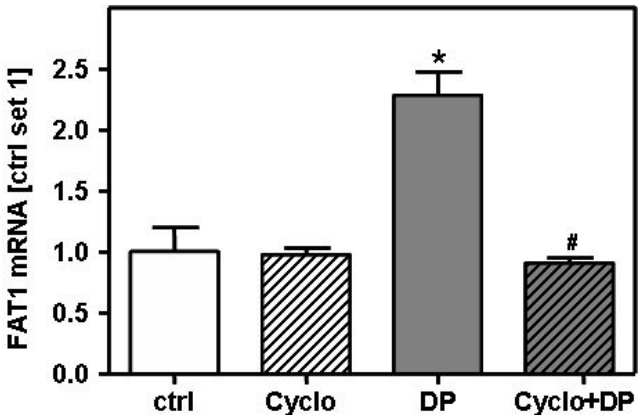

Figure 4.41 FAT1 mRNA expression in DP (100 µmol/L) stimulated cells with or without blocking protein synthesis by cycloheximide (Cyclo, 50 µg/ml). **p*<0.05 compared to control; #*p*<0.05 compared to DP.

Together, these data indicated that hypoxia or HIF1α, respectively, do not directly induce FAT1 expression on transcriptional level. It is known that hypoxia can cause epigenetic modifications as demethylation (Shahrzad et al. 2007). Of note, incubation with 5-azacytidine (Aza) and adenosine periodate oxidized (Adox),

inhibitors of DNA methylation, caused a dose-dependent upregulation of FAT1 expression in HCC cells (Figure 4.42).

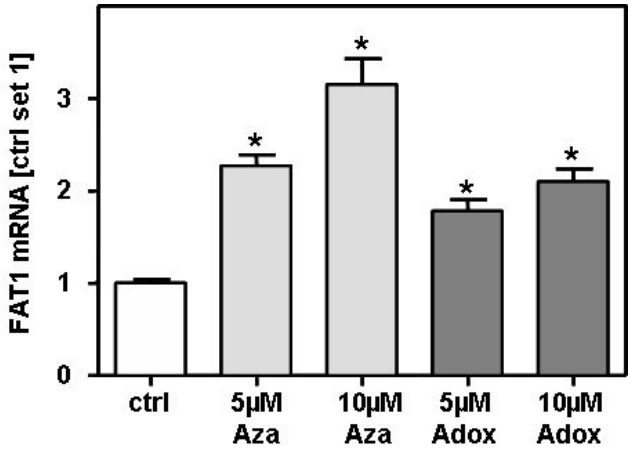

Figure 4.42 Fat1 mRNA expression in HCC treated with different doses of 5-azacytidine (Aza) and Adenosine periodate oxidized (Adox). *p<0.05 compared to control.

These data suggested that hypoxia induced FAT1 expression may also be caused by demethylation. Most recently, it has been shown by Liu et al., that hypoxia induced DNA demethylation in HCC is caused through activation of HIF1α and transcriptional upregulation of methionine adenosyltransferase II, alpha (MAT2A). Consecutively, increased MATII activity leads to reduced levels of the methyl donor S-adenosylmethionine (SAM) (Liu et al. 2011). Also we observed reduced SAM-levels in the supernatant of HCC cells in chemical hypoxia (Figure 4.43).

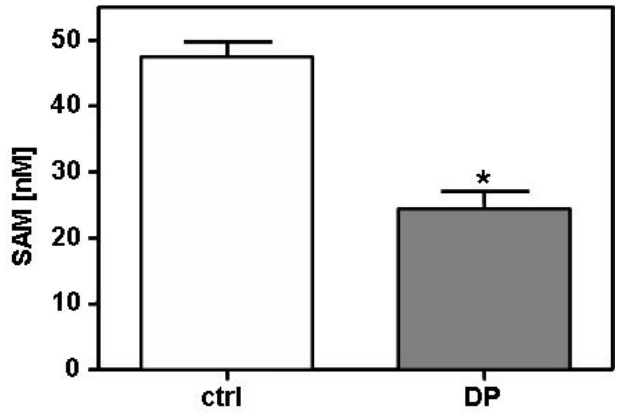

Figure 4.43 Analysis of S-adenosylmethionine (SAM) level in the supernatant of HCC cells after induction of hypoxia with DP (100 µmol/L) for 24 h. *p<0.05 compared to control.

Replenishment of SAM in culture medium of HCC cells dose-dependently inhibited hypoxia induced FAT1 expression (Figure 4.44). Cells were stimulated with higher concentrations of SAM than found in the supernatant, but in the literature even higher doses for stimulation of HCC cells can be found (Ou et al. 2007; Yang et al. 2004)

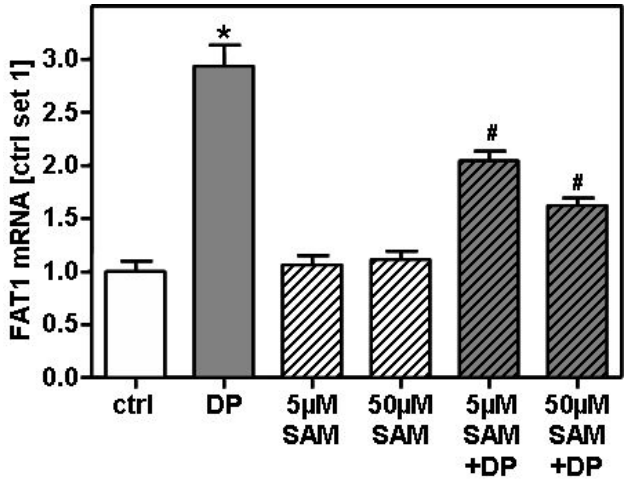

Figure 4.44 FAT1 mRNA expression in HCC cells stimulated with different doses of S-adenosylmethionine (SAM). Subsequently cells were stimulated with DP (100 µmol/L) to induce hypoxia (DP). *p<0.05 compared to control, #p<0.05 compared to DP.

These findings indicate that hypoxia induced FAT1 expression in HCC cells *via* MAT2A induced SAM depletion and subsequent demethylation.

To verify these findings *in vivo* we assessed FAT1 and vascular endothelial growth factor (VEGF) expression in 25 human HCC specimens. VEGF is highly regulated by HIF1α in HCC (Huang et al. 2005), and notably, we found a significant correlation between VEGF and FAT1 expression in HCC tissues Furthermore, FAT1 and MAT2A expression showed a significant correlation in HCC (Figure 4.45).

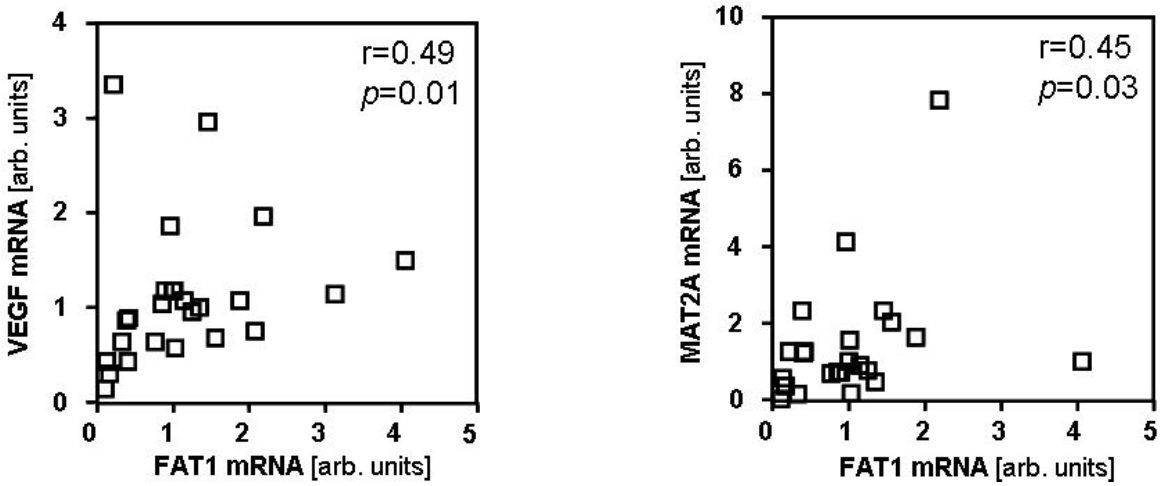

Figure 4.45 Correlation of FAT1 with vascular endothelial growth factor (VEGF, left panel) and methionine adenosyltransferase II, alpha (MAT2A, right panel) mRNA expression in HCC tissue (n=24).

Together, these data suggested that also *in vivo* hypoxia is a critical regulator of FAT1 expression in HCC. This effect seems to be at least in part mediated *via* enhanced MAT2A expression and subsequent depletion of SAM levels leading to demethylation of the FAT1 promoter.

5 Discussion

FAT1 is a member of the atypical cadherin family and has been implicated in various biological processes such as cell polarity, proliferation, and migration (see chapter 2.6.1.1). Cancer research revealed deregulated FAT1 expression (see chapter 2.6.1.2).
The aim of this thesis was to investigate FAT1 in the liver based on the fact that up till now no data addressing this issue existed. In particular, we analyzed FAT1 expression and function in chronic liver disease and hepatic stellate cells as central mediators of hepatic fibrosis as well as FAT1 expression and function in hepatocellular carcinoma *in vitro* and *in vivo*.

The discussion is divided into two main chapters according to the arrangement of the results in chapter 4:

5.1 FAT1 and chronic liver disease
5.2 FAT1 and hepatocellular carcinoma

5.1 FAT1 and chronic liver disease

While in healthy adult liver hepatocytes reveal only a minimal replication rate, they start to proliferate in response to liver injury (Taub 2004). We observed a marked upregulation of FAT1 expression in different murine models of liver injury as well as in diseased human livers. Unexpectedly, immunohistochemistry revealed no significant increase of FAT1 expression in hepatocytes of diseased livers compared to healthy control livers. However and interestingly, a strong immunosignal was observed in myofibroblast-like cells in fibrotic septa of cirrhotic livers, and we found a strong upregulation in HSCs during *in vitro* activation. Moreover, hepatic FAT1 expression revealed a striking correlation with the expression of collagen alpha I(1), the major component of type I collagen. Upon hepatic injury this fibrillar collagen is produced by activated HSCs and constitutes the most abundant extracellular matrix protein in fibrotic liver tissue. Together these data strongly indicate activated HSCs as the cellular source of increased FAT1 expression in diseased livers. A previous study showed increased FAT1 expression in injured arteries and identified vascular smooth muscle cells as

cellular source (Hou et al. 2006). In vascular injury as well as in chronic kidney disease and an epithelial cell wound model FAT1 seems to be necessary for efficient wound healing. Also HSC activation and hepatic fibrosis can be considered as physiological wound healing process in response to acute hepatic injury. However, upon persistent hepatocellular injury excessive or dysregulated fibrosis leads to a distortion of the hepatic architecture and can lead to severe organ dysfunction. The correlation between FAT1 and collagen alpha I (1) expression and the increased expression during HSC activation strongly suggest that this atypical cadherin also plays a critical role in hepatic fibrosis. Furthermore, we newly link FAT1 expression to apoptosis resistance in activated HSCs. We and others have shown that the activation of the transcription factor NFκB markedly increases during HSC activation and strongly contributes to the resistance to apoptosis in activated HSCs (Hellerbrand et al. 1998; Oakley et al. 2005). Notably, we found that suppression of FAT1 led to a significant reduction of NFκB-activity in activated HSCs. This strongly indicates that the effect of FAT1 on apoptosis is at least in part mediated *via* NFκB activation.

Although fibrosis is a progressive pathological process there is emerging experimental and clinical evidence that even cirrhosis is potentially reversible. Key to this is the discovery that reversion of fibrosis is accompanied by clearance of activated HSCs by apoptosis (Elsharkawy et al. 2005).

5.2 FAT1 and hepatocellular carcinoma

The specific function of FAT1 in cancer development and progression is still under investigation. There are contrasting studies about the role of FAT1 in human cancers, pointing towards a dual role of FAT1 as both an oncogene as well as a tumor suppressor (Kwaepila et al. 2006; Settakorn et al. 2005). Here, we found increased FAT1 expression in HCC cells and tissues compared to primary human hepatocytes and non-tumorous liver tissue, and strong FAT1 expression significantly correlated with higher tumor stages and higher mitotic activity. These findings indicated a protumorigenic effect of FAT1 in HCC, and functional studies confirmed that FAT1 promotes the tumorigenicity of HCC cells *in vitro* and *in vivo.* FAT1 has been shown to affect different biological mechanisms. Similar as described in squamous cell carcinoma and glioma cells, we observed reduced migratory potential in HCC cells upon FAT1 suppression (Chosdol et al. 2009;

Dikshit et al. 2012), while FAT1 seems to inhibit progression to invasive phenotype in breast cancer (Lee et al. 2012). In cholangiocarcinoma, Settakorn *et al.* found that FAT1 expression showed a significant inverse association with the Ki67 index and that loss of membrane localization for FAT1 correlated with more aggressive tumors (Settakorn et al. 2005). In non-malignant vascular smooth muscle cells FAT1 knockdown decreased migration *in vitro*, but surprisingly and in contrast to our findings in HCC cells, enhanced proliferation *in vitro* (Hou et al. 2006).

These findings indicate varying effects of FAT1 on proliferation and migration in different cell types. FAT1 has also been engaged in several other biological functions as cell polarity (Moeller et al. 2004), but available literature had not yet functionally linked FAT1 to apoptosis. Here, we demonstrated that FAT1 downregulation impairs the resistance of HCC cells against induced apoptosis *in vitro*, and also *in vivo* tumors derived from FAT1 cells with repressed FAT1 expression revealed significantly more apoptotic cells than tumors derived from control cells. Together these data indicate that increased FAT1 expression in HCC acts protumorigenic.

In search for the molecular mechanism responsible for the transcriptional upregulation of FAT1 in HCC we first looked at factors secreted by activated hepatic stellate cells. These cells do not only form and infiltrate the HCC stroma (Dubuisson et al. 2001; Faouzi et al. 1999; Le Bail B. et al. 1999), but also induce tumorigenicity in HCC cells *in vitro* and *in vivo* (Amann et al. 2009a). We identified HGF as a strong inducer of FAT1 expression in HCC cells. The exact role of HGF in HCC development and progression has not yet been defined. On the one hand, the growth of different HCC cell lines was reduced in the presence of HGF (Shiota et al. 1992; Tajima et al. 1991), and transgenic animals expressing HGF in the liver inhibited hepatocarcinogenesis in bitransgenic mice overexpressing c-myc (Santoni-Rugiu et al. 1996) or transforming growth factor alpha (TGFα) (Shiota et al. 1995). On the other hand, HGF transgenic mice which are overexpressing HGF more rapidly developed HCC in the DEN model of chemically induced hepatocancerogenesis (Horiguchi et al. 2002).

We found that HGF effects on FAT1 activation are not mediated *via* the classical HGF-c-Met signaling pathway but *via* increased activation of HIF1α. Activation of this transcription factor has been shown to play a critical role in HCC progression (Huang et al. 2005; Kim et al. 2002; Tanaka et al. 2006). In addition to HGF

induction HIF1α is typically stabilized and herewith leads to an activation of this pathway by hypoxia. Hypoxic conditions frequently occur in tumor tissue and are another critical promoter of HCC progression (Rosmorduc and Housset 2010). Interestingly, we found that hypoxia and HIF1α effects, respectively, on FAT1 expression are not mediated on the transcriptional level but epigenetic mechanisms. Specifically, we found that hypoxia leads to reduced levels of the methyl donor S-adenosylmethionine (SAM) in HCC cells, and replenishment of SAM abrogates hypoxia induced FAT1 expression in HCC cells *in vitro*. A recent study by Liu *et al.* identified HIF1α dependent upregulation of methionine adenosyl transferase 2A (MAT2A) as novel mechanism how hypoxia induces DNA demethylation (Liu et al. 2011).

Methionine adenosyltransferase is the only enzyme responsible for the reaction from methionine and ATP to SAM. There are two genes (MAT1A, MAT2A) for two homologous catalytic MAT subunits (MATI, MATII). While MAT1A is mainly expressed in healthy liver, during the progression of HCC a switch from MAT1A to MAT2A takes place (Cai et al. 1996). This leads to reduced SAM levels due to the lower enzymatic activity of MATII compared to MATI (Lu and Mato 2008).

Here, we found that incubation with demethylating agents significantly enhanced FAT1 expression in HCC cells *in vitro* and observed a significant correlation between FAT1 and MAT2A in HCC tissues. A model of FAT1 regulation in HCC cells can be postulated as follows: HGF induced or hypoxia mediated HIF1α activation enhances MAT2A expression. Consecutively, increased MATII activity and consequently reduced MATI activity in summary cause reduced levels of the methyl donor SAM, and subsequently, reduced methylation including the FAT1 promoter and higher FAT1 expression, respectively. This working model is summarized in Figure 5.1

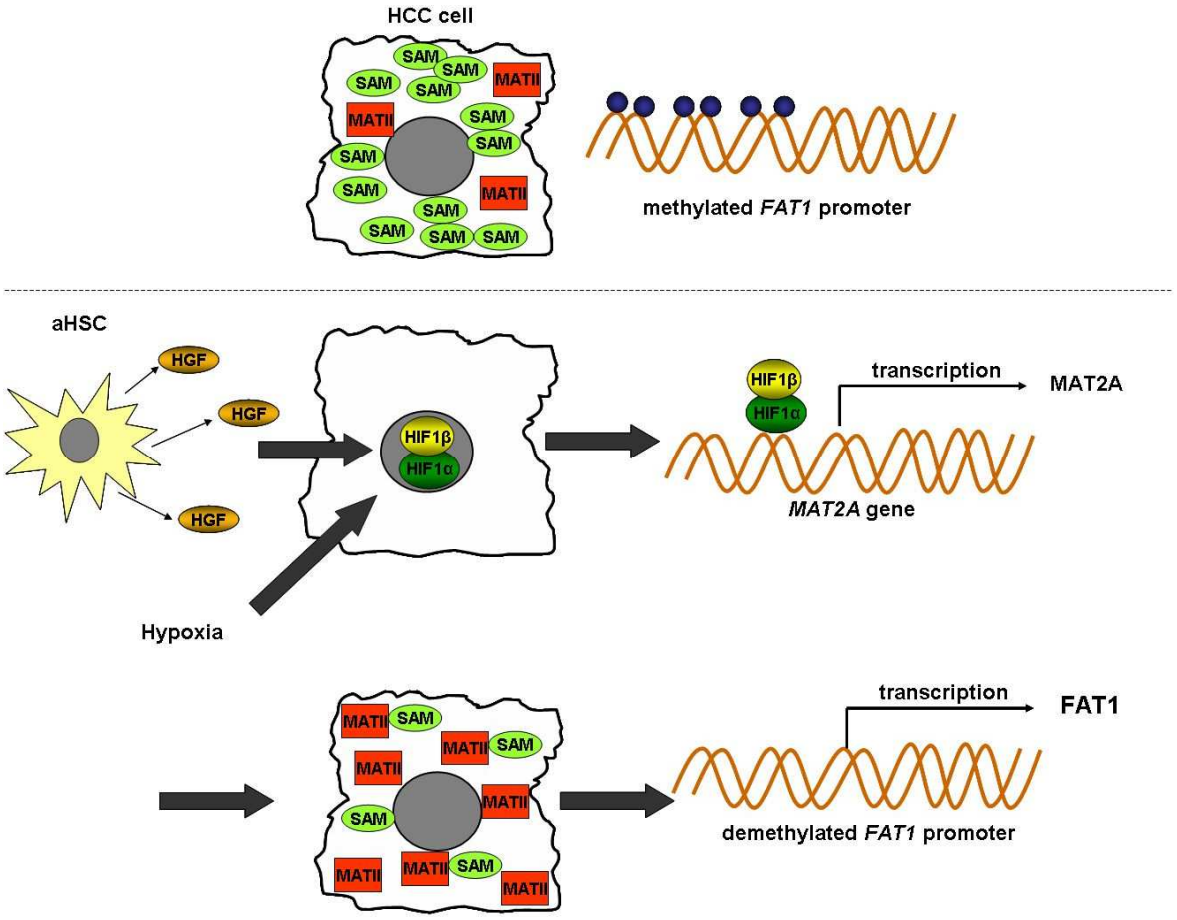

Figure 5.1 Working model for regulation of FAT1 expression in HCC cells. HGF secreted from activated hepatic stellate cells (aHSC) or hypoxia stabilizes HIF1α which transcriptionally upregulates MAT2A expression. Enhanced MATII activity causes reduced levels of the methyl donor S-adenosylmethionine (SAM), which leads to reduced methylation of the FAT1 promoter, and higher FAT1 transcription.

HGF has been linked to the polyamine pathway *via* NFκB regulated ornithine decarboxylase (ODC) expression (Tacchini et al. 2004). Recent studies demonstrated the regulatory role of SAM in HGF-mediated hepatocytes proliferation through a mechanism that implicates the activation of the non-canonical LKB1/AMPK/eNOS cascade and the function of HuR, which stabilizes MAT2A mRNA (Gomez-Santos et al. 2012). Here, we newly demonstrate a novel regulatory pathway by which HGF can effect SAM levels and herewith promoter methylation and transcription of the atypical cadherin FAT1.

Four FAT genes have now been identified in vertebrates, and Sopko and coworkers (Sopko et al. 2009) have shown that mammalian FAT4 is the true structural orthologues of *Drosophila* Fat, which has been identified as regulator of the Hippo pathways (Bennett and Harvey 2006). Despite this, several studies

suggest that FAT1 also shares the functional role as regulator of the Hippo pathway at least during development (Skouloudaki et al. 2009). The Hippo signaling pathway has a conserved role in growth control and is of fundamental importance during both normal development and oncogenesis. Thus, this pathway also has a prominent role in suppressing tumor growth, with the most evident contribution in HCC (Liu et al. 2012). FAT1 may be a mediator linking HGF and hypoxia induced HIF1α activation with this complex yet important growth-control signaling pathway.

Signaling pathways propagated from the cell surface through transmembrane receptors to intracellular regulatory mechanisms are critical from normal as well as aberrant cellular functions. Here, we demonstrated that increased FAT1 expression in HCC induces proliferation, migration and resistance to apoptosis. The FAT1 effect on apoptosis is a novel finding as well as the identification of FAT1 as potential mediator of hypoxia and growth receptor signaling to critical HCC related mechanisms.

5.3 Conclusion

In this work it could be shown that FAT1 is overexpressed in hepatocellular carcinoma and promotes its tumorigenicity. Furthermore, FAT1 is upregulated in human cirrhotic liver tissues, which represents a precancerous condition for HCC. Further, FAT1 was found to be increased during activation of hepatic stellate cells, i.e. an early event of the fibrosis-cirrhosis-carcinoma course. In these cells, FAT1 is involved in apoptosis-resistance and proinflammatory gene expression of HSCs. In addition, we found that activated HSCs are able to induce FAT1 expression in HCC cells *via* secretion of HGF which represents another example for the protumorigenic interaction between HSCs in the tumor stroma and HCC.

The fact that FAT1 is involved in different stages and mechanisms of liver disease progression suggests it as a novel and promising prognostic and therapeutic target.

6 References

Ala, A., Walker, A.P., Ashkan, K., Dooley, J.S., & Schilsky, M.L. 2007. Wilson's disease. *Lancet*, 369, (9559) 397-408 available from: PM:17276780

Amann, T., Bataille, F., Spruss, T., Muhlbauer, M., Gabele, E., Scholmerich, J., Kiefer, P., Bosserhoff, A.K., & Hellerbrand, C. 2009a. Activated hepatic stellate cells promote tumorigenicity of hepatocellular carcinoma. *Cancer Sci.*, 100, (4) 646-653 available from: PM:19175606

Amann, T., Maegdefrau, U., Hartmann, A., Agaimy, A., Marienhagen, J., Weiss, T.S., Stoeltzing, O., Warnecke, C., Scholmerich, J., Oefner, P.J., Kreutz, M., Bosserhoff, A.K., & Hellerbrand, C. 2009b. GLUT1 expression is increased in hepatocellular carcinoma and promotes tumorigenesis. *Am.J.Pathol.*, 174, (4) 1544-1552 available from: PM:19286567

Angst, B.D., Marcozzi, C., & Magee, A.I. 2001. The cadherin superfamily: diversity in form and function. *J.Cell Sci.*, 114, (Pt 4) 629-641 available from: PM:11171368

Angulo, P. 2002. Nonalcoholic fatty liver disease. *N.Engl.J.Med.*, 346, (16) 1221-1231 available from: PM:11961152

Bartosch, B., Thimme, R., Blum, H.E., & Zoulim, F. 2009. Hepatitis C virus-induced hepatocarcinogenesis. *J.Hepatol.*, 51, (4) 810-820 available from: PM:19545926

Bennett, F.C. & Harvey, K.F. 2006. Fat cadherin modulates organ size in Drosophila via the Salvador/Warts/Hippo signaling pathway. *Curr.Biol.*, 16, (21) 2101-2110 available from: PM:17045801

Benyon, R.C., Iredale, J.P., Goddard, S., Winwood, P.J., & Arthur, M.J. 1996. Expression of tissue inhibitor of metalloproteinases 1 and 2 is increased in fibrotic human liver. *Gastroenterology*, 110, (3) 821-831 available from: PM:8608892

Boonstra, K., Beuers, U., & Ponsioen, C.Y. 2012. Epidemiology of primary sclerosing cholangitis and primary biliary cirrhosis: a systematic review. *J.Hepatol.*, 56, (5) 1181-1188 available from: PM:22245904

Braun, G.S., Kretzler, M., Heider, T., Floege, J., Holzman, L.B., Kriz, W., & Moeller, M.J. 2007. Differentially spliced isoforms of FAT1 are asymmetrically distributed within migrating cells. *J.Biol.Chem.*, 282, (31) 22823-22833 available from: PM:17500054

Brodehl, J. 1961. [Thioacetamide in experimental liver research]. *Klin.Wochenschr.*, 39, 956-962 available from: PM:13873282

Bryant, P.J., Huettner, B., Held, L.I., Jr., Ryerse, J., & Szidonya, J. 1988. Mutations at the fat locus interfere with cell proliferation control and epithelial morphogenesis in Drosophila. *Dev.Biol.*, 129, (2) 541-554 available from: PM:3417051

Cabibbo, G., Enea, M., Attanasio, M., Bruix, J., Craxi, A., & Camma, C. 2010. A meta-analysis of survival rates of untreated patients in randomized clinical trials of hepatocellular carcinoma. *Hepatology*, 51, (4) 1274-1283 available from: PM:20112254

Cai, J., Sun, W.M., Hwang, J.J., Stain, S.C., & Lu, S.C. 1996. Changes in S-adenosylmethionine synthetase in human liver cancer: molecular characterization and significance. *Hepatology*, 24, (5) 1090-1097 available from: PM:8903381

Chosdol, K., Misra, A., Puri, S., Srivastava, T., Chattopadhyay, P., Sarkar, C., Mahapatra, A.K., & Sinha, S. 2009. Frequent loss of heterozygosity and altered expression of the candidate tumor suppressor gene 'FAT' in human astrocytic tumors. *BMC.Cancer*, 9, 5 available from: PM:19126244

Dandri, M. & Locarnini, S. 2012. New insight in the pathobiology of hepatitis B virus infection. *Gut*, 61 Suppl 1, i6-17 available from: PM:22504921

Day, C.P. & James, O.F. 1998. Steatohepatitis: a tale of two "hits"? *Gastroenterology*, 114, (4) 842-845 available from: PM:9547102

de Alwis, N.M. & Day, C.P. 2008. Non-alcoholic fatty liver disease: the mist gradually clears. *J.Hepatol.*, 48 Suppl 1, S104-S112 available from: PM:18304679

de Bock, C.E., Ardjmand, A., Molloy, T.J., Bone, S.M., Johnstone, D., Campbell, D.M., Shipman, K.L., Yeadon, T.M., Holst, J., Spanevello, M.D., Nelmes, G., Catchpoole, D.R., Lincz, L.F., Boyd, A.W., Burns, G.F., & Thorne, R.F. 2012. The Fat1 cadherin is overexpressed and an independent prognostic factor for survival in paired diagnosis-relapse samples of precursor B-cell acute lymphoblastic leukemia. *Leukemia*, 26, (5) 918-926 available from: PM:22116550

De Minicis, S. & Brenner, D.A. 2008. Oxidative stress in alcoholic liver disease: role of NADPH oxidase complex. *J.Gastroenterol.Hepatol.*, 23 Suppl 1, S98-103 available from: PM:18336675

Dikshit, B., Irshad, K., Madan, E., Aggarwal, N., Sarkar, C., Chandra, P.S., Gupta, D.K., Chattopadhyay, P., Sinha, S., & Chosdol, K. 2012. FAT1 acts as an upstream regulator of oncogenic and inflammatory pathways, via PDCD4, in glioma cells. *Oncogene* available from: PM:22986533

Dubuisson, L., Lepreux, S., Bioulac-Sage, P., Balabaud, C., Costa, A.M., Rosenbaum, J., & Desmouliere, A. 2001. Expression and cellular localization of fibrillin-1 in normal and pathological human liver. *J.Hepatol.*, 34, (4) 514-522 available from: PM:11394650

Dunne, J., Hanby, A.M., Poulsom, R., Jones, T.A., Sheer, D., Chin, W.G., Da, S.M., Zhao, Q., Beverley, P.C., & Owen, M.J. 1995. Molecular cloning and tissue expression of FAT, the human homologue of the Drosophila fat gene that is located on chromosome 4q34-q35 and encodes a putative adhesion molecule. *Genomics*, 30, (2) 207-223 available from: PM:8586420

El-Serag, H.B. 2011. Hepatocellular carcinoma. *N.Engl.J.Med.*, 365, (12) 1118-1127 available from: PM:21992124

El-Serag, H.B. & Rudolph, K.L. 2007. Hepatocellular carcinoma: epidemiology and molecular carcinogenesis. *Gastroenterology*, 132, (7) 2557-2576 available from: PM:17570226

Elsharkawy, A.M., Oakley, F., & Mann, D.A. 2005. The role and regulation of hepatic stellate cell apoptosis in reversal of liver fibrosis. *Apoptosis.*, 10, (5) 927-939 available from: PM:16151628

Faouzi, S., Le, B.B., Neaud, V., Boussarie, L., Saric, J., Bioulac-Sage, P., Balabaud, C., & Rosenbaum, J. 1999. Myofibroblasts are responsible for collagen synthesis in the stroma of human hepatocellular carcinoma: an in vivo and in vitro study. *J.Hepatol.*, 30, (2) 275-284 available from: PM:10068108

Farazi, P.A. & DePinho, R.A. 2006. Hepatocellular carcinoma pathogenesis: from genes to environment. *Nat.Rev.Cancer*, 6, (9) 674-687 available from: PM:16929323

Ferlay, J., Shin, H.R., Bray, F., Forman, D., Mathers, C., & Parkin, D.M. 2010. Estimates of worldwide burden of cancer in 2008: GLOBOCAN 2008. *Int.J.Cancer*, 127, (12) 2893-2917 available from: PM:21351269

Forner, A., Llovet, J.M., & Bruix, J. 2012. Hepatocellular carcinoma. *Lancet*, 379, (9822) 1245-1255 available from: PM:22353262

Friedman, S.L. & Arthur, M.J. 2002. Reversing hepatic fibrosis. *Science & Medicine*, 8, (4) 194-205

Frith, J., Day, C.P., Henderson, E., Burt, A.D., & Newton, J.L. 2009. Non-alcoholic fatty liver disease in older people. *Gerontology*, 55, (6) 607-613 available from: PM:19690397

Gabele, E., Froh, M., Arteel, G.E., Uesugi, T., Hellerbrand, C., Scholmerich, J., Brenner, D.A., Thurman, R.G., & Rippe, R.A. 2009. TNFalpha is required for cholestasis-induced liver fibrosis in the mouse. *Biochem.Biophys.Res.Commun.*, 378, (3) 348-353 available from: PM:18996089

Gervais, D.A. & Arellano, R.S. 2011. Percutaneous tumor ablation for hepatocellular carcinoma. *AJR Am.J.Roentgenol.*, 197, (4) 789-794 available from: PM:21940565

Gomez-Santos, L., Vazquez-Chantada, M., Mato, J.M., & Martinez-Chantar, M.L. 2012. SAMe and HuR in liver physiology: usefulness of stem cells in hepatic differentiation research. *Methods Mol.Biol.*, 826, 133-149 available from: PM:22167646

Gumbiner, B.M. 2005. Regulation of cadherin-mediated adhesion in morphogenesis. *Nat.Rev.Mol.Cell Biol.*, 6, (8) 622-634 available from: PM:16025097

Hellerbrand, C., Jobin, C., Licato, L.L., Sartor, R.B., & Brenner, D.A. 1998. Cytokines induce NF-kappaB in activated but not in quiescent rat hepatic stellate cells. *Am.J.Physiol*, 275, (2 Pt 1) G269-G278 available from: PM:9688654

Horiguchi, N., Takayama, H., Toyoda, M., Otsuka, T., Fukusato, T., Merlino, G., Takagi, H., & Mori, M. 2002. Hepatocyte growth factor promotes hepatocarcinogenesis through c-Met autocrine activation and enhanced angiogenesis in transgenic mice treated with diethylnitrosamine. *Oncogene*, 21, (12) 1791-1799 available from: PM:11896611

Hou, R., Liu, L., Anees, S., Hiroyasu, S., & Sibinga, N.E. 2006. The Fat1 cadherin integrates vascular smooth muscle cell growth and migration signals. *J.Cell Biol.*, 173, (3) 417-429 available from: PM:16682528

Hou, R. & Sibinga, N.E. 2009. Atrophin proteins interact with the Fat1 cadherin and regulate migration and orientation in vascular smooth muscle cells. *J.Biol.Chem.*, 284, (11) 6955-6965 available from: PM:19131340

Huang, G.W., Yang, L.Y., & Lu, W.Q. 2005. Expression of hypoxia-inducible factor 1alpha and vascular endothelial growth factor in hepatocellular carcinoma: Impact on neovascularization and survival. *World J.Gastroenterol.*, 11, (11) 1705-1708 available from: PM:15786555

Iredale, J.P. 2003. Cirrhosis: new research provides a basis for rational and targeted treatments. *BMJ*, 327, (7407) 143-147 available from: PM:12869458

Iredale, J.P. 2007. Models of liver fibrosis: exploring the dynamic nature of inflammation and repair in a solid organ. *J.Clin.Invest*, 117, (3) 539-548 available from: PM:17332881

Kim, K.R., Moon, H.E., & Kim, K.W. 2002. Hypoxia-induced angiogenesis in human hepatocellular carcinoma. *J.Mol.Med.(Berl)*, 80, (11) 703-714 available from: PM:12436347

Kivirikko, K.I. & Myllyharju, J. 1998. Prolyl 4-hydroxylases and their protein disulfide isomerase subunit. *Matrix Biol.*, 16, (7) 357-368 available from: PM:9524356

Koff, R.S. 1998. Hepatitis A. *Lancet*, 351, (9116) 1643-1649 available from: PM:9620732

Kong, D., Park, E.J., Stephen, A.G., Calvani, M., Cardellina, J.H., Monks, A., Fisher, R.J., Shoemaker, R.H., & Melillo, G. 2005. Echinomycin, a small-molecule inhibitor of hypoxia-inducible factor-1 DNA-binding activity. *Cancer Res.*, 65, (19) 9047-9055 available from: PM:16204079

Krause, M., Dent, E.W., Bear, J.E., Loureiro, J.J., & Gertler, F.B. 2003. Ena/VASP proteins: regulators of the actin cytoskeleton and cell migration. *Annu.Rev.Cell Dev.Biol.*, 19, 541-564 available from: PM:14570581

Krawitt, E.L. 2006. Autoimmune hepatitis. *N.Engl.J.Med.*, 354, (1) 54-66 available from: PM:16394302

Kwaepila, N., Burns, G., & Leong, A.S. 2006. Immunohistological localisation of human FAT1 (hFAT) protein in 326 breast cancers. Does this adhesion molecule have a role in pathogenesis? *Pathology*, 38, (2) 125-131 available from: PM:16581652

Lavanchy, D. 2004. Hepatitis B virus epidemiology, disease burden, treatment, and current and emerging prevention and control measures. *J.Viral Hepat.*, 11, (2) 97-107 available from: PM:14996343

Le Bail B., Faouzi, S., Boussarie, L., Guirouilh, J., Blanc, J.F., Carles, J., Bioulac-Sage, P., Balabaud, C., & Rosenbaum, J. 1999. Osteonectin/SPARC is overexpressed in human hepatocellular carcinoma. *J.Pathol.*, 189, (1) 46-52 available from: PM:10451487

Lee, S., Stewart, S., Nagtegaal, I., Luo, J., Wu, Y., Colditz, G., Medina, D., & Allred, D.C. 2012. Differentially Expressed Genes Regulating the Progression of Ductal Carcinoma in Situ to Invasive Breast Cancer. *Cancer Res.* available from: PM:22751464

Liu, A.M., Xu, Z., & Luk, J.M. 2012. An update on targeting Hippo-YAP signaling in liver cancer. *Expert.Opin.Ther.Targets.*, 16, (3) 243-247 available from: PM:22335485

Liu, Q., Liu, L., Zhao, Y., Zhang, J., Wang, D., Chen, J., He, Y., Wu, J., Zhang, Z., & Liu, Z. 2011. Hypoxia induces genomic DNA demethylation through the activation of HIF-1alpha and transcriptional upregulation of MAT2A in hepatoma cells. *Mol.Cancer Ther.*, 10, (6) 1113-1123 available from: PM:21460102

Llovet, J.M. & Bruix, J. 2008. Novel advancements in the management of hepatocellular carcinoma in 2008. *J.Hepatol.*, 48 Suppl 1, S20-S37 available from: PM:18304676

Lu, S.C. & Mato, J.M. 2008. S-Adenosylmethionine in cell growth, apoptosis and liver cancer. *J.Gastroenterol.Hepatol.*, 23 Suppl 1, S73-S77 available from: PM:18336669

Ludwig, J., Viggiano, T.R., McGill, D.B., & Oh, B.J. 1980. Nonalcoholic steatohepatitis: Mayo Clinic experiences with a hitherto unnamed disease. *Mayo Clin.Proc.*, 55, (7) 434-438 available from: PM:7382552

Magg, T., Schreiner, D., Solis, G.P., Bade, E.G., & Hofer, H.W. 2005. Processing of the human protocadherin Fat1 and translocation of its cytoplasmic domain to the nucleus. *Exp.Cell Res.*, 307, (1) 100-108 available from: PM:15922730

Maluf, D., Cotterell, A., Clark, B., Stravitz, T., Kauffman, H.M., & Fisher, R.A. 2005. Hepatic angiosarcoma and liver transplantation: case report and literature review. *Transplant.Proc.*, 37, (5) 2195-2199 available from: PM:15964377

Martinez-Hernandez, A. & Amenta, P.S. 1995. The extracellular matrix in hepatic regeneration. *FASEB J.*, 9, (14) 1401-1410 available from: PM:7589981

Moeller, M.J., Soofi, A., Braun, G.S., Li, X., Watzl, C., Kriz, W., & Holzman, L.B. 2004. Protocadherin FAT1 binds Ena/VASP proteins and is necessary for actin dynamics and cell polarization. *EMBO J.*, 23, (19) 3769-3779 available from: PM:15343270

Nakaya, K., Yamagata, H.D., Arita, N., Nakashiro, K.I., Nose, M., Miki, T., & Hamakawa, H. 2007. Identification of homozygous deletions of tumor suppressor

gene FAT in oral cancer using CGH-array. *Oncogene*, 26, (36) 5300-5308 available from: PM:17325662

Navarro, V.J. & Senior, J.R. 2006. Drug-related hepatotoxicity. *N.Engl.J.Med.*, 354, (7) 731-739 available from: PM:16481640

Nishikawa, Y., Miyazaki, T., Nakashiro, K., Yamagata, H., Isokane, M., Goda, H., Tanaka, H., Oka, R., & Hamakawa, H. 2011. Human FAT1 cadherin controls cell migration and invasion of oral squamous cell carcinoma through the localization of beta-catenin. *Oncol.Rep.*, 26, (3) 587-592 available from: PM:21617878

Oakley, F., Meso, M., Iredale, J.P., Green, K., Marek, C.J., Zhou, X., May, M.J., Millward-Sadler, H., Wright, M.C., & Mann, D.A. 2005. Inhibition of inhibitor of kappaB kinases stimulates hepatic stellate cell apoptosis and accelerated recovery from rat liver fibrosis. *Gastroenterology*, 128, (1) 108-120 available from: PM:15633128

Ou, X., Yang, H., Ramani, K., Ara, A.I., Chen, H., Mato, J.M., & Lu, S.C. 2007. Inhibition of human betaine-homocysteine methyltransferase expression by S-adenosylmethionine and methylthioadenosine. *Biochem.J.*, 401, (1) 87-96 available from: PM:16953798

Park, S.K., Dadak, A.M., Haase, V.H., Fontana, L., Giaccia, A.J., & Johnson, R.S. 2003. Hypoxia-induced gene expression occurs solely through the action of hypoxia-inducible factor 1alpha (HIF-1alpha): role of cytoplasmic trapping of HIF-2alpha. *Mol.Cell Biol.*, 23, (14) 4959-4971 available from: PM:12832481

Peinado, H., Portillo, F., & Cano, A. 2004. Transcriptional regulation of cadherins during development and carcinogenesis. *Int.J.Dev.Biol.*, 48, (5-6) 365-375 available from: PM:15349812

Pietrangelo, A. 2004. Hereditary hemochromatosis--a new look at an old disease. *N.Engl.J.Med.*, 350, (23) 2383-2397 available from: PM:15175440

Pinzani, M. 1995. Novel insights into the biology and physiology of the Ito cell. *Pharmacol.Ther.*, 66, (2) 387-412 available from: PM:7667403

Rinta-Valkama, J., Palmen, T., Lassila, M., & Holthofer, H. 2007. Podocyte-associated proteins FAT, alpha-actinin-4 and filtrin are expressed in Langerhans islets of the pancreas. *Mol.Cell Biochem.*, 294, (1-2) 117-125 available from: PM:16841182

Rosmorduc, O. & Housset, C. 2010. Hypoxia: a link between fibrogenesis, angiogenesis, and carcinogenesis in liver disease. *Semin.Liver Dis.*, 30, (3) 258-270 available from: PM:20665378

Sadeqzadeh, E., de Bock, C.E., Zhang, X.D., Shipman, K.L., Scott, N.M., Song, C., Yeadon, T., Oliveira, C.S., Jin, B., Hersey, P., Boyd, A.W., Burns, G.F., & Thorne, R.F. 2011. Dual processing of FAT1 cadherin protein by human melanoma cells generates distinct protein products. *J.Biol.Chem.*, 286, (32) 28181-28191 available from: PM:21680732

Sangro, B., Inarrairaegui, M., & Bilbao, J.I. 2012. Radioembolization for hepatocellular carcinoma. *J.Hepatol.*, 56, (2) 464-473 available from: PM:21816126

Santoni-Rugiu, E., Preisegger, K.H., Kiss, A., Audolfsson, T., Shiota, G., Schmidt, E.V., & Thorgeirsson, S.S. 1996. Inhibition of neoplastic development in the liver by hepatocyte growth factor in a transgenic mouse model. *Proc.Natl.Acad.Sci.U.S.A*, 93, (18) 9577-9582 available from: PM:8790372

Schnabl, B., Choi, Y.H., Olsen, J.C., Hagedorn, C.H., & Brenner, D.A. 2002. Immortal activated human hepatic stellate cells generated by ectopic telomerase expression. *Lab Invest*, 82, (3) 323-333 available from: PM:11896211

Schofield, C.J. & Ratcliffe, P.J. 2005. Signalling hypoxia by HIF hydroxylases. *Biochem.Biophys.Res.Commun.*, 338, (1) 617-626 available from: PM:16139242

Schreiner, D., Muller, K., & Hofer, H.W. 2006. The intracellular domain of the human protocadherin hFat1 interacts with Homer signalling scaffolding proteins. *FEBS Lett.*, 580, (22) 5295-5300 available from: PM:16979624

Schuppan, D. & Afdhal, N.H. 2008. Liver cirrhosis. *Lancet*, 371, (9615) 838-851 available from: PM:18328931

Schwimmer, J.B., Deutsch, R., Kahen, T., Lavine, J.E., Stanley, C., & Behling, C. 2006. Prevalence of fatty liver in children and adolescents. *Pediatrics*, 118, (4) 1388-1393 available from: PM:17015527

Semela, D. & Dufour, J.F. 2004. Angiogenesis and hepatocellular carcinoma. *J.Hepatol.*, 41, (5) 864-880 available from: PM:15519663

Semenza, G.L. & Wang, G.L. 1992. A nuclear factor induced by hypoxia via de novo protein synthesis binds to the human erythropoietin gene enhancer at a site required for transcriptional activation. *Mol.Cell Biol.*, 12, (12) 5447-5454 available from: PM:1448077

Settakorn, J., Kaewpila, N., Burns, G.F., & Leong, A.S. 2005. FAT, E-cadherin, beta catenin, HER 2/neu, Ki67 immuno-expression, and histological grade in intrahepatic cholangiocarcinoma. *J.Clin.Pathol.*, 58, (12) 1249-1254 available from: PM:16311342

Shahrzad, S., Bertrand, K., Minhas, K., & Coomber, B.L. 2007. Induction of DNA hypomethylation by tumor hypoxia. *Epigenetics.*, 2, (2) 119-125 available from: PM:17965619

Shiota, G., Kawasaki, H., Nakamura, T., & Schmidt, E.V. 1995. Characterization of double transgenic mice expressing hepatocye growth factor and transforming growth factor alpha. *Res.Commun.Mol.Pathol.Pharmacol.*, 90, (1) 17-24 available from: PM:8581343

Shiota, G., Rhoads, D.B., Wang, T.C., Nakamura, T., & Schmidt, E.V. 1992. Hepatocyte growth factor inhibits growth of hepatocellular carcinoma cells. *Proc.Natl.Acad.Sci.U.S.A*, 89, (1) 373-377 available from: PM:1309612

Shiraishi-Yamaguchi, Y. & Furuichi, T. 2007. The Homer family proteins. *Genome Biol.*, 8, (2) 206 available from: PM:17316461

Shukla, V., Coumoul, X., & Deng, C.X. 2007. RNAi-based conditional gene knockdown in mice using a U6 promoter driven vector. *Int.J.Biol.Sci.*, 3, (2) 91-99 available from: PM:17304337

Skouloudaki, K., Puetz, M., Simons, M., Courbard, J.R., Boehlke, C., Hartleben, B., Engel, C., Moeller, M.J., Englert, C., Bollig, F., Schafer, T., Ramachandran, H., Mlodzik, M., Huber, T.B., Kuehn, E.W., Kim, E., Kramer-Zucker, A., & Walz, G. 2009. Scribble participates in Hippo signaling and is required for normal zebrafish pronephros development. *Proc.Natl.Acad.Sci.U.S.A*, 106, (21) 8579-8584 available from: PM:19439659

Sopko, R. & McNeill, H. 2009. The skinny on Fat: an enormous cadherin that regulates cell adhesion, tissue growth, and planar cell polarity. *Curr.Opin.Cell Biol.*, 21, (5) 717-723 available from: PM:19679459

Sopko, R., Silva, E., Clayton, L., Gardano, L., Barrios-Rodiles, M., Wrana, J., Varelas, X., Arbouzova, N.I., Shaw, S., Saburi, S., Matakatsu, H., Blair, S., & McNeill, H. 2009. Phosphorylation of the tumor suppressor fat is regulated by its ligand Dachsous and the kinase discs overgrown. *Curr.Biol.*, 19, (13) 1112-1117 available from: PM:19540118

Stefanovic, B., Hellerbrand, C., Holcik, M., Briendl, M., Aliebhaber, S., & Brenner, D.A. 1997. Posttranscriptional regulation of collagen alpha1(I) mRNA in hepatic stellate cells. *Mol.Cell Biol.*, 17, (9) 5201-5209 available from: PM:9271398

Stevens, A.P., Dettmer, K., Kirovski, G., Samejima, K., Hellerbrand, C., Bosserhoff, A.K., & Oefner, P.J. 2010. Quantification of intermediates of the methionine and polyamine metabolism by liquid chromatography-tandem mass spectrometry in cultured tumor cells and liver biopsies. *J.Chromatogr.A*, 1217, (19) 3282-3288 available from: PM:20117790

Tacchini, L., Dansi, P., Matteucci, E., & Desiderio, M.A. 2001. Hepatocyte growth factor signalling stimulates hypoxia inducible factor-1 (HIF-1) activity in HepG2 hepatoma cells. *Carcinogenesis*, 22, (9) 1363-1371 available from: PM:11532856

Tacchini, L., De, P.C., Matteucci, E., Follis, R., & Desiderio, M.A. 2004. Hepatocyte growth factor-activated NF-kappaB regulates HIF-1 activity and ODC expression, implicated in survival, differently in different carcinoma cell lines. *Carcinogenesis*, 25, (11) 2089-2100 available from: PM:15240510

Tajima, H., Matsumoto, K., & Nakamura, T. 1991. Hepatocyte growth factor has potent anti-proliferative activity in various tumor cell lines. *FEBS Lett.*, 291, (2) 229-232 available from: PM:1657643

Tanaka, H., Yamamoto, M., Hashimoto, N., Miyakoshi, M., Tamakawa, S., Yoshie, M., Tokusashi, Y., Yokoyama, K., Yaginuma, Y., & Ogawa, K. 2006. Hypoxia-independent overexpression of hypoxia-inducible factor 1alpha as an early change in mouse hepatocarcinogenesis. *Cancer Res.*, 66, (23) 11263-11270 available from: PM:17145871

Tanimoto, K., Makino, Y., Pereira, T., & Poellinger, L. 2000. Mechanism of regulation of the hypoxia-inducible factor-1 alpha by the von Hippel-Lindau tumor suppressor protein. *EMBO J.*, 19, (16) 4298-4309 available from: PM:10944113

Tanoue, T. & Takeichi, M. 2004. Mammalian Fat1 cadherin regulates actin dynamics and cell-cell contact. *J.Cell Biol.*, 165, (4) 517-528 available from: PM:15148305

Tanoue, T. & Takeichi, M. 2005. New insights into Fat cadherins. *J.Cell Sci.*, 118, (Pt 11) 2347-2353 available from: PM:15923647

Taub, R. 2004. Liver regeneration: from myth to mechanism. *Nat.Rev.Mol.Cell Biol.*, 5, (10) 836-847 available from: PM:15459664

Tyson, G.L. & El-Serag, H.B. 2011. Risk factors for cholangiocarcinoma. *Hepatology*, 54, (1) 173-184 available from: PM:21488076

Venook, A.P., Papandreou, C., Furuse, J., & de Guevara, L.L. 2010. The incidence and epidemiology of hepatocellular carcinoma: a global and regional perspective. *Oncologist.*, 15 Suppl 4, 5-13 available from: PM:21115576

Wang, G.L. & Semenza, G.L. 1995. Purification and characterization of hypoxia-inducible factor 1. *J.Biol.Chem.*, 270, (3) 1230-1237 available from: PM:7836384

Wang, L. & Tsai, C.C. 2008. Atrophin proteins: an overview of a new class of nuclear receptor corepressors. *Nucl.Recept.Signal.*, 6, e009 available from: PM:19043594

Warnecke, C., Zaborowska, Z., Kurreck, J., Erdmann, V.A., Frei, U., Wiesener, M., & Eckardt, K.U. 2004. Differentiating the functional role of hypoxia-inducible factor (HIF)-1alpha and HIF-2alpha (EPAS-1) by the use of RNA interference: erythropoietin is a HIF-2alpha target gene in Hep3B and Kelly cells. *FASEB J.*, 18, (12) 1462-1464 available from: PM:15240563

Wedemeyer, H. & Manns, M.P. 2010. Epidemiology, pathogenesis and management of hepatitis D: update and challenges ahead. *Nat.Rev.Gastroenterol.Hepatol.*, 7, (1) 31-40 available from: PM:20051970

Wenger, R.H. 2002. Cellular adaptation to hypoxia: O2-sensing protein hydroxylases, hypoxia-inducible transcription factors, and O2-regulated gene expression. *FASEB J.*, 16, (10) 1151-1162 available from: PM:12153983

Yang, H., Sadda, M.R., Li, M., Zeng, Y., Chen, L., Bae, W., Ou, X., Runnegar, M.T., Mato, J.M., & Lu, S.C. 2004. S-adenosylmethionine and its metabolite induce apoptosis in HepG2 cells: Role of protein phosphatase 1 and Bcl-x(S). *Hepatology*, 40, (1) 221-231 available from: PM:15239106

7 Abbreviations

α-sma	*alpha*-smooth muscle actin
°C	degree Celsius
µg	microgram
µl	microliter
µm	micrometer
µM	micromolar
µm	micrometer
Adox	Adenosine-2′,3′-dialdehyde
ALF	acute liver failure
ALL	acute lymphatic leukemia
AMV-RT	avian myeloblastosis virus reverse transcriptase
arb.	arbituary
APS	ammonium persulfate
ATP	adenosine triphosphate
Aza	5-Aza-2‘deoxycytidine
BCA	bicinchonic acid
BDL	bile duct ligation
bp	base pairs
BSA	bovine serum albumin
ca.	circa
CAM	cell adhesion molecule
cDNA	complementary DNA
coll I	collagen type I
ctrl.	control
Cyclo	Cycloheximide
d	day
Da	dalton (=1.66018 x 10^{-24} g)
DAPI	4’, 6-diamino-2-phenylindole
dest.	destilled
DMEM	Dulbecco’s modified eagle medium
DMSO	dimethyl sulfoxide
DNA	deoxyribonucleic acid
DP	2,2-dipyridyl
e.g.	*exempli gratia*
ECM	extracellular matrix
EDTA	ethylene diamine tetraacetic acid
EGTA	ethylene glycol tetraacetic acid
ELISA	enzyme linked immunosorbent assay
EMT	epithelial-mesenchymal transition

et al.	*et alii*
FCS	fetal calf serum
FITC	fluorescein isothiocyanate
g	gram
h	hour
$H_2O_{dest.}$	destilled water
HCC	hepatocellular carcinoma
HGF	hepatocyte growth factor
HIF	hypoxia inducible factor
HRP	horse radish peroxidase
HSC	hepatic stellate cells
hTERT	human telomerase reverse transcriptase
Ig	immunoglobulin
IκBα	inhibitory *kappa* B *alpha*
kDa	kilodalton
l	liter
LOH	loss of heterozygosity
LSEC	liver sinusoidal endothelial cells
M	molar, mol/l
mA	milliampere
MCP-1	monocyte chemoattractant protein-1 = CCL2
MET	mesenchymal-epithelial transition
mg	milligram
Mg	magnesium
min	minute
ml	milliliter
mM	millimolar
mm	millimeter
mmol	millimol
MMP	matrix metalloproteinase
mRNA	messenger RNA
NAFLD	non-alcoholic fatty liver disease
NASH	non-alcoholic steatohepatitis
NFκB	nuclear factor *kappa* B
ng	nanogram
NLS	nuclear localization sequence
nm	nanometer
OD	optical density
OSCC	oral squamous cell carcinomas
PBC	primary biliary cirrhosis
PBS	phosphate buffered saline
PCR	polymerase chain reaction

PDGF	platelet-derived growth factor
PEI	percutaneous ethanol injection
pH	*pondus hydrogenii*
PHH	primary human hepatocytes
PI	propidium iodide
PCP	planar cell polarity
PMH	primary murine hepatocytes
PSC	primary sclerosing cholangitis
p-value	probability value (statistics)
qRT-PCR	quantitative realtime-PCR
r	radius
RFA	radiofrequency ablation
RNA	ribonucleic acid
RNase	ribonuclease
ROS	reactive oxygen species
rpm	rounds per minute
RT	room temperature
s	second
SDS	sodium dodecyl sulfate
SIRT	selective internal radiation therapy
STS	staurosporine
TAA	thioacetamide
TACE	transarterial chemoembolization
TE	tris EDTA
TEMED	N, N, N', N'-tetramethylethylenediamine
TIMP	tissue inhibitors of matrix metalloproteinases
TMA	tissue microarray
TNF	tumor necrosis factor
Tris	tris(hydroxymethyl)aminomethane
TWEEN	Polyoxyethylene sorbitan monolaurate
U	unit
U.S.	United States
UV	ultraviolet
V	volt
v/v	volume per volume
VEGF	vascular endothelial growth factor
Vol.	volume
vs.	versus
VSMC	vascular smooth muscle cells
w/v	weight per volume
XTT	2,3-bis(2-methoxy-4-nitro-5-sulfophenyl)-5-[phenylamino)carbonyl]-2H-tetrazolium hydroxide

8 Appendix

8.1 Curriculum vitae

Daniela Valletta

Geburtsdatum: 03.03.1981

Geburtsort: Neumarkt i.d.OPf

Staatsangehörigkeit: deutsch, italienisch

1987-1991	Grundschule Bräugasse, Neumarkt
1991-2000	Ostendorfer Gymnasium, Neumarkt, Allgemeine Hochschulreife (Abitur)
Okt. 2000 – März 2004	Diplomstudiengang Biologie, Universität Regensburg
April 2004 – Juli 2008	Diplomstudiengang Molekulare Medizin, Friedrich-Alexander Universität, Erlangen-Nürnberg
Sept. – Dez. 2007	Diplomprüfungen Hauptfach: Molekulare Zellfunktionen Nebenfächer: Pharmakologie und Toxikologie, Molekulare Humangenetik, Molekulare Pathomechanismen
Jan. – Juli 2008	Diplomarbeit,. Universitätsklinikum Erlangen, Frauenklinik, Labor für Molekulare Medizin; Titel: „Die Rolle der GnRH-Rezeptor-vermittelten Signaltransduktion in der Proliferation von Endometriose“
Feb. 2006 – Dez. 2007	Studentische Hilfskraft, Universitätsklinikum Erlangen, Frauenklinik, Labor für Molekulare Medizin;

8.2 Advanced training and courses

März 2006	Fachkundenachweis nach § 9 Tierschutzgesetz
März 2007	Fachkundenachweis nach Strahlenschutzverordnung (StrlSchV)
30. - 31. März 2009	Fortbildungsveranstaltung für Projektleiter und Beauftragte für Biologische Sicherheit (BBS) in Regensburg
28. – 29. Jan. 2010	Falk Workshop “The Gut and the Liver”
27. – 28. Jan. 2011	Falk Workshop “Liver and Immunology“
26. – 27. Jan. 2012	Falk Workshop “Inflammation & Cancer“

8.3 Publications

Valletta D., Czech B., Thasler W.E., Müller M., Bosserhoff A.K., Hellerbrand C.
Expression and function of the atypical cadherin FAT1 in chronic liver disease. *Biochem Biophys Res Commun*. (2012) [in press]

Schnabl B., Czech B., Valletta D., Weiss T.S., Kirovski G., Hellerbrand C.
Increased expression of zinc finger protein 267 in non-alcoholic fatty liver disease. *Int J Clin Exp Pathol.* (2011) 4: 661-666.

Schnabl B., Valletta D., Kirovski G., Hellerbrand C.
Zinc finger protein 267 is upregulated in hepatocellular carcinoma and promotes tumor cell proliferation and migration. *Exp Mol Pathol.* (2011) 3:695-701.

Oppelt P., Renner S.P., Strick R., Valletta D., Mehlhorn G., Fasching P.A., Beckmann M.W., Strissel P.L.
Correlation of high risk human papilloma viruses but not of herpes viruses or Chlamydia trachomatis with endometriosis lesions. *Fertil Steril.* (2010) 6: 1778-1786.

8.4 Presentations

8.4.1 Oral poster presentation

47th Annual Meeting of the European Association for the Study of the Liver (18. – 22. April 2012, Barcelona, Spain)

- ☐ Valletta D., Czech B., Weiss T.S., Bosserhoff A.K., Hellerbrand C.
  FAT1 expression is increased in hepatocellular carcinoma and promotes tumorigenesis

8.4.2 Poster presentations

26. Jahrestagung der Deutschen Arbeitsgemeinschaft zum Studium der Leber (29. – 30. Jan. 2010, Bonn, Germany)

- ☐ Valletta D., Amann T., Bosserhoff A., Hellerbrand C.
  Increased expression of FAT1 in hepatocellular carcinoma promotes tumorigenicity

33rd Annual Meeting of the German Society for Cell Biology (10. – 13. March 2010, Regensburg, Germany)

- ☐ Valletta D., Amann T., Bosserhoff A., Hellerbrand C.
  Increased expression of FAT1 in hepatocellular carcinoma promotes tumorigenicity

45th Annual Meeting of the European Association for the Study of the Liver (14. – 18. April 2010, Vienna, Austria)

- ☐ Valletta D., Amann T., Bosserhoff A.K., Hellerbrand C.
  Increased expression of FAT1 in hepatocellular carcinoma promotes tumorigenicity

27. Jahrestagung der Deutschen Arbeitsgemeinschaft zum Studium der Leber (28. – 29. Jan. 2011, Regensburg, Germany)

- ☐ Valletta D., Dorn C., Saugspier M., Amann T., Czech B., Gäbele E., Bosserhoff A., Hellerbrand C.
  Expression and function of the atypical cadherin FAT1 in liver fibrosis
- ☐ Valletta D., Amann T., Czech B., Weiss T., Bosserhoff A., Hellerbrand C.
  FAT1 expression is increased in hepatocellular carcinoma and promotes tumorigenesis

Falk Workshop, Inflammation & Cancer (26. – 27. Jan. 2012, Hamburg, Germany)

- Valletta D., Czech B., Hellerbrand C
  Atrophin 2 expression and function in hepatocellular carcinoma

28. Jahrestagung der Deutschen Arbeitsgemeinschaft zum Studium der Leber (27. – 28. Jan. 2012, Hamburg, Germany)

- Valletta D., Czech B., Sauspier M., Dorn C., Bosserhoff A., Hellerbrand C.
  Expression of the atypical cadherin FAT1 in hepatic fibrosis
- Valletta D., Czech B., Weiss T.S., Dorn C., Hellerbrand C.
  Atrophin 2 expression in chronic liver disease functionally affects activated hepatic stellate cells
- Valletta D., Czech B., Weiss T.S., Bosserhoff A., Hellerbrand C.
  FAT1 expression is increased in hepatocellular carcinoma and promotes tumorigenesis

47th Annual Meeting of the European Association for the Study of the Liver (18. – 22. April 2012, Barcelona, Spain)

- Valletta D., Czech B., Saugspier M., Dorn C., Bosserhoff A.K., Hellerbrand C.
  Expression and function of the atypical cadherin FAT1 in hepatic fibrosis

8.5 Awards/Grants

- EASL (European Association for the Study of the Liver) Registration Award 2010, Vienna, Austria
- Falk Foundation Travel Award 2012, Hamburg, Germany
- EASL (European Association for the Study of the Liver) Travel Award 2012, Barcelona, Spain

8.6 Danksagung

An dieser Stelle ist es mir sehr wichtig, den vielen Menschen zu danken, die mich bei dieser Arbeit unterstützt haben.

Ich danke **Herrn Prof. Claus Hellerbrand** für die viele Zeit, die er sich während der letzten Jahre für die Betreuung genommen hat, für die ertragreichen Diskussionen, den Ansporn, die hin und wieder nötige Motivation und seine freundschaftliche und offene Art.

Mein Dank gilt auch **Frau Prof. Anja-Katrin Bosserhoff** für die engagierte Betreuung und das fortwährende Interesse an dieser Arbeit.

Herrn Prof. Ralf Weiskirchen danke ich für die Übernahme des Mentorats und die wissenschaftlichen Diskussionen im Rahmen der Colloquien.

Ich danke **Herrn PD Dr. Sven Lang** und **Frau Prof. Marina Kreutz** für ihre Bereitschaft als Drittprüfer bzw. Vorsitzende der Prüfungskommission zu fungieren.

Frau Prof. Martina Müller-Schilling danke ich für das forschungsfreundliche Umfeld in der Inneren Medizin I, das mir die Erstellung dieser Arbeit ermöglicht hat.

Herrn Dr. Thilo Spruss und seinen Mitarbeitern danke ich für das Management der Nacktmausversuche.

Danke an **Herrn Peter Karl** und **Herrn Herbert Gabler** für die gute Zusammenarbeit im Versuchtierlabor.

Ich danke auch **Herrn Rudi Jung** für die Unterstützung bei den immunhistochemischen Färbungen.

Frau Martina Meisinger danke ich für die vielen stillen Arbeiten im Hintergrund, die einem das Leben im Labor sehr erleichtern.

Danke der gesamten **Arbeitsgruppe Bosserhoff** und allen **Kollegen im H1** für die selbstverständliche Hilfe bei den verschiedensten Fragen und für den angenehmen Laboralltag.

Tausend Dank an die gesamte Lebergruppe, die mir die Zeit im Labor – im wahrsten Sinne des Wortes – versüßt hat. Jederzeit mit Rat und Tat standen mir zur Seite: **Abdo Mahli, Andreas Koch, Barbara Czech, Birgitta Ott-Rötzer, Dr. Christoph Dorn, Heidi Gschwendtner, Karin Grünberger, Kornelia Elser, Leandra Koletzko, Margit Nützel, Marina Fink, Dr. Michael Saugspier, Monika Artinger und Ruth Schewior**.
Ein besonderer Dank geht dabei auch an unseren ehemaligen Kollegen **Dr. Thomas Amann**, der mich in der ersten Zeit geduldig eingewiesen hat und mich an seiner Erfahrung teilhaben hat lassen.

Herzlichen Dank an **Barbara** für jede Form von Kohlenhydraten, das Korrekturlesen, den Seelenbeistand und die tolle Zeit auch außerhalb des Labors.

Ich danke allen meinen Freunden für ihre Unterstützung. Danke **Co** und **Susi**, für das Korrekturlesen, den Zuspruch, die Telefonseelsorge und das Care-Paket.

Ein ganz lieber Dank gilt meinen **Eltern,** die mich all die Jahre geduldig unterstützt haben. Ich danke ihnen für ihr Verständnis und für alles, was sie mir ermöglicht haben. Ein großes Dankeschön auch an meine Schwester **Elisa**, die immer für mich da war und an mich geglaubt hat.

Danke **Jo**, dass Du - einmal mehr - manche Laune und den Verzicht auf gemeinsam verbrachte Zeit geduldig ertragen hast und mir oft genug den Zuspruch und Rückhalt gegeben hast, den ich gebraucht habe.

8.7 Selbständigkeitserklärung

Ich, Valletta Daniela geboren am 03.03.1981 in Neumarkt i.d.OPf erkläre hiermit, dass ich die vorliegende Arbeit ohne unzulässige Hilfe Dritter und ohne Benutzung anderer als der angegebenen Hilfsmittel angefertigt habe.

Die aus anderen Quellen direkt oder indirekt übernommenen Daten und Konzepte sind unter Angabe der Quelle gekennzeichnet. Insbesondere habe ich nicht die entgeltliche Hilfe von Vermittlungs- bzw. Beratungsdiensten (Promotionsberater oder andere Personen) in Anspruch genommen.

Die Arbeit wurde bisher weder im In- noch im Ausland in gleicher oder ähnlicher Form einer anderen Prüfungsbehörde vorgelegt.

…….. ……..

(Ort, Datum) (Unterschrift)